NASA Contractor Report 3829

Investigation, Development, and Application of Optimal Output Feedback Theory

Volume II—Development of an Optimal Limited State Feedback Outer-Loop Digital Flight Control System for 3-D Terminal Area Operation

John R. Broussard and Nesim Halyo

CONTRACT NAS1-15759
AUGUST 1984

NASA

NASA Contractor Report 3829

Investigation, Development, and Application of Optimal Output Feedback Theory

Volume II—Development of an Optimal Limited State Feedback Outer-Loop Digital Flight Control System for 3-D Terminal Area Operation

John R. Broussard and Nesim Halyo
Information & Control Systems, Incorporated
Hampton, Virginia

Prepared for
Langley Research Center
under Contract NAS1-15759

National Aeronautics
and Space Administration

**Scientific and Technical
Information Branch**

1984

FOREWORD

The investigation described in this report was performed by Information & Control Systems, Incorporated (ICS) under Contract Number NAS1-15759 for the National Aeronautics and Space Administration, Langley Research Center, Hampton, Virginia. This work was sponsored by the Applied Controls Branch of the Flight Control Systems Division. Mr. Richard M. Hueschen served as Technical Representative monitoring this contract. Use of trade names or names of manufacturers in this report does not constitute an official endorsement of such products or manufacturers, either expressed or implied, by the National Aeronautics and Space Administration.

ABSTRACT

This report contains the development of a digital outer-loop three dimensional radio navigation (3-D RNAV) flight control system for a small commercial jet transport. The outer-loop control system is designed using optimal stochastic limited state feedback techniques. Options investigated using the optimal limited state feedback approach include integrated versus hierarchical control loop designs, 20 samples per second versus 5 samples per second outer-loop operation and alternative Type 1 integration command errors. Command generator tracking techniques used in the digital control design enable the jet transport to automatically track arbitrary curved flight paths generated by waypoints. The performance of the design is demonstrated using detailed nonlinear aircraft simulations in the terminal area, frequency domain multi-input sigma plots, frequency domain single-input Bode plots and closed-loop poles. The response of the system to a severe wind shear during a landing approach is also presented.

TABLE OF CONTENTS

TABLE OF CONTENTS (CONTINUED)

LIST OF TABLES

LIST OF FIGURES

LIST OF FIGURES (CONCLUDED)

I. INTRODUCTION

To meet the higher volume aviation requirements projected for the 1980 - 1990 period, NASA is conducting research and development under the Advanced Transport Operating Systems (ATOPS) Program at the Langley Research Center. The major effects of higher volume will be felt in terminal area operations. The goals of the ATOPS program include increased efficiency in the utilization of an airport's terminal area airspace, optimization of aircraft and airport operations, and safe take-off and landing in most types of weather conditions.

An important step in the achievement of these goals is the development of technology and system design procedures which provide the ability to fly specified curved paths with high accuracy during the radio naviation (RNAV) and Microwave Landing System (MLS) phases of the flight. In an effort to achieve the ATOPS goals, Ref. 1, has developed an advanced digital flight control system synthesis procedure using the concept of optimal stochastic limited state feedback. This report is the application of the synthesis procedure in Ref. 1, to the design of an outer-loop digital flight control system for the ATOPS research aircraft. The digital control system is designed to process guidance information from external sources and aircraft aerodynamic and kinetic information from onboard aircraft sensors in order to command control effectors so that the aircraft flies arbitrary curved paths. The three-dimensional curved paths are generated by waypoints supplied by the pilot or a flight schedule. The commerical jet follows the path and a specified calibrated airspeed profile without regard to positional timing errors along the path. The advanced autopilot described in this report is viewed as a three-dimensional radio navigation (3-D RNAV) outer-loop digital flight control system. The airspeed proflie could be selected so as to achieve some 4-D objectives, however, without much difficulty.

The block diagram in Fig. 1b is a simplified depiction of the way the control system in this report should be implemented. The digital control system is composed of an inner-loop operating at 20 samples per second and an outer-loop control system operating at either 20 sps or 5 sps. The inner-loop control system feeds back accelerometer and rate gyro signals in order to stabilize the aircraft's "fast" dynamics such as the short period, Dutch roll and roll modes, (Ref. 2). The inner-loop system used here was previously designed using classical control design techniques, and is taken as is in this study. The outer-loop control system processes information about the aircraft's slower responding dynamics, such as vehicle attitude and geographical position, to perform a variety of functions. Examples of outer-loop control functions include flight path angle select, pitch attitude control wheel steering, altitude select, horizontal path tracking, heading select and the 3-D curved path tracking autopilot designed in this report. The inner-loop, outer-loop terminology used in Fig. 1 is often employed in what is historically referred to as "classical" control structure synthesis methodology.

NASA has previously researched and flight tested a three-dimensional area naviation (3-D RNAV) path tracking control system described in Ref. 3. The control design discussed in Ref. 3 is arrived at primarily using the

classical control synthesis methodology previously mentioned. The classical control system has a structured Laplace transform (s-domain) block diagram configuration. Control modules such as gain elements, wash-out filters, low-pass filters, complementary filters, integrators and signal limiting operations are used throughout the block diagrams. The control loops operate in a decentralized manner (no roll angle feedback to rudder except during decrab, no pitch attitude feedback to throttle, etc., ...). The inner-loop and outer-loop control designs discussed in Ref. 3 are implemented digitally using the Tustin transform.

The control design presented in this report uses the modern control approach. The outer-loop control design is synthesized directly in the discrete-time domain by minimizing a quadratic performance index defined by a weighted sum of mean-square steady state responses and controls. The inner-loop control system used with the outer-loop design consists of the primary feedback paths of the inner-loop design discussed in Ref. 3.

The inner-loop control system discussed in Ref. 3 has a simple block diagram structure and is straightforward to implement. The inner-loop control system has been extensively analyzed and successfully flight tested. Some inner-loop control elements are eliminated when the inner-loop control system is modeled and combined with the aircraft model in order to perform the outer-loop control system design in this report. The integrity and stability characteristics of the reduced inner-loop control system are retained, however. Imposing a predefined control structure that is not to be altered in the modern control approach, is a problem that is both practical to solve and is a better representation of control design philosophy practiced in industry.

The modern control state-space methodology is often synonymous with the full state feedback Linear Quadratic Gaussian (LQG) approach to control design. A quadratic performance index is minimized to yield feedback paths from all states to all controls. Unmeasured or unavailable states are estimated using a full order Kalman filter that should vary with flight condition. The use of the full state feedback LQG method for the outer-loop design would cause the inner-loop control design to be altered. The meaning of inner-loop/outer-loop would be vague if the full state feedback LQG approach were to be used for the 3-D RNAV control problem.

In order to design the outer-loop control system, a departure is made from the full state feedback LQG approach. The quadratic cost function is minimized using a control system restricted to use limited state feedback. Reference 1, presents the theoretical development of the optimal stochastic limited state feedback approach. Reference 1 also formulates and proves the convergence of a new numerical algorithm which determines an optimal limited state feedback gain. Sufficient conditions for the existance of the gain are also presented. The advantages of using optimal limited state feedback in the outer-loop control system are as follows:

- Only chosen states are used for feedback purposes. The inner-loop control system remains unaltered as desired.

- Estimates of all states are not required. A time-varying Kalman filter with its associated complexity and real-time implementation requirements is not used.

- Low-order filters such as analog prefilters and digital complementary filters can be included in the aircraft design model and their effect on control performance is accommodated when the control gains are computed.

- Actuator dynamics and gust dynamics can be included in the aircraft design model, their effect on control performance is taken into account when the quadratic cost is minimized, but their states are not fed back and hence do not have to be measured or estimated.

- There is no separation of stochastic performance and closed-loop performance for optimal limited state feedback even though all noise sources are assumed to be white Gaussian noise. Increasing the measurement noise on some feedback variables causes the corresponding feedback gains to be reduced when the quadratic cost function is minimized.

- There is an increased flexibility in choosing a control structure when using optimal output feedback. Each control loop can be designed individually in a hierarchical approach using different measurements for each loop closure. LON1, an outer-loop longitudinal control system which is discussed later, is designed using the hierarchical approach.

- The control law can also be designed in an integrated manner, i.e., the various controls work in cooperation to achieve the desired maneuvers. All other outer-loop control systems designed in this report are formulated using the integrated approach.

- The new numerical algorithm discussed in Ref. 1 can be applied to relatively large order plant models without difficulty. The largest plant model used in this report has 18 states.

- The proportional-integral-filter (PIF) control structure can be used in the outer-loop design.

The PIF structure in incremental form has been successfully flight tested as discussed in Refs. 4 and 5. DIALS in Ref. 6 was successfully flight tested using a PIF-like structure in position form. The PIF structure accommodates computation delay, has good high-frequency roll-off characteristics, uses integral control and allows command generator tracking theory, Refs. 7 and 8, to be used. The theoretical derivation of the optimal output feedback PIF control system used in this report has not appeared elsewhere.

The outer-loop control system discussed in this report may be flight tested using the ATOPS B-737 aircraft, a small commerical jet transport. Control of the aircraft is provided by commands to the elevator, ailerons, rudder, throttle, spoilers, stabilators and flaps. Based on experience gained during the flight tests of autopilots discussed in Ref. 4, more than one outer-loop control system design is presented for both the longitudinal and lateral dynamics. The primary difference between the designs are the gain elements and the way the command errors are constructed. The control structure remains the same. Multiple designs increase the probability of success and allow for inflight comparisons between gain sets as an indication of the direction of improved pilot acceptance.

A. ORGANIZATION OF THE REPORT

The state-space control system design model is discussed in Chapter II. Linear continuous-time models are presented for individual subsystems. The subsystem models are combined into a large order design model representation. The procedure for representing the design model in discrete-time is summarized. The inner-loop control system operates at 20 samples per second (sps). Outer-loop designs are performed for 20 sps and 5 sps. In the later case, the digital control system is implemented multirate, although only single-rate synthesis techniques are used in this report.

Chapter III begins with a short summary of the optimal output feedback problem and the solution presented in Ref. 1. The outer-loop PIF control system causes the aircraft to follow a curved path in the terminal area. Chapter III discusses how this is accomplished. A waypoint path construction procedure, derived and investigated in Ref. 9, generates a smooth path using specified waypoints and a spherical earth assumption. A command model is constructed, as in Ref. 4, which can generate the important attributes of the path, i.e., height profile, roll profile and airspeed profile. The command model follows the path; the outer-loop control system forces the aircraft to follow the command model.

The control designs and time-domain evaluation are presented in Chapter IV. The gains are designed at eight flight conditions. The gains are scheduled using calibrated airspeed (CAS) as the independent variable. The scheduled gain designs are simulated and evaluated using a full nonlinear six-degree of freedom (6-DOF) simulation.

A frequency domain evaluation of the outer-loop PIF control system designs are presented in Chapter V. Sigma plots, Ref. 10, and Bode plots are graphically portrayed and discussed. Chapter VI shows the performance of the control system, inner-loop and outer-loop, along a curved descending trajectory in the terminal area. Chapter VII summarizes the report and suggest areas where further developments could improve optimal digital implementable control systems. The product of the control design effort is software subroutines that can be programmed onboard the flight computer. Appendices A and B present the FORTRAN control subroutines used in the nonlinear simulation.

II. PLANT MODEL

The application of the linear optimal stochastic output feedback control synthesis procedure to outer-loop control design requires mathematical models for the aircraft, wind disturbances, actuator dynamics, outer-loop filters and inner-loop control system dynamics. This chapter provides a summary of the models and the state variable definitions. Further documentation of the actuator dynamics and inner-loop dynamics are provided in Refs. 11 and 12.

A. AIRCRAFT OPEN-LOOP DYNAMICS

The nonlinear equations of motion of the aircraft are determined by constructing kinematic relationships between aircraft translation and angular position states and by applying Newton's Second Law to the dynamics of the vehicle. A body-fixed axis system is used in this report. The origin is located at the body center of mass, and is fixed in orientation with respect to the vehicle. The body x-axis extends forward out the vehicle's nose, the y-axis extends out the right wind, and the z-axis extends out the bottom of the vehicle.

The aircraft dynamics fall into the general state equation

$$\dot{\underline{x}} = \underline{f}(\underline{x}, \underline{u}) \tag{1}$$

by noting that aerodynamic forces and moments are functions of aircraft states, $\underline{x}$, controls, $\underline{u}$, and to some extent the state history. A linear time-invariant model representation is required to perform the control design. The model is determined by modeling small changes in aircraft motion due to small changes in control position.

The linearization procedure is performed by the construction of a Taylor series expansion representing the nonlinear equations about some nominal trajectory:

$$\dot{\underline{x}} = \dot{\underline{x}}_0 + \Delta\dot{\underline{x}} + \text{Higher Order Terms} \tag{2}$$

$$= \underline{f}(\underline{x}_0, \underline{u}_0) + \left.\frac{\partial \underline{f}}{\partial \underline{x}}\right|_{\substack{\underline{x}=\underline{x}_0 \\ \underline{u}=\underline{u}_0}} \Delta\underline{x} + \left.\frac{\partial \underline{f}}{\partial \underline{u}}\right|_{\substack{\underline{x}=\underline{x}_0 \\ \underline{u}=\underline{u}_0}} \Delta\underline{u} + \text{Higher Order Terms} \tag{3}$$

Here, the subscript "0" indicates the nominal value and the prefix "Δ" denotes a small perturbation. All except first-order terms are then neglected by arguing that the higher-order terms are small compared to linear terms. The results of this procedure are separated into a nonlinear equation describing the nominal trajectory and a linear equation defining ther perturbation motion dynamics,

$$\dot{\underline{x}}_0 = f(\underline{x}_0, \underline{u}_0) \tag{4}$$

$$\Delta\dot{\underline{x}} = A\Delta\underline{x} + B\Delta\underline{u} \tag{5}$$

The linear model is further separated by noting that the lateral-directional dynamics and the longitudinal dynamics tend to decouple for straight and level flight. The states in $\Delta\underline{x}$ for the lateral-directional dynamics are ordered Δv, Δr, Δp, $\Delta\phi$, $\Delta\zeta$ and Δc. The states are, respectively, y-axis velocity, yaw rate, roll rate, roll angle, track angle error and cross track error. The states in $\Delta\underline{x}$ for the longitudinal dynamics are ordered Δu, Δw, Δq, $\Delta\theta$, Δz and are, respectively, x-axis velocity, z-axis velocity, pitch rate, pitch angle and z-axis position. The control system is to operate as a three dimensional path tracking system (i.e., Δc, ΔCAS and Δh are to be regulated to zero) hence, longitudinal horizontal path error, Δx, is not included in the model and is not regulated to zero by the control system. The state, Δh, is the vertical height from the earth's surface to the aircraft's cg. For small pitch angles, Δz and Δh are essentially equal in magnitude.

Eight linear aircraft models are used to design the control system. The aircraft is trimmed for straight and level flight at 1524 m (5,000 ft) and 8,500 lb. The eight different CAS values used are 62 m/s (120 kt), 69 m/s (135 kt), 77 m/s (150 kt), 85 m/s (165 kt), 93 m/s (180 kt), 124 m/s (240 kt), 139 m/s (270 kt), 154 m/s (300 kt). Flaps are positioned as a function of CAS for each flight condition as shown in Appendix B.

B. GUST MODEL

The predominate random disturbance affecting the aircraft dynamics is wind gusts. The wind gusts can be modeled using the well-known Dryden spectrum. The modeling effort consists of using spectral factorization methods to obtain a dynamical system which generates a random process having the specified power spectral density when driven by a white noise process. The gusts affect the body-axis aircraft velocites. Rotational gusts around the aircraft are ignored. The transfer functions for the gust dynamics are as follows:

$$u_g = \sigma_u \left[\frac{L_u}{V_{TAS}}\right]^{\frac{1}{2}} \frac{\sqrt{2}}{\left(1 + \frac{L_u}{V_{TAS}} s\right)} \tag{6}$$

$$v_g = \sigma_v \left[\frac{L_v}{V_{TAS}}\right]^{\frac{1}{2}} \frac{1 + \sqrt{3}\ \frac{L_v}{V_{TAS}}\, s}{\left(1 + \frac{L_v}{V_{TAS}}\, s\right)^2} \tag{7}$$

$$w_g = \sigma_w \left[\frac{L_v}{V_{TAS}}\right]^{\frac{1}{2}} \frac{1 + \sqrt{3}\ \frac{L_w}{V_{TAS}}\, s}{\left(1 + \frac{L_w}{V_{TAS}}\, s\right)^2} \tag{8}$$

In the gust models, V_{TAS} is the true airspeed, L_u, L_v, and L_w are the scales of turbulence, and σ_u, σ_v, and σ_w are the variance of the gust. The scales and gust variances are shown in Table 1.

A state-space realization of Eqs. 6 to 8 is

$$\begin{bmatrix} \Delta u_g \\ \Delta v_g \\ \Delta w_g \end{bmatrix} = H_w \underline{\Delta w}_g \tag{9}$$

$$\dot{\underline{w}} = A_w \underline{\Delta w}_g + B_w \underline{\Delta w} \tag{10}$$

Where

$$\underline{\Delta w}^T = [\Delta\eta_u \quad \Delta\eta_v \quad \Delta\eta_w] \tag{11}$$

$\underline{\Delta w}$ is a vector of independent Gaussian white noise process with unit variance. Combining Eq. 10 and Eq. 5 yields the aircraft model

$$\Delta\dot{\underline{x}} = A\Delta\underline{x} + B\Delta\underline{u} + E\Delta\underline{w} \tag{12}$$

As new states are added to the design model representation, the vector $\Delta\underline{x}$ and matrices A, B and E are increased appropriately in dimension. It should be, clear however, that A in Eq. 5, Eq. 12 and Eq. 32 are of course, not equal.

C. ACTUATOR DYNAMICS

Block diagrams for each actuator and a short description of the block diagrams are presented in Ref. 11. Only the linear perturbation dynamics are presented in this section.

In the aileron actuator system, a lead/lag filter processes the aileron position command to provide phase advance. The output of the lead/lag filter drives the aileron hydraulic value. The rate limited valve position drives the cable system that rotates the aileron surface. Cable stretch caused by increased dynamic pressure is modeled as a gain reduction of the value commanded to the aileron surface. Cable hysteresis (~0.2 deg aileron) is modeled in the nonlinear simulation. If the aileron command from the valve exceeds ~2.5 deg, then spoilers are also deflected.

Raising left or right spoilers reduces the lift on the left or right wing resulting in a lift differential and rolling moment which serves to boost the roll power. Decreasing the lift on a wing affects the longitudinal dynamics. If spoilers are deflected beyond ~3.5 deg, then a spoiler feedback loop is closed to produce a gain which decreases the original aileron command. The gain which reduces the aileron command is also a function of flap position.

The spoiler feedback and the lead/lag filter are used to eliminate a limit cycle problem that occurs when roll attitude is regulated through the aileron actuator system for the outer-loop control system discussed in Ref. 3. The spoiler feedback and lead/lag filter is also used in the outer-loop control design in this report.

A linear model of the aileron/spoiler system is as follows:

$$\begin{bmatrix} \Delta\dot{\delta}_a \\ \Delta\dot{\delta}_s \end{bmatrix} = \begin{bmatrix} -12.38 & -1.021k_1(\delta_F)k_2(\delta_{SPR}) \\ 202.6 & -20.0 \end{bmatrix} \begin{bmatrix} \Delta\delta_a \\ \Delta\delta_s \end{bmatrix} + \begin{bmatrix} 1.021 + 0.510k_1(\delta_F) \\ 0.0 \end{bmatrix} \Delta\delta_{AC} \tag{13}$$

$$\begin{bmatrix} \Delta\delta_A \\ \Delta\delta_{SPL} \\ \Delta\delta_{SPR} \end{bmatrix} = \begin{bmatrix} \frac{11.0}{1.0+0.0015\bar{q}} & 0 \\ 0 & 0 \\ 0 & 1.0 \end{bmatrix} \begin{bmatrix} \Delta\delta_a \\ \Delta\delta_s \end{bmatrix} \tag{14}$$

The model ignores hysteresis, rate limits, position limits, and residualizes and eliminates the lead/lag filter pole. The function $k_1(\delta_F)$ represents the effect of nominal flap position. The function $k_2(\delta_{SPR})$ represents the gain of the spoiler feedback loop as a function of spoiler position and $\bar{q}$ is dynamic pressure. Only the right spoiler is used for design purposes but it is assumed to have positive and negative values.

The rudder dynamics are straight forward and are modeled simply as

$$\Delta\dot{\delta}_r = -32.68\ \Delta\delta_r + 2.438\ \Delta\delta_{RC} \tag{15}$$

$$\Delta\delta_R = 13.4\ \Delta\delta_r \tag{16}$$

The model ignores rate limits and position limits.

Throttle position commands engine thrust. Throttle position, which is limited to 0 - 60 deg, commands EPR (engine pressure ratio). The EPR command is subjected to upper and lower rate limits that vary as a function of EPR and the direction EPR is moving in. A table of look up functions is used to compute engine thrust from the value of EPR, i.e., $\delta_T = f(EPR)$. The model for throttle becomes,

$$\Delta\dot{EPR} = -\frac{1}{\zeta}\Delta EPR + \frac{a}{\zeta}\Delta\delta_{TC} \tag{17}$$

$$\Delta\delta_T = b\Delta EPR \tag{18}$$

The value of a is the steady state relationship between throttle position and the EPR command for the nominal flight conditions. The value for ζ is chosen so that the resulting throttle control system design behaves well in nonlinear simulations. The ζ value was varied from 0.2 to 2.0 seconds, with the later value becoming the one used in the outer-loop design model. The parameter, b, is the perturbation linear relationship between EPR and δ_T.

The linear model for elevator is straightforward and given by,

$$\Delta\dot{\delta}_e = -23.23\ \Delta\delta_e + 2.0779\ \Delta\delta_{EC} \tag{19}$$

$$\Delta\delta_E = \frac{10.76}{1.0 + 0.0023\ \bar{q}}\ \Delta\delta_e \tag{20}$$

The model includes the effect of cable stretch. The position of elevator drives the stabilator. If elevator moves above a certain computed value and remains there for a length of time, (1.2 sec), the stabilator moves in a direction which causes elevator trim to return to a neutral position. Stabilator moves at a constant rate of ± 0.03 deg/sec or ± 0.18 deg/sec depending on the flap position. Stabilator serves as a trimming device and a linear model is not necessary for analysis and design. Flaps are similarly used for trimming purposes at low speeds (see Appendix B) and a linear model is not necessary for analysis and design.

D. INNER-LOOP CONTROL SYSTEM

The inner-loop control system block diagrams, reported in a preliminary version in Ref. 12, are shown in Figs. 2 to 5. After an analysis of the

inner-loop designs and their interaction with modern control outer-loop structures, a number of deletions were made to arrive at a desirable inner-loop system.

All of the control loops in the autothrottle block diagram shown in Fig. 4 were eliminated. The V_{TAS} and V_{GS} feedback loop at lower left in Fig. 4 is a wind shear detection system used to advance or retard throttle in wind shears. The EPR protection system in the upper part of the figure is used to keep EPR below the maximum value MXEPR - 0.10. The haversin washout roll function in the upper left part of the figure is used to advance throttle during turn initiation.

The output feedback outer-loop counter part to the EPR protection system is the upper limit placed on the throttle command as a function of EPR as shown in Appendix B. The response of the output feedback outer-loop control system to wind shear is shown in Section IV F. The simulations indicate that the integrated approach to autothrottle design, whereby all feedback loops (such as height error, pitch attitude error, height integral error, etc.) are feedback to throttle, causes autothrottle to react appropriately during severe atmospheric conditions. The roll crossfeed to throttle in Fig. 4 is not used and airspeed loss in a turn is not particularly noticeable.

All inner-loop elements for the elevator control system in Fig. 5 are retained except for the integrator feedback through the k_{24} gain. The outer-loop control system uses integral feedback directly on the outer-loop tracking errors. Washed-out pitch rate and vertical acceleration feedback in the inner-loop damp the short period mode. Roll squared feedback improves vertical height tracking in turns. The outer-loop control system uses individual gain scheduling as a function of CAS as well as retaining the inner-loop gain schedule shown in Fig. 5.

Roll rate feedback and the gain schedule shown in Fig. 2 are also retained in the aileron/spoiler inner-loop control system. Roll rate feedback damps the roll mode response of the aircraft. The roll angle tracking loop in Fig. 2 is deleted from the inner-loop control system. Roll angle tracking error is used directly in the outer-loop integral feedback expression. The yaw damper inner-loop control system for rudder is shown in Fig. 3. The washed-out yaw rate signal has authority to ± 4 deg and serves to damp the Dutch roll mode. The yaw damper is retained in the inner-loop control system.

Linear continuous-time models for the inner-loop control systems can be directly inferred from the block diagrams as follows:

Throttle:

$$\Delta\delta_{TC} = \Delta u_t \tag{21}$$

Elevator:

$$\Delta\delta_{EC} = K_{CAS}\ [k_{27}\quad k_{25}{*}k_{22}] \begin{bmatrix} \Delta\hat{q} \\ \Delta\hat{a}_h \end{bmatrix} + K_{CAS}\ [k_{27}\quad 0.0] \begin{bmatrix} \Delta q + \Delta\nu_q \\ \Delta a_h + \Delta\nu_{a_h} \end{bmatrix} \tag{22}$$

$$+ K_{CAS}\ \Delta u_e$$

$$\begin{bmatrix} \dot{\hat{\Delta q}}_{WO} \\ \dot{\hat{\Delta a}}_h \end{bmatrix} = \begin{bmatrix} -1.0/k_{28} & 0.0 \\ 0.0 & -1.0/k_{20} \end{bmatrix} \begin{bmatrix} \Delta\hat{q}_{WO} \\ \Delta\hat{a}_h \end{bmatrix} \tag{23}$$

$$+ \begin{bmatrix} -1.0/k_{28} & 0.0 \\ 0.0 & -1.0/k_{20} \end{bmatrix} \begin{bmatrix} \Delta q + \Delta\nu_q \\ \Delta a_h + \Delta\nu_{a_h} \end{bmatrix}$$

Aileron/Spoiler:

$$\Delta\delta_{AC} = [-k_v{*}k_{33}]\ \Delta\hat{p} + k_v\ \Delta u_a \tag{24}$$

$$\dot{\Delta\hat{p}} = [-1.0/k_{32}]\ \Delta\hat{p} + [1.0/k_{32}]\ [\Delta p + \Delta\nu_p] \tag{25}$$

Rudder:

$$\Delta\delta_{RC} = [1.0\quad 1.0] \begin{bmatrix} \Delta r_{WO} \\ \Delta\hat{r} \end{bmatrix} + [\Delta u_r] \tag{26}$$

$$\begin{bmatrix} \Delta\dot{r}_{WO} \\ \dot{\Delta\hat{r}} \end{bmatrix} = \begin{bmatrix} -1.0/k_{42} & -1.0/k_{42} \\ 0.0 & -1.0/k_{41} \end{bmatrix} \begin{bmatrix} \Delta r_{WO} \\ \Delta\hat{r} \end{bmatrix} + \begin{bmatrix} 0 \\ KYD{*}k_{40}/k_{41} \end{bmatrix} (\Delta r + \Delta\nu_r) \tag{27}$$

Combining the inner-loop control system subsystems yields

$$\Delta\dot{\underline{x}}_{IL} = A_{IL}\,\Delta\underline{x}_{IL} + B_{IL}\,\Delta y_{MEAS} \tag{28}$$

The inner-loop discrete-time representation used in Appendix B is determined using Eqs. 39, 40 and 41 in conjunction with Eq. 28.

E. OUTER-LOOP COMPLEMENTARY FILTERS

Outer-loop filters are used to suppress sensor measurement noise and can be included in the control system design model using the limited state feedback approach. Flight tests results in Ref. 4 indicate that the vertical height complementary filter has a significant effect on closed-loop stability of the longitudinal control system. The complementary filter combines a vertical height position measurement with onboard body-axis accelerometer measurements to provide a smooth estimate of vertical position and vertical velocity. A discussion of the filter structure and design is given in Refs. 4 and 5. The discrete-time version of the third-order complementary filter used in the longitudinal outer-loop control system is

Update:

$$\begin{bmatrix} \hat{h}(+) \\ \dot{\hat{h}}(+) \\ \hat{b}(+) \end{bmatrix}_k = \begin{bmatrix} \hat{h}(-) \\ \dot{\hat{h}}(-) \\ \hat{b}(-) \end{bmatrix}_k + \begin{bmatrix} 0.004 \\ 0.016 \\ -0.000475 \end{bmatrix}_k \left[h_{MEAS} - \hat{h}(-)_k \right] \tag{29}$$

Propagate:

$$\begin{bmatrix} \hat{h}(-) \\ \dot{\hat{h}}(-) \\ \hat{b}(-) \end{bmatrix}_{k+1} = \begin{bmatrix} 1 & \Delta t & 0 \\ 0 & 1 & 0 \\ 0 & 0 & 1 \end{bmatrix} \begin{bmatrix} h(+) \\ \dot{\hat{h}}(+) \\ \hat{b}(+) \end{bmatrix}_k + \begin{bmatrix} \Delta t/2 \\ \Delta t \\ 0 \end{bmatrix} \left[a_{h,k} - \hat{b}_k(+) \right] \tag{30}$$

The digital filter operates at 20 iterations per second. The state, b, is an estimate of accelerometer bias. The local-level accelerometer measurement is corrected for gravity to obtain a_h.

Similiar filters are used to compute the horizontal x and y position of the aircraft. Flight tests in Ref. 6 indicate that including the complementary filter for y in the lateral dynamic model is not necessary. The position complementary filter is not included in the lateral model for the outer-loop control design.

The accelerometer bias estimator dynamics have little effect on the outer-loop control system. The bias state is neglected when the digital filter is expressed in analog form for inclusion in the outer-loop continuous-time design model. The analog form is

$$\begin{bmatrix} \dot{\hat{h}} \\ \ddot{\hat{h}} \end{bmatrix} = \begin{bmatrix} -0.8 & 1.0 \\ -.32 & 0.0 \end{bmatrix} \begin{bmatrix} \hat{h} \\ \dot{\hat{h}} \end{bmatrix} + \begin{bmatrix} 0.8 \\ 0.32 \end{bmatrix} h_m + \begin{bmatrix} 0.0 \\ 1.0 \end{bmatrix} a_h \tag{31}$$

F. DISCRETE REPRESENTATION

Combining the linear models for the aircraft, actuators, gusts, outer-loop filters and inner-loop control system yields the outer-loop control system design model,

$$\Delta\dot{\underline{x}} = A\Delta\underline{x} + B\Delta\underline{u} + E\Delta\underline{w} \tag{32}$$

The states in the longitudinal and lateral-directional design models are

Longitudinal:

$$\Delta\underline{x}^T = [\Delta u\ \Delta w\ \Delta\theta\ \Delta q\ \Delta z\ \Delta\delta_e\ \Delta EPR\ \Delta\hat{q}_{WO}\ \Delta\hat{a}_h\ \Delta\hat{h}\ \Delta\dot{\hat{h}}\ u_g\ w_{g1}\ w_{g2}] \tag{33}$$

$$\Delta\underline{u}^T = [\Delta u_e\ \Delta u_t] \tag{34}$$

$$\Delta\underline{w}^T = [\Delta\nu_q\ \Delta\nu_{a_h}\ \Delta\eta_u\ \Delta\eta_w] \tag{35}$$

Lateral-Directional:

$$\Delta\underline{x}^T = [\Delta v\ \Delta p\ \Delta r\ \Delta\phi\ \Delta\zeta\ \Delta c\ \Delta\delta_a\ \Delta\delta_s\ \Delta\delta_r\ \Delta\hat{p}\ \Delta r_{WO}\ \Delta\hat{r}\ v_{g1}\ v_{g2}] \tag{36}$$

$$\Delta\underline{u}^T = [\Delta u_a\ \Delta u_r] \tag{37}$$

$$\Delta\underline{w}^T = [\Delta\nu_p\ \Delta\nu_r\ \Delta\eta_v] \tag{38}$$

The method used to represent the plant for direct digital design of the outer-loop control system is to assume the control, $\Delta\underline{u}$, is constant over the sampling interval, Δt; resulting in the plant representation;

$$\Delta\underline{x}_{k+1} = \Phi\Delta\underline{x}_k + \Gamma\Delta\underline{u}_k + \Gamma_w\Delta\underline{w}_k \tag{39}$$

The matrices in Eq. 39 are obtained from

$$\Phi = e^{A\Delta t} \tag{40}$$

$$\Gamma = \int_0^{\Delta t} e^{As}ds\ B \tag{41}$$

$$\Gamma_w\Delta\underline{w}_k = \int_0^{\Delta t} e^{As}E\underline{w}(s)ds \tag{42}$$

It is not necessary to know Γ_w and $\Delta\underline{w}_k$ in Eq. 39. Only the mean and covariance of the Gaussian white noise vector, $\Gamma_w\Delta\underline{w}_k$, are required for design.

Equation 39 is an exact discrete representation of the plant if the inner-loop control system and outer-loop filter are implemented as analog networks. The inner-loop control system and outer-loop filter are implemented digitally, hence, Eq. 39 is not an exact representation of the plant dynamics. If the outer-loop control system is designed at a slow rate (5 sps is used in Chapter V) and the inner-loop control system and outer-loop filter were modeled correctly, the control synthesis model would become multirate. Techniques for handling optimal, multirate, multivariable control synthesis have been determined in Ref. 13, but are outside the scope of this work. The single-rate plant model representation in Eq. 39 proved to be adequate for outer-loop control synthesis for either 20 sps or 5 sps outer-loop operation.

In Ref. 12, step response comparisons are made between Eq. 39, a linear time-invariant model, and a nonlinear simulation of the commerical jet transport dynamics with the correct discrete implementation of the inner-loop control systems. A summary of the comparisons follows:

Elevator: Good match in both actuator and inner-loop dynamics.

Rudder : Good match in both actuator and inner-loop dynamics.

Aileron/
Spoiler : Adequate match which deteriorates as the control input step size increases. Highly nonlinear behavior of the aileron/spoiler actuators and vehicle aerodynamics is the likely cause of the problem.

Throttle: Poor match due to the highly nonlinear behavior of the engine dynamics.

III. DIGITAL FLIGHT CONTROL SYSTEM

This chapter presents a brief derivation of the linear part of the digital flight control system. The derivation is accomplished by formulating a tracking problem embedded in a limited state feedback, sampled-data regulator problem; then converting the limited state feedback/feedforward optimal solution to a final implementable structure. A full state feedback derivation of the outer-loop control structure used in this report is presented in Ref. 4. The modifications needed for limited state feedback are shown in the following sections.

A. OUTER-LOOP TRACKING

The tracking problem is formulated in Chapter I as a model following problem. The control law must cause the output of the linear aircraft model

$$\Delta \underline{y}_k = H\Delta \underline{x}_k + D\Delta \underline{u}_k \tag{43}$$

to optimally track the output of a linearized command model

$$\Delta \underline{x}_{m,k+1} = \Phi_m \, \Delta \underline{x}_{m,k} + \Gamma_m \Delta \underline{u}_{m,k+1} \tag{44}$$

$$\Delta \underline{y}_{m,k} = H_m \, \Delta \underline{x}_{m,k} + D_m \Delta \underline{u}_{m,k+1} \tag{45}$$

at the equally spaced sample times t_k. The number of commands in Eq. 45 is assumed to be equal to the number of aircraft controls used for tracking purposes.

The command model input, $\Delta \underline{u}_m$, is assumed to be constant previous to $t_k=0$, changes at $t_k=0$, then remains constant thereafter. The $\Delta \underline{u}_m$ assumption results in excellent control system performance in implementation when $\Delta \underline{u}_m$ is allowed to vary slowly or intermittently. Each change in $\Delta \underline{u}_m$ is viewed as a new initial condition.

When $\Delta \underline{y}_k$ equals $\Delta \underline{y}_{m,k}$, the plant states and controls follow a trajectory, $\Delta \underline{x}^*_k$ and $\Delta \underline{u}^*_k$ which satisfy the equation, (Refs. 7, 4 and 8).

$$\begin{bmatrix} \Delta \underline{x}^*_k \\ \Delta \underline{u}^*_k \end{bmatrix} = \begin{bmatrix} A_{11} & A_{12} \\ A_{21} & A_{22} \end{bmatrix} \begin{bmatrix} \Delta \underline{x}_{m,k} \\ \Delta \underline{u}_m \end{bmatrix} \tag{46}$$

The feedforward matrices, A_{ij}, satisfy the solvable matrix algebraic equation

$$\begin{bmatrix} (\Phi-I) & \Gamma \\ H & D \end{bmatrix} \begin{bmatrix} A_{11} & A_{12} \\ A_{21} & A_{22} \end{bmatrix} = \begin{bmatrix} A_{11}(\Phi_m-I) & A_{11}\Gamma_m \\ H_m & D_m \end{bmatrix} . \tag{47}$$

The algebraic equation has a solution when the plant has no transmission zeroes at one and no plant transmission zero equals a command model eigenvalue. The trajectory in Eq. 46 is not actually generated when the control law is implemented, but is useful in constructing the quadratic cost function and the u_m feedforward gain in the next section.

B. PROPORTIONAL-INTEGRAL-FILTER CONTROL LAW

The control law is synthesized using the mathematical model of perturbation aircraft motion shown in Eq. 32. The perturbation state vector of the linear time-invariant model is further augmented to contain the perturbation control and is driven by the control rate. The control position and the control rate are both weighted in the linear quadratic cost function.

Control rate weighting affects the discrete plant representation so that the discrete control system is synthesized to use one-step delayed sensor state information. The result is that a one sample period computation delay is accommodated by the control law. Integral states are also augmented to the state vector to operate on the error between the aircraft states, $\Delta\underline{y}$, and the command generator output $\Delta\underline{y}_m$. The integral states cause Δy to track a constant $\Delta\underline{y}_m$ in steady state if: 1) the control system is stable, 2) the integrator gain is invertible, and 3) the discrete plant has no transmission zeroes at 1.0 (i.e., the plant quad partition matrix in Eq. 47 is invertible).

Assuming that the control, $\Delta\underline{u}$, the control difference, $\Delta\underline{v}$, and the Euler implemented integrator states, $\Delta\underline{\xi}$, are constant over a sampling interval, Δt, the discrete plant representation becomes:

$$\begin{bmatrix} \Delta\underline{x} \\ \Delta\underline{u} \\ \Delta\underline{\xi} \end{bmatrix}_{k+1} = \overbrace{\begin{bmatrix} \Phi & \Gamma & 0 \\ 0 & I & 0 \\ \Delta tH & \Delta tD & I \end{bmatrix}}^{\overline{\Phi}} \begin{bmatrix} \Delta\underline{x} \\ \Delta\underline{u} \\ \Delta\underline{\xi} \end{bmatrix}_k + \overbrace{\begin{bmatrix} 0 \\ \Delta tI \\ 0 \end{bmatrix}}^{\overline{\Gamma}} \Delta\underline{v}_k + \overbrace{\begin{bmatrix} \Gamma_w \\ 0 \\ 0 \end{bmatrix}}^{\overline{\Gamma}_w} \Delta\underline{w}_k \tag{48}$$

Φ is the state transition matrix and Γ is the control effect matrix. The matrices H and D determine the aircraft output that is integrated to produce the control law's Type 1 property.

The tracking objective of the control law is introduced into the design by defining the variables

$$\Delta\tilde{\underline{x}}_k = \Delta\underline{x}_k - \Delta\underline{x}^*_k \quad ; \quad \Delta\tilde{\underline{u}} = \Delta\underline{u}_k - \Delta\underline{u}^*_k \tag{49}$$

$$\Delta\tilde{\underline{v}}_k = \Delta\underline{v}_k - A_{21}\,(\Delta\underline{x}_{m,k+1} - \Delta\underline{x}_{m,k})/\Delta t \tag{50}$$

$$\Delta\tilde{\underline{\xi}}_k = \Delta\underline{\xi}_k - \Delta\underline{\xi}^*_k \quad ; \quad \Delta\bar{\underline{x}}^T_k = \left[\Delta\tilde{\underline{x}}^T_k \quad \Delta\tilde{\underline{u}}^T_k \quad \Delta\tilde{\underline{\xi}}^T_k\right] \tag{51a,b}$$

and the discrete cost function

$$J = \lim_{N\to\infty} \frac{1}{N} E\left\{ \sum_{k=-1}^{N} \Delta\bar{\underline{x}}^T_k \hat{Q}\, \Delta\bar{\underline{x}}_k + 2\, \Delta\bar{\underline{x}}^T_k \hat{M}\, \Delta\tilde{\underline{v}}_k + \Delta\tilde{\underline{v}}^T_k \hat{R}\, \Delta\tilde{\underline{v}}_k \right\} \tag{52}$$

The cost function weighting matrices are determined by first specifying a continuous cost function for the continues plant model augmented with $\Delta\underline{u}$ and $\Delta\underline{\xi}$; then converting to the equivalent discrete form which accounts for vehicle behavior between iterations.

The states that are available for feedback are represented as

$$\begin{bmatrix} \Delta\tilde{\underline{y}}_{MEAS} \\ \Delta\tilde{\underline{u}} \\ \Delta\tilde{\underline{\xi}} \end{bmatrix}_k = \overbrace{\begin{bmatrix} C & 0 & 0 \\ 0 & I & 0 \\ 0 & 0 & I \end{bmatrix}}^{\bar{C}} \begin{bmatrix} \Delta\tilde{\underline{x}} \\ \Delta\tilde{\underline{u}} \\ \Delta\tilde{\underline{\xi}} \end{bmatrix}_k + \overbrace{\begin{bmatrix} \Delta\underline{v}_k \\ 0 \\ 0 \end{bmatrix}}^{\Delta\bar{\underline{v}}_k} \tag{53}$$

The states observed from the aircraft model are corrupted by white Gaussian measurement noise $\Delta\underline{v}_k$ with covariance, V. The control internal states $\Delta\underline{u}$ and $\Delta\underline{\xi}$ are noise free. The class of control laws considered are restricted to be of the form

$$\Delta\tilde{v}_k = -[\overbrace{K_y \; K_u \; K_\xi}^{K}] \begin{bmatrix} \Delta\tilde{y}_{MEAS} \\ \Delta\tilde{u} \\ \Delta\tilde{\xi} \end{bmatrix}_k \tag{54}$$

The necessary conditions for the feedback gain in Eq. 54 to be optimal are in the next section. The derivation from Eq. 54, to the implementable control equations is the same as in Ref. 4, except for the computation of $\Delta\xi^*_k$. The star trajectory for $\Delta\xi^*_k$ is derived in Eqs. 74 to 77. Using $\Delta\xi^*_k$ as defined in Eq. 76, the implementable equations for the control law are

$$u_k = u_{k-1} + \Delta t \; v_{k-1} + A_{21}(x_{m,k} - x_{m,k-1}) \tag{55}$$

$$e_{k-1} = y_{MEAS,k-1} - C \; A_{11} \; x_{m,k-1} \tag{56}$$

$$v_{k-1} = (I - \Delta t \; K_u) \; v_{k-2} - K_y(e_{k-1} - e_{k-2}) - \Delta t \; K_\xi(y_{k-2} - y_{m,k-2})$$
$$+ (\overbrace{K_\xi \; A + K_y \; C \; A_{12} + K_u \; A_{22}}^{K_{um}})(u_{m,k} - u_{m,k-1}) \tag{57}$$

The perturbation variables and trim variables have been eliminated in the above control law expression in incremental form, using a large number of substitutions and cancellations.

The gain, K_{um}, which feeds forward the command generator forcing function increment, is a linear combination of feedback, feedforward and Liapunov solution matrices. The effect of K_{um} is to improve the transient response of the outer-loop control system by changing closed-loop system zeroes without affecting closed-loop poles. The A_{21} feedforward gain in Eq. 55 is zero for the curved path command generator models used in this report. K_y is the limited state feedback gain which primarily stabilizes the outer-loop aircraft dynamics. $K\xi$ is the integrator gain and $I-\Delta tK_u$ is the control filter gain.

C. OPTIMAL OUTPUT FEEDBACK

For the plant dynamics shown in Eq. 48, the feedback gain constraint shown in Eq. 54 and the following conditions:

$$E\{\Delta w_k\} = 0 \qquad E\{\bar{\Gamma}_w \; \Delta w_k \; \Delta w_j^T \; \bar{\Gamma}_w^T\} = W\delta_{kj} \tag{58 a,b}$$

$$E\{\Delta\bar{v}_k\} = 0 \qquad E\{\Delta\bar{v}_k \; \Delta\bar{v}_j\} = V\delta_{kj} \tag{59 a,b}$$

$$E\left\{\Delta\bar{x}_{-1}\ \Delta\bar{x}_{-1}^T\right\} = X_o \tag{60}$$

$$E\left\{\Delta w_k\ \Delta\bar{v}_j^T\right\} = E\left\{\Delta w_k\ \Delta\bar{x}_{-1}^T\right\} = E\left\{\Delta\bar{v}_k\ \Delta\bar{x}_{-1}^T\right\} = 0 \tag{61}$$

the cost function in Eq. 52 can be modified as follows, (Ref. 1),

$$J(\bar{K}) = \frac{1}{2}\ (J_t + J_s) \tag{62}$$

$$J_t = \sum_{k=0}^{\infty} \Delta\bar{x}_{tk}^T\ \hat{Q}\ \Delta x_{tk} + 2\ \Delta\bar{x}_{tk}^T\ \hat{M}\ \Delta\tilde{v}_{tk} + \Delta\tilde{v}_{tk}^T\ \hat{R}\ \Delta\tilde{v}_{tk} \tag{63}$$

$$J_s = \lim_{N\to\infty} \frac{1}{N+1}\ E\left\{\sum_{k=0}^{N} \Delta\bar{x}_{sk}^T\ \hat{Q}\ \Delta\bar{x}_{sk} + 2\ \Delta\bar{x}_{sk}^T\ \hat{M}\ \Delta\tilde{v}_{sk} + \Delta\tilde{v}_{sk}^T\ \hat{R}\ \Delta\tilde{v}_{sk}\right\} \tag{64}$$

$$J(\bar{K}) = \frac{1}{2}\ tr\left\{P(W + X_o)\right\} + \frac{1}{2}\ tr\left\{\bar{K}^T(\bar{\Gamma}^T\ P\bar{\Gamma} + \hat{R})\ \bar{K}\ V\right\} \tag{65}$$

The notation tr denotes the trace of a matrix. J_t is the transient cost with noise sources set to zero while J_s is the average stochastic cost. The trade-off between J_t and J_s is accomplished by varying X_o with respect to W. The effect of X_o is like adding pseudo process noise to the plant to improve control system robustness. The benefits of using Eq. 62 as the cost function are discussed further in Ref. 1 and Ref. 14.

The matrix, P, in Eq. 65, satisfies the Riccati-like equation

$$P = \bar{\Phi}_{CL}^T\ P\ \bar{\Phi}_{CL} + \bar{C}^T\ \bar{K}^T\ \hat{R}\ \bar{K}\ \bar{C} + \hat{Q} - \hat{M}\ \bar{K}\ \bar{C} - \bar{C}^T\ \bar{K}^T\ \hat{M}^T \tag{66}$$

$\bar{\Phi}_{CL}$ is the stable closed-loop plant matrix,

$$\bar{\Phi}_{CL} = \bar{\Phi} - \bar{\Gamma}\ \bar{K}\ \bar{C} \tag{67}$$

The necessary conditions for $J(\bar{K})$ to have a minimum, are derived in Ref. 1. The necessary conditions are:

- The gain $\bar{K}$ must satisfy

$$\left[\bar{\Gamma}^T P \bar{\Gamma} + \hat{R}\right] \bar{K} \left[\bar{C} S \bar{C}^T + V\right] = \left[\bar{\Gamma}^T P \Phi + \hat{M}^T\right] S\bar{C}^T \tag{68}$$

where

$$S = \bar{\Phi}_{CL} S \Phi_{CL}^T + (W + X_o) + \bar{\Gamma} \bar{K} V \bar{K}^T \bar{\Gamma}^T \tag{69}$$

A gain which satisfies the necessary condition is not necessarily unique.

Sufficient conditions for the existence of a gain $\bar{K}$ which minimizes $J(K)$, with $\hat{M}$ the zero matrix, are derived in Ref. 1. The existence conditions are:

- There must exist a gain $\bar{K}$ so that $\bar{\Phi}_{CL}$ is stable.
- $(\bar{\Gamma}^T \hat{Q} \bar{\Gamma} + \hat{R}) > 0$, $(\bar{C}(W + X_o)\bar{C}^T + V) > 0$ (70 a,b)
- $\hat{Q} \geq \varepsilon \bar{C}^T \bar{C}$ for some scalar $\varepsilon > 0$ (71)
- $W \geq \varepsilon \bar{\Gamma} \bar{\Gamma}^T$ for some scalar $\varepsilon > 0$ (72)

The existence conditions can be violated and an optimal gain may still exist.

In Ref. 4, $\Delta\underline{\xi}_k^*$ in Eq. 51a, is determined by minimizing the performance index after the full state feedback optimal gains are determined, i.e.,

$$\text{Min } J(\Delta\underline{\bar{x}}_{-1})\Big|_{\forall\Delta\xi^*} = \text{Min } \Delta\underline{\bar{x}}_{-1} P_f \Delta\underline{\bar{x}}_{-1}\Big|_{\forall\Delta\xi^*} \tag{73}$$

P_f is the full state feedback Riccati equation solution. The minimum cost for output feedback is expressed differently from Eq. 73 as shown in Eq. 65. If a feedback gain is suboptimal with respect to full state feedback, the suboptimal cost, $J_s(\Delta\underline{\bar{x}}_{-1})$ is given by,

$$J_s(\Delta\underline{\bar{x}}_{-1}) = \Delta\underline{\bar{x}}_{-1}^T \bar{P} \Delta\underline{\bar{x}}_{-1} \geq J(\Delta\underline{\bar{x}}_{-1}) \tag{74}$$

where $\bar{P}$ is the unique, symmetric, and positive definite solution of the Lyapunov equation

$$\bar{P} = \bar{\Phi}_{CL}^{T}\ \bar{P}\ \bar{\Phi}_{CL} + \bar{C}^{T}\ \bar{K}^{T}\ \hat{R}\ \bar{K}\ \bar{C} + \hat{Q} - \hat{M}\ \bar{K}\ \bar{C} - \bar{C}^{T}\ \bar{K}^{T}\ \hat{M}^{T} \tag{75}$$

Note that $\bar{P}$ and P in Eq. 66 are equal. The value for $\Delta\underline{\xi}^{*}$ can be determined exactly as in Ref. 4, using P. The $\Delta\underline{\xi}^{*}$ equation derived in Ref. 4 is given by

$$\Delta\underline{\xi}_{k}^{*} = \begin{bmatrix} 0 & A \end{bmatrix} \begin{bmatrix} \underline{x}_{m,k} \\ \underline{u}_{m,k+1} \end{bmatrix} \tag{76}$$

where

$$A = -P_{\xi\xi}^{-1} \left[P_{x\xi}^{T}\ A_{12} + P_{u\xi}^{T}\ A_{22} \right] \tag{77}$$

The partitions $P_{\xi\xi}$, $P_{x\xi}$, $P_{u\xi}$ of P in Eq. 77 match the partitions of $\Delta\underline{\bar{x}}$ in Eq. 51b.

D. WAYPOINT PATH CONSTRUCTION SUMMARY

The procedure for constructing a desired path consisting of great circles connected by arcs of circles, fixed on the surface of a rotating spherical earth, and rotating with the earth, is presented in Ref. 9. In this section, the input data needed to construct the path and the output data the path generates are summarized.

If N is the number of waypoints (N must be at least three), then at each waypoint the following is supplied,

$$\lambda(I) = \text{longitude in degrees} \tag{78}$$

$$\delta(I) = \text{latitude in degrees} \tag{79}$$

$$h(I) = \text{altitude in meters} \tag{80}$$

$$CAS(I) = \text{airspeed in meters/sec} \tag{81}$$

$$I = 1, N$$

At each interior waypoint, the following is needed

$$R_{T}(I) = \text{radius of the turn (meters)} \tag{82}$$

$$I = 1, N-2$$

Quoting from Ref. 9, "The path is constructed by sequentially connecting each pair of waypoints by a great circle arc on the surface of the earth. At each interior waypoint, a circle is constructed by the intersection of a circular cone from the center of the earth to the surface of the earth. The radius of the circular conical base is taken to be the input turn radius at that interior waypoint. The center of the cone is chosen so that the circle is tangent to both the incoming great circle and the outgoing great circle".

The initial and final waypoints as well as each interior middle-of-the-turn waypoints are assigned a desired altitude and airspeed from Eqs. 80 and 81. The gradient in altitude and airspeed over each segment is determined by dividing the difference in altitude or airspeed by the ground track distance. Altitude and airspeed commands are smooth ramps between desired values.

After the path is constructed and the aircraft is flying the path, the following RNAV guidance parameters are generated,

Cross track error - Δc
Track angle error - $\Delta\zeta$
Distance to go to the end of the leg - - - - - - - - - - - - - - R_L
Time to go to the end of the leg - - - - - - - - - - - - - - - - T_L
Desired altitude and altitude rate - - - - - - - - - - - - - - - $h_c, \dot{h}_c$
Desired airspeed - CAS_c
Desired flight path angle - γ_c
Desired bank angle in the turn - - - - - - - - - - - - - - - - - ϕ_c

The bank angle command is switched to the value it should have in the turn as soon as the time to go to the great circle is less than the bank command divided by the maximum bank rate, $\dot{\phi}_{MAX}$. At the end of the turn, the bank command is returned to zero when the time to go is less than the time to return the bank angle to zero at the maximum bank rate. Anticipatory bank angle commands decrease the cross track error.

The information in the waypoint commands shown above is used to develop the command models and the command errors in the next section. In the lateral dynamics, only command errors are available, Δc and $\Delta\zeta$, while in the longitudinal dynamics, absolute command values are available, h_c and CAS_c.

E. LONGITUDINAL COMMAND MODEL CONTROL SYSTEM

The outer-loop control system uses a command model which is regulated by a non-linear command model control system. When the outer-loop control system is engaged, the internal states in the command model are initialized to the aircraft states. After initialization, the control law follows state trajectories generated by the command model. The command model control system is designed simultaneously with the feedback/feedforward gains in Eq. 57 to provide good ride quality and command limiting.

The longitudinal command model uses a double integration of vertical acceleration to generate the vertical path trajectory. The CAS trajectory is one integration of forward acceleration,

$$\begin{bmatrix} h_m \\ \dot{h}_m \\ CAS_m \end{bmatrix}_k = \begin{bmatrix} 1.0 & \Delta t & 0 \\ 0 & 1.0 & 0 \\ 0 & 0 & 1.0 \end{bmatrix} \begin{bmatrix} h_m \\ \dot{h}_m \\ CAS_m \end{bmatrix}_{k-1} + \begin{bmatrix} \Delta t^2/2 & 0 \\ \Delta t & 0 \\ 0 & \Delta t \end{bmatrix} \begin{bmatrix} \ddot{h}_m \\ \dot{CAS}_m \end{bmatrix}_{k-1} \tag{83}$$

The command model controls are computed using

$$\begin{bmatrix} \ddot{h}_m \\ \dot{CAS}_m \end{bmatrix}_k = \begin{bmatrix} k_h & k_{\dot{h}} & 0 \\ 0 & 0 & k_{CAS} \end{bmatrix} \begin{bmatrix} (h_c - h_m) \\ (\dot{h}_c - \dot{h}_m) \\ (CAS_c - CAS_m) \end{bmatrix}_k \tag{84}$$

The variables with the c subscript are the commands from the waypoint path generator. The command model controls are magnitude limited to acceptable values $|\ddot{h}_m| \leq \ddot{h}_{MAX}$, $|\dot{CAS}_m| \leq \dot{CAS}MAX$. Flight tests of a similiar vertical command model in Ref. 4 provided values shown in Table 2 for k_h, $k_{\dot{h}}$ and the acceleration magnitude limits that pilots favor. All of the equations for the command model control system are shown in Appendix B.

The outer-loop control system detects if the command model is initialized away from the desired path and internally chooses a vertical velocity command, $\dot{h}_c$=2.53 m/s (8.3 fps), to return to the path. The linear model version of Eq. 83 is used in Eq. 44. The linear model controls are assumed to be $\ddot{h}_m$ and CAS_m as discussed in Ref. 4.

The construction of the command error, $\underline{y}-\underline{y}_m$, fundamentally affects the control system feedback robustness properties as well as the closed-loop plant transient response to commands and disturbances. A generic longitudinal command error of the form

$$\underline{y}-\underline{y}_m = \begin{bmatrix} k_1(\hat{h}_k - h_{m,k}) + k_2(\dot{\hat{h}}_k - \dot{h}_{m,k}) + k_3(CAS_k^2 - CAS_{m,k}^2) \\ CAS_k - CAS_{m,k} \end{bmatrix} \tag{85}$$

was investigated. If k_1=1.0, k_2=0.0, and k_3=1.0/2g, for example, the longitudinal control system causes h to track h_m and CAS to track CAS_m, but energy error and CAS error are the quantities regulated in the control system during transients. A number of combinations of k_1, k_2, and k_3 were investigated. Three designs were completed and are candidates for flight testing:

LON1: $k_1 = 1.0,\ k_2 = 0.1,\ k_3 = 0.0$

LON2: $k_1 = 1.0,\ k_2 = 10.0,\ k_3 = 0.0$

LON3: $k_1 = 1.0,\ k_2 = 20.0,\ k_3 = 0.1$

The results in Chapters IV, V and VI make comparisons between the different longitudinal command error designs.

F. LATERAL COMMAND MODEL CONTROL SYSTEM

The lateral command model operates differently from the longitudinal command model because of the different commands generated by the path guidance system in Section III D. The command model is used to smoothly capture the horizontal path when the system is engaged. After capture, the command model states are essentially zero and the command model calculations are deactivated. The command model uses the dynamical relationship between lateral position and velocity heading and the relationship between heading and roll angle for a coordinated turn, Ref. 15,

$$\Delta c_{m,k+1} = \Delta c_{m,k} + \Delta t\ V_{GS,k}\ \sin\Delta\zeta_{m,k} \tag{86}$$

$$\Delta\zeta_{m,k+1} = \Delta\zeta_{m,k} + \Delta t\ \frac{g}{V_{GS,k}}\ \tan\phi_{m,k} \tag{87}$$

$$\phi_{m,k+1} = \phi_{m,k} + \Delta t\ \dot{\phi}_{m,k} \tag{88}$$

The model control is $\dot{\phi}_m$. The linear model used in Eq. 44 is a linearized version of Eqs. 86 and 87 for straight-and-level flight. The linear model control is ϕ_m. The variable g is gravity. The variable V_{GS} is ground speed.

The control system for the nonlinear command model is

$$\dot{\phi}_{m,k} = -k_c\ \Delta c_{m,k} - (k_\zeta\ \frac{V_{GS}}{150})\Delta\zeta_{m,k} \tag{89}$$

The gain feeding back $\Delta\zeta_m$ varies as a function of ground speed in an attempt to keep the command model closed-loop system eigenvalues invariant with respect to changing V_{GS}. The roll rate is limited to a maximum value,

$$|\dot{\phi}_{m,k}| \leq \dot{\phi}_{MAX} \tag{90}$$

If the aircraft is close to the desired path, i. e., $|\Delta c| \leq 900m$ or $|\Delta\zeta| \leq 30$ deg, the control system uses a maximum bank angle, ϕ_{MAX1}, to turn. If the aircraft is far from the desired path, a new bank angle maximum is calculated to ensure that the capture can be performed without over-shooting the path,

$$\phi_{MAX2} = \left| \tan^{-1}\left(\frac{-V_{GS}^2 \ (COS\Delta\zeta_o - 1)}{(\Delta c_o - SIGN(\Delta c_o)600)g} \right) \right| \tag{91}$$

Equation 91 is determined by integrated Eqs. 86 to 88 for the constant bank angle that results in $\Delta c=0$ from some initial condition $\Delta\zeta_o$ and $\Delta\dot{\zeta}_o$. For safety reasons, ϕ_{MAX2} cannot exceed an absolute maximum bank angle ϕ_{MAX3}. The values for ϕ_{MAX1} and ϕ_{MAX3} are shown in Table 2. If the intercept angle $\Delta\zeta_o$ exceeds 30 deg, the command model control system is activated only when the roll rate command causes the bank angle to roll away from the horizontal path, i. e., $\dot{\phi}_{m,k}\ \Delta\zeta \leq 0.0$; a capture feature pilots favor.

The command model shown in Eqs. 86 to 88 was flight tested and the results are reported in Ref. 4. Three different command errors were flight tested

LOC1

$$\underline{y}_k - \underline{y}_{m,k} = \begin{bmatrix} \phi_k \\ \underline{\Delta\hat{c}}_k \end{bmatrix} - \begin{bmatrix} \phi_{m,k} \\ \underline{\Delta c}_{m,k} \end{bmatrix} \tag{92}$$

LOC2

$$\underline{y}_k - \underline{y}_{m,k} = \begin{bmatrix} \phi_k \\ \delta_{r,k} \end{bmatrix} - \begin{bmatrix} 1.0 & 0.0 \\ a_k & 1.0 \end{bmatrix} \begin{bmatrix} k_4(\Delta\zeta_k - \Delta\zeta_{m,k} - k_5(\Delta\hat{c}_k - \Delta c_{m,k})) \\ \delta_{mr,k} \end{bmatrix} \tag{93}$$

LOC3

$$\underline{y}_k - \underline{y}_{m,k} = \begin{bmatrix} \phi_k \\ \delta_{r,k} \end{bmatrix} - \begin{bmatrix} 1.0 & 0.0 \\ a_k & 1.0 \end{bmatrix} \begin{bmatrix} k_6(\Delta\hat{c}_k - \Delta c_{m,k}) \\ \delta_{mr,k} \end{bmatrix} \tag{94}$$

Yaw angle, Ψ, was used in Ref. 4, instead of $\Delta\zeta$ but the conclusions and operations are essentially the same because sideslip is usually zero and the angle of attack is small.

In LOC1, the objective of the aileron and rudder is to null roll angle and cross track errors. The control system will track a straight horizontal path wings level. LOC2 uses the philosophy of a three tiered nested approach commonly used in commerical autopilots. A wings leveler, which causes the error $\phi_k - \phi_{m,k}$ to be zero, can be upgraded to a track angle hold autopilot by replacing the roll command with a track angle error command, $\phi_k - k_4(\Delta\zeta_k - \Delta\zeta_{m,k})$. The track hold autopilot can be upgraded to a cross track autopilot by replacing $\Delta\zeta_{m,k}$ with cross track error as shown in Eq. 93.

The parameter a_k is a roll command to rudder command crossfeed gain and is used to change rudder trim position in a turn so that the steady-state sideslip angle is zero. If a_k is zero, then commanding steady state rudder position to a trim value, δ_{mr}, as shown in Eq. 93 operates much like a yaw damper. The rudder is used to stabilize the aircraft, and damp Dutch roll in the transients; but is forced back to δ_{mr} in steady state. LOC2 is similiar in philosophy to a localizer autopilot discussed in Ref. 2. In LOC3, only the cross track error is used to command the bank angle. The δ_{mr} command in Eq. 93 and Eq. 94 can be either programmed in software or the measure value of rudder at control system engage can be used.

The flight tests in Ref. 4 clearly showed, that from a capture and track viewpoint, LOC3 is the better all around design. LOC3 is used for the outer-loop lateral control system in this report but with the following modification

$$\underline{y}_k - \underline{y}_{m,k} = \begin{bmatrix} \phi_k \\ \delta_{r,k} \end{bmatrix} - \begin{bmatrix} 1.0 & 0.0 \\ a_k & 1.0 \end{bmatrix} \begin{bmatrix} \phi_{c,k} + \phi_{m,k} + k_7(\Delta\hat{c}_k - \Delta c_{m,k}) \\ \delta_{rm,k} \end{bmatrix} \tag{95}$$

The known value for the roll command from the waypoint guidance system is included in the command error equation. Two different lateral control designs were investigated and are candidates for flight testing.

LAT1: $k_7 = 0.5$

LAT2: $k_7 = 1.0$

IV. CONTROL DESIGN AND NONLINEAR SIMULATIONS

This chapter presents the control system design parameters and some of the closed-loop simulation evaluations. There are three different designs for the longitudinal dynamics: LON1, LON2 and LON3 as discussed in Chapter III. LON1 and LON2 are designed using 5 and 20 samples per second. LON3 is designed using 5 sps for a total of five longitudinal control system options. There are two different designs for the lateral dynamics: LAT1 and LAT2. LAT1 is designed using 5 and 20 samples per second and LAT2 is designed using 5 sps for a total of three lateral control system options.

LON1 is a hierarchical design. First the elevator control loop is designed using the height error integrator. The elevator loop is closed, then the throttle loop is designed using the CAS error integrator. The height error integrator is not fed back to throttle and the CAS error integrator is not fed back to elevator. Elevator has a higher bandwidth than throttle and the control system can be considered to have vertical path error priority over airspeed error. During maneuvers, the throttle sometimes saturates and the control system must stabilize the vehicle using only elevator. The hierarchical approach guarantees that the control system is stable when throttle saturates.

LON2 is an integrated design. Throttle and elevator are designed simultaneously using the multivariable plant model. Both Type 1 integrators have feedback paths to both control effectors. When throttle saturates, there is no guarantee that the remaining elevator control loop is stable. Numerical tests for stability are necessary using closed-loop eigenvalues. The single elevator control loop achieves closed-loop stability throughout the aircraft's design flight conditions. The LON2 control system has neither path error or airspeed error dominating control priority.

LON3 is also an integrated design. As shown in Chapter III, airspeed error appears in both integrators. The control system is considered to have airspeed error priority over path error priority. Chapter V indicates that LON3 has slightly better stability margins than LON2 and LON1. This chapter shows that LON3 also has better simulation performance.

LAT1 and LAT2 are integrated designs. A hierarchical design for the lateral dynamics proved to be a poor approach. The hierarchical approach had difficulty in determining control gains which yielded a coordinated turn in simulation. LAT2 is included primarily to have at least two control options for comparison purposes. Chapter V indicates that LAT1 has better stability margins than LAT2. This chapter shows LAT1 also has better simulation performance.

The 20 iterations per second nonlinear simulation of the aircraft includes 6 degree of freedom motion for the aircraft, nonlinear actuator dynamics, sensor models, wind shear models and random noise generators. The nonlinear simulation uses aerodynamic forces generated using the stability derivatives of the ATOPS B-737 aircraft. When the outer-loop control system operates at 5 sps, the control effector command can be released at any 1/20 sec interval within the 1/5 sec sampling interval. (NMUCATI and NMUCOTI in Appendix B are subroutine inputs that control the command release time period). Releasing the control effector command early within the 1/5 sec control cycle does not seem to improve control performance significantly and is not further discussed. The control command is released as designed, at the end of the control sampling interval for all the simulations in this report.

A. OUTPUT FEEDBACK AND DESIGN VALUES

In this section, the states in the plant model and the output vector used for feedback are presented for each longitudinal design:

LON1: FIRST LOOP-ELEVATOR

$$\Delta \underline{x}^T = [\Delta u\ \Delta w\ \Delta q\ \Delta\theta\ \Delta z\ \Delta\delta_e\ \Delta\hat{a}_h\ \Delta\hat{q}_{WO}\ \Delta u_e\ \Delta\xi_{h1}\ \Delta\hat{h}\ \Delta\dot{\hat{h}}\ u_g\ w_{g1}\ w_{g2}]$$

$$\Delta u = \Delta v_e$$

$$\Delta \underline{y}^T = [\Delta\theta\ \Delta\hat{h}\ \Delta\dot{\hat{h}}\ \Delta\hat{a}_h\ \Delta u_e\ \Delta\xi_{h1}]$$

SECOND LOOP-THROTTLE

$$\Delta \underline{x}^T = [\Delta u\ \Delta w\ \Delta q\ \Delta\theta\ \Delta z\ \Delta\delta_e\ \Delta EPR\ \Delta\hat{a}_h\ \Delta\hat{q}_{WO}\ \Delta u_e\ \Delta u_t\ \Delta\xi_{h1}\ \Delta\xi_{CAS}\ \ \Delta\hat{h}\ \Delta\dot{\hat{h}}\ u_g\ w_{g1}\ w_{g2}]$$

$$\Delta u = \Delta v_t$$

$$\Delta \underline{y}^T = [\Delta CAS\ \Delta\theta\ \Delta u_t\ \Delta\xi_{CAS}]$$

The integrator states, ξ_{h1} and ξ_{CAS}, using Eq. 85 can be expressed in continuous time as,

$$\xi_{h1} = \int \left\{ (\hat{h} - h_m) + 0.1\ (\dot{\hat{h}} - \dot{h}_m) \right\} dt \qquad (96)$$

$$\xi_{CAS} = \int (CAS - CAS_m)\, dt \tag{97}$$

The observations used for feedback in the elevator loop are pitch attitude, the complementary filter outputs, filtered vertical acceleration, control command position and the height integrator. The feedback paths in the throttle loop are CAS, pitch attitude, control command position and the CAS integrator. From a control design viewpoint, pitch attitude provides the throttle control system with lead information concerning the movement of elevator and aircraft height.

LON2: ELEVATOR AND THROTTLE

$$\Delta\underline{x}^T = [\Delta u\ \Delta w\ \Delta q\ \Delta\theta\ \Delta z\ \Delta\delta_e\ \Delta EPR\ \Delta\hat{a}_h\ \Delta\hat{q}_{WO}\ \Delta u_e\ \Delta u_t\ \Delta\xi_{h2}\ \Delta\xi_{CAS}\ \Delta\hat{h}\ \Delta\dot{\hat{h}}\ \Delta u_g\ \Delta w_{g1}\ \Delta w_{g2}]$$

$$\Delta\underline{u}^T = [\Delta v_e\ \ \Delta v_t]$$

$$\Delta\underline{y}^T = [\Delta CAS\ \Delta\theta\ \Delta\hat{h}\ \Delta\dot{\hat{h}}\ \Delta\hat{a}_h\ \Delta u_e\ \Delta u_t\ \Delta\xi_{h2}\ \Delta\xi_{CAS}]$$

$$\xi_{h2} = \int \{(\hat{h} - h_m) + 10.0(\dot{\hat{h}} - \dot{h}_m)\}\, dt$$

LON3: ELEVATOR AND THROTTLE

$$\Delta\underline{x}^T = [\Delta u\ \Delta w\ \Delta q\ \Delta\theta\ \Delta z\ \Delta\delta_e\ \Delta EPR\ \Delta\hat{a}_h\ \Delta\hat{q}_{WO}\ \Delta u_e\ \Delta u_t\ \Delta\xi_{h3}\ \Delta\xi_{CAS}\ \Delta\hat{h}\ \Delta\dot{\hat{h}}\ \Delta u_g\ \Delta w_{g1}\ \Delta w_{g2}]$$

$$\Delta\underline{u}^T = [\Delta v_e\ \ \Delta v_t]$$

$$\Delta\underline{y}^T = [\Delta CAS\ \Delta\theta\ \Delta\hat{h}\ \Delta\dot{\hat{h}}\ \Delta\hat{a}_h\ \Delta u_e\ \Delta u_t\ \Delta\xi_{h3}\ \Delta\xi_{CAS}]$$

$$\xi_{h3} = \int \{(\hat{h} - h_m) + 20.0(\dot{\hat{h}} - \dot{h}_m) + 0.1(CAS^2 - CAS_m^2)\}\, dt$$

The different integrators in LON2 and LON3 are determined as in LON1 using Eq. 85. The observations used for feedback in LON2 and LON3 are the combination of the LON1 observation vectors. Throttle and elevator have access to the same sensor information feedback paths in LON2 and LON3.

The design of the control system is achieved by choosing the elements in the matrices Q, R, X_o, W and V iteratively until the control system has desired closed-loop properties. The elements in W, the process noise covariance matrix, and V, the measurement noise covariance matrix, are predetermined from the values shown in Table 1 and Table 3. All internal control

states, such as an integrator state, have zero measurement noise. Iterative adjustments are made to Q, R, and X_o until one set of numbers could be used for all three longitudinal control designs at all eight design flight conditions.

The design parameters for the longitudinal control systems are shown in Table 4. The large initial condition values for X_o dominate over the process noise covariance matrix W, when the two matrices are added in Eq. 69. The large initial condition values for the control states are useful in increasing frequency domain stability margins as discussed in Refs. 14 and 10.

The states in the plant model and the output vector for each lateral design are presented next.

LAT1: AILERON AND RUDDER

$$\Delta\underline{x}^T = [\Delta v\ \Delta p\ \Delta r\ \Delta\phi\ \Delta\zeta\ \Delta c\ \Delta\delta_a\ \Delta\delta_r\ \Delta\hat{p}\ \Delta r_{WO}\ \Delta\hat{r}\ \Delta u_a\ \Delta u_r\ \Delta\xi_{c1}\ \Delta\xi_{r1}\ \Delta v_{g1}\ \Delta v_{g2}]$$

$$\Delta\underline{u}^T = [\Delta v_a\ \ \Delta v_r]$$

$$\Delta\underline{y}^T = [\Delta\phi\ \Delta\zeta\ \Delta c\ \Delta u_a\ \Delta u_r\ \Delta\xi_{c1}\ \Delta\xi_{r1}]$$

$$\xi_{c1} = \int \{\phi - \phi_c - \phi_m - 0.5(\Delta c - \Delta c_m)\ \ dt$$

$$\xi_{r1} = \int \{\delta_r - \delta_{rm} - a(\phi_c + \phi_m + 0.5(\Delta c - \Delta c_m))\}\ dt$$

LAT2: AILERON AND RUDDER

$$\Delta\underline{x}^T = [\Delta v\ \Delta p\ \Delta r\ \Delta\phi\ \Delta\zeta\ \Delta c\ \Delta\delta_a\ \Delta\delta_r\ \Delta\hat{p}\ \Delta r_{WO}\ \Delta\hat{r}\ \Delta u_a\ \Delta u_r\ \Delta\xi_{c2}\ \Delta\xi_{r2}\ \Delta v_{g1}\ \Delta v_{g2}]$$

$$\Delta\underline{u}^T = [\Delta v_a\ \ \Delta v_r]$$

$$\Delta\underline{y}^T = [\Delta\phi\ \Delta\zeta\ \Delta c\ \Delta u_a\ \Delta u_r\ \Delta\xi_{c2}\ \Delta\xi_{r2}]$$

$$\xi_{c2} = \int \{\phi - \phi_c - \phi_m - (\Delta c - \Delta c_m)\}\ dt$$

$$\xi_{r2} = \int \{\delta_r - \delta_{rm} - a(\phi_c + \phi_m + \Delta c - \Delta c_m)\}\ dt$$

The observations used for feedback in the lateral control loops are roll attitude, track angle error, cross track error, control command position and the integrators.

The design parameters for all the lateral control systems are shown in Table 5. The measurement noise for Δp and Δr are absorbed into the process noise covariance when the inner loops are introduced into the aircraft model. A large weight is placed on Δv in an attempt to make the aircraft bank-to-turn with little sideslip, i.e., a coordinated turn. A large weight is placed on Δv_r to keep the outer-loop command rudder rate small.

B. GAIN SCHEDULING AND CLOSED-LOOP EIGENVALUES

The control laws are adapted to changing airspeed by scheduling their gains as a function of CAS. Figure 6 shows the pitch LON3 optimal gain and scheduled gain as a function of CAS. The abrupt change in the two gains in Fig. 6 at 92.6 m/s (180 kt), a trend evident in most of the other gains, caused the gain schedule for all the gains to be computed in two groups. One group uses the four design flight conditions 61.7 m/s (120 kt), 69.4 m/s (135 kt), 77.2 m/s (150 kt), and 84.9 m/s (165 kt) to find a_1 and a_2 in the scheduling equation

$$GAIN = a_1\ CAS + a_2 \tag{98}$$

The other group uses the four design flight conditions 92.6 m/s (180 kt), 123.5 m/s (240 kt), 138.9 m/s (270 kt) and 154.3 m/s (300 kt) and regression analysis to determine a_3 and a_4 in

$$GAIN = a_3\ CAS + a_4 \tag{99}$$

The coefficients a_1-a_4 for all the control designs are given in Appendix A. The correlation coefficient for more than eighty percent of the gains is above 0.9.

The gains are updated in flight and simulation once every second. An easy-on is used to transition the gains between updates,

$$\hat{GAIN}_k = (1 - e^{-a\Delta t})\ \hat{GAIN}_{k-1} + e^{-at}\ GAIN_k \tag{100}$$

The easy-on operates at the outer-loop sample rate. The parameter a in Eq. 100 is 2.0. The easy-on is particularly useful during the 92.6 m/s (180 kt) gain transition point in CAS shown in Fig. 6.

The stability characteristics of the closed-loop digital flight control system are described by the eigenvalues of the closed-loop linear model system matrix. The closed-loop linear model system matrix, Φ_{CL}, is computed as follows,

$$\Phi_{CL} = \begin{bmatrix} \Phi & \Gamma & 0 \\ 0 & I & 0 \\ \Delta th & \Delta tD & I \end{bmatrix} - \begin{bmatrix} 0 \\ \Delta tI \\ 0 \end{bmatrix} \begin{bmatrix} K_y & K_u & K_\xi \end{bmatrix} \begin{bmatrix} C & 0 & 0 \\ 0 & I & 0 \\ 0 & 0 & I \end{bmatrix} \tag{101}$$

The degree of involvement of each state variables in each mode of motion is identified by the corresponding eigenvectors of Φ_{CL}. For discrete-time systems, root locations within the "unit circle" indicate stability, but these root locations are difficult to interpret. A useful method for evaluating discrete root locations is to map them into an equivalent continuous-time representation using natural logrithms.

Table 6 shows mapped closed-loop eigenvalues for each longitudinal and lateral control design at one flight condition. The mode definition in Table 6 is representative, since the table indicates that some complex modes split and recombine with other modes as the control structure alters. The column marked INNER-LOOP shows the plant eigenvalues before the outer-loop control system is closed. The inner-loop control system stabilizes the fast aircraft modes of motion (short period and Dutch roll) with good damping. The outer-loop control system alters the short-period root locations, but further increases the damping ratio to near critical damping (ζ=0.707). The lateral outer-loop control system tends to destabilize the Dutch roll mode.

The different sampling rates used for the outer-loop designs (20 sps and 5 sps) have a small effect on eigenvalue locations. In most cases, the complex mode damping actually increases when the 5 sps design is compared to the 20 sps design. The LON1 control design has complex eigenvalues (associated with $\Delta\xi_{h1}$) with the poorest damping.

The effect of the gain schedule on closed-loop eigenvalue location is small. There are differences but the scheduled gain closed-loop eigenvalues remain close to their optimal counterparts with reasonable damping. The LON3 control system has the best match between optimal and scheduled closed-loop eigenvalues and is closely followed in eigenvalue match performance by the LAT1 design. The LON1 control system has the poorest match.

A demonstration of the effect of airspeed on closed-loop eigenvalues is shown in Table 7. The real part of the Dutch roll mode remains almost constant while the imaginary part decreases with velocity. Dutch roll damping is increased as the natural frequency decreases with airspeed. The damping of the short period mode, the task of the inner-loop control system, is significantly decreased as velocity increases. The short period damping reaches a value of 0.22 near 154 m/s.

The inner-loop phugoid mode in Table 7 is stable below 84 m/s, then changes abruptly near 92 m/s and becomes unstable as airspeed increases. The gain scheduled outer-loop control systems stabilize the phugoid mode with high damping as the airspeed changes from landing approach values to high speed cruise velocities. In the LAT1 control system, the cross track mode is almost critically damped at low velocities as shown in Table 7. Increasing airspeed causes the cross track mode natural frequency to decrease but the damping remains high (ζ>0.59).

C. ALTITUDE CAPTURE SIMULATION

The command model interface between the waypoint path generator and the outer-loop control system allows the aircraft to be remote from the desired path when the control system is engaged. When the aircraft is engaged above the flight path, the command model establishes a path the aircraft follows using a standard rate of descent, 2.5 m/s (8.3 ft/s), to capture the waypoint path with no overshoot as depicted in Fig. 7.

Nonlinear six degree-of-freedom simulations of the three longitudinal control systems operating at 5 sps for an altitude capture are shown in Fig. 8. The wind, measurement noise and gust disturbances are inactive in the simulation. The captures are smooth with little overshoot. The lower damping of the modes in the LON1 control system, as shown in Table 6, are evident in the LON1 simulation for $\dot{h}$. Maximum CAS deviations during the descent are approximately 2 m/s (~4 kts), for all three designs.

D. CAS CAPTURE SIMULATION

Changing the calibrated airspeed of the aircraft over a wide range is an important test of the gain schedule part of the outer-loop control system. Figure 9 shows each control system changing CAS from an initial value of 77.2 m/s (150 kt) to 129 m/s (250 kt) at an altitude of 305 m (1000 ft). The initial CAS rate of change is limited to 0.76 m/s^2. The CAS command model control system causes the CAS response to have a smooth capture. Flaps change position as a function of airspeed in Fig. 9 and is one source of height error as airspeed increases. The other source of height error in Fig. 9 is the manner in which the different longitudinal outer-loop control systems regulate potential and kinetic energy.

The airspeed increases faster if the aircraft is allowed to descend slightly at the beginning of the maneuver. In other words, potential energy is allowed to decrease initially to obtain a fast increase in kinetic energy. The integrated designs, LON2 and LON3 both exhibit an initial loss in altitude of approximately 25 m (~ 80 ft). The LON1 hierarchical design simulation on the other hand, actually shows an initial increase in height at the beginning of the simulation.

The LON1 hierarchical design keeps total height variation small (10 m < (~ 30 ft <)) as airspeed increases. Airspeed responds slower, however, in the LON1 hierarchical design approach. LON2 and LON3 require approximately 100

sec to complete the CAS change while LON1 requires 160 sec to perform the same velocity maneuver. Smaller height variations with changing airspeed could be made by LON2 and LON3 if the maximum rate of change of the command model CAS command is reduced. The maximum rate of change of CAS is an input variable to the control subroutine in Appendix B and has no effect on closed-loop stability.

An important transfer point in the CAS simulation occurs when CAS crosses 92.6 m/s (180 kt). Some control gains change quickly in this region, but little effect of the change is evident in the simulation.

The only noticeable CAS simulation difference between LON2 and LON3 occurs in throttle. Throttle is smoother and settles faster in LON3 past 78 seconds into the simulation.

E. HORIZONTAL PATH CAPTURE

A horizontal path capture is similiar to a localizer bean centerline capture during a landing approach. Figure 10 shows the horizontal path geometry. The aircraft is heading towards the desired path and the aircraft control system is engaged approximately 5500 m (4 mi) from the path. The nonlinear 6-DOF simulation for the LAT1 control system is shown in Fig. 11. The command generator leaves the aircraft on course after computing the desired maximum bank angle using Eq. 91 which captures the path in one turning sequence. The command generator begins the turn when the command generator control system indicates the aircraft should roll away from the path. The coordinated turn is accomplished with a no overshoot capture.

F. WIND SHEAR SIMULATION

Wind shear has been recognized as a significant factor in commercial transport accidents during takeoff and landing, (Ref. 16). The nonlinear 6-DOF simulation used to evaluate the control designs, contains the wind shear/turbulence package developed by the Standard Research Institude, (SRI) (Ref. 17). The control designs in this report are not specifically designed to counteract wind shear and do not contain wind shear internal models for estimation and disturbance accommodation. The effect of wind shear is an important indication of the control systems performance, however, and simulations are presented in this section for the three longitudinal control designs.

One of the most severe wind shear models in the SRI package is Profile D4, a high severity thunderstorm wind shear. The horizontal wind increases from 0 to a 50 kt head wind initially, then rapidly changes to a 30 kt tail-wind as the aircraft nears the touchdown point during landing. Coincident with the change from a headwind to a tail wind, a vertical downdraft of 10 kt and of short duration, 15 sec, is also simulated as part of the shear profile. Figure 12 shows the atmospheric condition which could generate the Profile D4 wind shear. All three longitudinal control designs fly successfully through the wind shear avoiding both stall and premature ground interception.

The effect of the wind shear for each longitudinal control design is shown in Figs. 13 and 14. The aircraft is simulated progressing down a 3 deg glidelsope with wind gust and sensor measurement errors not activated. The glideslope descent path changes to level flight 9 m (32 ft) above the runway at approximately 125 secs into the simulation. The wind shear and vertical downdraft occur between 110 and 120 seconds into the simulation.

LON3 exhibits the best, i.e., the smallest, path error response in vertical height (± 12 m). LON1, the hierarchical design, has the largest path error (23 m below - 44 m above the glideslope). LON2 operating at 20 sps, has the best CAS response, i.e., CAS stays above 59 m/s (115 kt). LON1 experiences the worst CAS response but still avoids stall.

Throttle response for each control design is shown in Fig. 14. The upper limit on throttle is a function of engine pressure ratio, EPR, and the CAS error in the control integrator $y-y_m$ as shown in Appendix B. If the CAS error is small, then the upper limit on throttle decreases from 60.0 deg (the physical maximum) at EPR = 1.2 to 42.0 deg when EPR = 1.85. The throttle limits are determined using the steady state relationship between EPR and throttle. The objective of the throttle limit is to keep EPR below 1.85 under normal operating conditions. Keeping EPR below 1.85 is also the objective of the inner-loop autothrottle control system shown in Fig. 4. If the CAS error is large (> 4.1 m/s (8 kts)), EPR and throttle for the outer-loop control design in this report are allowed to increase as CAS error increases up to the physical maximums (60 deg for throttle). The lower limit on throttle is increased from 0 at 131 m/s to 10 deg at 101.8 m/s to keep the engines from completely spooling down at low velocities.

In all four wind shear simulations, throttle increases to the 60 deg limit at 20 sec into the simulations and EPR reached a value of ~2.1 as shown in Fig. 14. The control systems recognized the abnormal situation and allowed throttle to reach full authority in order to reduce the command errors. The 42 deg limit for throttle is activated for the LON3 (at 5 sps) and LON2 (at 20 sps) control systems 135 sec into the simulations. The CAS error for these two control designs is kept within tolerance values during the 135 sec - 145 sec time period.

V. FREQUENCY DOMAIN EVALUATION

The linear control systems designed in Chapters III and IV are evaluated in this chapter using frequency domain concepts. Frequency domain evaluation is useful in judging control system performance when the plant is subjected to various types of uncertainties. An excellant discussion of these concepts is given in Ref. 10.

The evaluation in this chapter concentrates on the effect of additive alterations at the input to the plant model. In Fig. 15, the plant loop is broken at point i and the loop transfer function is computed as (with $\Delta G(s)$ zero),

$$\underline{u} = (I + K(s)G(s))^{-1}\, \underline{u}^* \tag{102}$$

In single-input, single-output plants, the performance objective is usually viewed as observing how close $K(s)G(s)$ evaluated at $s=j\omega$ is to -1.0 as the frequency, ω, is varied over a frequency range of interest. The resulting Bode gain/phase plot gives an indication of how close $1 + K(s)G(s)$ is to being zero.

For multi-input, multi-output plants, Ref. 10 argues that one type of performance evaluation for a closed-loop system is to compute how close the return difference matrix, $I + K(s)G(s)$, is to being singular using singular values. The singular values are computed by substituting $j\omega$ for s and varying ω in the return difference matrix, $I + K(j\omega)G(j\omega)$, over a frequency range of interest. A plot of the singular values of the complex matrix, i.e., $\sigma[I + K(j\omega)G(j\omega)]$, is called a sigma plot. The singular values are plotted in this report in units of dB using $20 \log \sigma$. As σ approaches 0, the dB values approaches $-\infty$.

Unlike Bode plots, a problem with sigma plots is that it is not clear what constitutes a poor sigma plot, i.e., a less than satisfactory control design. Recent publications, Refs. 18 and 19, have shown that sigma plots tend to be conservative. If a sigma plot indicates a potentially poor design, the actual performance of the control system, when physically realizable uncertainties occur, is unclear. It is clear, however, that a "good" sigma plot <u>does</u> result in a satisfactory control design. If the performance characteristics of the full state feedback continuous-time linear quadratic regulator (LQR) is judged as a potentially "good" design, the performance characteristics are, Ref. 8, (with $R = \rho I$, ρ is a scalar).

$$\underline{\sigma}[I + K_{LQR}(j\omega I - A)B] \geq 1 \qquad 0 \leq \omega < \infty \tag{103}$$

Expressed in dB, sigma plots above 0 dB indicate a good design while sigma plots below 0 dB are potentially poor. In the single-input case, sigma plots above 0 dB correspond to 60 deg of phase margin and infinite gain margin.

Past research efforts in sigma plots have primarily concentrated on continuous-time additive alterations, $\Delta G(s)$ in Fig. 15, and multiplicative alterations to continuous-time plants. The outer-loop control design in this report is discrete. The discrete system counterpart to Fig. 15 and Eq. 102, as discussed in Ref. 8, is determined using the z-transform. The loop transfer function is computed as (with $\Delta G(z)$ zero),

$$\underline{u} = (I + K(z)G(z))^{-1} \underline{u}^* \tag{104}$$

The discrete system sigma plots in this report are computed by substituting $z = e^{j\omega\Delta t}$ into the discrete return difference matrix $I + K(z)G(z)$. Singular values are computed using the complex matrix, $I + K(e^{j\omega\Delta t})G(e^{j\omega\Delta t})$, and varying the frequency ω. What constitutes a "good" sigma plot for the discrete-time systems is currently an open question. As the sampling time approaches zero, it has been shown in Ref. 20 that the discrete-time sampled-data linear quadratic regulator frequency domain properties approach the continuous-time properties.

A. SINGULAR VALUES AND BODE PLOTS

This section compares outer-loop sigma plots and Bode plots for the control system designs. The comparisons are computed for the LON2 and LAT1 outer-loop control systems operating at 5 sps and 77 m/s CAS. The point where the control loop is broken for the outer-loop control design is shown in Fig. 1a. The inner-loop control system, actuator dynamics and aircraft dynamics are lumped together as the continuous-time plant. Sigma plots can be determined at point i for the 5 sps and 20 sps control designs. If the control loop is broken at the actuator input, the inner-loop control system would have to be modeled as a discrete system and the control system would be multirate when the outer-loop controller operates at 5 sps. Multirate control evaluation using sigma plots is beyond the scope of this work.

Single loop Bode plots in this report are obtained by opening one control loop while leaving the other control loop closed and plotting gain and phase of the scalar complex number $K(e^{j\omega\Delta t})G(e^{j\omega\Delta t})$. A single loop singular value plot is obtained by adding 1.0 to $K(e^{j\omega\Delta t})G(e^{j\omega\Delta t})$ and plotting the resulting complex number magnitude in dB. Breaking the throttle loop at point i' for the LON2 outer-loop control system operating at 5 sps and 77 m/s CAS produces the sigma plot and Bode plot in Fig. 16. The smallest value for $\underline{\sigma}$ is -2.7 dB at 0.2 rad/sec. At 0.2 rad/sec, the LON2 throttle Bode plot has a gain of -7.3 dB and a phase of -138 deg. The LON2 throttle phase margin is 57 deg and the gain margin is -18.5 dB, an excellent design. The minimum singular value does not usually occur at the crossover frequency as shown in Fig. 16. The LON2 control system's high gain feedback in the low frequency range is caused by the integrators. The LON2 control system's good roll off at high frequencies is caused by the u_t filter in PIF.

Breaking the loop at i' for the LAT1 rudder outer-loop control system operating at 5 sps and 77 m/s CAS produces the sigma plot and Bode plot in Fig. 17. The rudder command error integrator causes the control system to "wash-out" low frequency inputs to rudder. The smallest singular value is -3.5 dB at 0.53 rad/sec. At 0.53 rad/sec, the LAT1 rudder Bode plot in Fig. 17 has a gain of -8.7 dB and a phase of -160 deg. The phase margins for the LAT1 rudder loop are 174 deg and 93.1 deg. The gain margins for the LAT1 rudder loop is -10 dB and -50 dB, all good single-input design values.

Breaking the loop at point i for the LON2 control system operating at 5 sps and 77 m/s produces the maximum and minimum singular value plots in Fig. 18. The first minimum singular value, -3.0 dB at 0.21 rad/sec, corresponds to the single-input throttle minimum in Fig. 16. The second minimum singular value, -3.2 dB at 1.1 rad/sec, corresponds to the single-input elevator minimum in Fig. 19. Overall, there is not a significant difference between single-input sigma plots and multi-input sigma plots for the longitudinal control systems.

The lateral control system has a completely different conclusion. Breaking the loop at i for the LAT2 control system operating at 5 sps and 77 m/s CAS produces the two singular value plots in Fig. 18. The minimum singular value in Fig. 18b is 12.3 dB below either minimum single-input singular value in Figs. 17 and 20. The minimum singular value of -17.3 dB at 0.44 rad/sec in Fig. 18b is a strong departure from the single-input indications of control system robustness for aileron and rudder. Figure 18 is considered to be an example of the conservativeness inherent in singular value analysis. Numerous quadratic weight adjustments did not improve the minimum value in Fig. 18b significantly. The frequency of the minimum singular value indicates the inner-loop control system is actively involved in generating the result shown in the figure. Contrary to Fig. 18b; nonlinear simulations, closed-loop eigenvalues and single-input Bode plots all indicate that the lateral control system design has acceptable performance.

B. EFFECT OF SAMPLE RATE

Two longitudinal control system configurations, LON1 and LON2, and one lateral control system, LAT1, are designed at two sample rates, 20 sps and 5 sps. Figures 21 and 22 show the effect of different sample rates for single loop breaks at point i'. The different sample rates have little effect on LAT1 and LON2 control system gain as a function of frequency. The different sample rates have a larger effect on the control system phase, especially at high frequencies. The phase margin for the aileron loop changes from 45 deg at 20 sps to 35 deg at 5 sps, a significant degradation. The phase margin for the rudder loop changes from 100 deg to 90 deg. The LON2 throttle loop shows no change in phase margin with sample rate. The elevator loop phase margin degrades only 2.0 deg.

The multi-input singular value effects of different sample rates can be observed by comparing Table 8 and Table 9 for the LON2 design and comparing

the results in Table 10 for the LAT1 design. There is a 0.5 dB (approximate) minimum singular value improvement using the higher sample rate for LON2 (this corresponds to a 3.0 deg phase change). The singular value improvement for LAT1 is 0.3 dB or less. Single-input Bode plots give a better relative indication of control system performance degradation as the sample rate decreases when compared to multi-input sigma plots for the control designs in this report.

C. EFFECT OF AIRSPEED

The primary effect of airspeed on the longitudinal designs is that the control system low frequency stability properties improve with airspeed. The increase is apparent when the minimum singular values are compared in Tables 11, 8 and 12 for the LON1, LON2 and LON3 control systems, respectively. The high frequency stability properties degrade in LON1 and LON2 but remain fairly constant in LON3 as airspeed increases. Another trend evident in the tables is that LON3 has better frequency domain stability properties than LON2 and LON2 has better stability properties than LON1.

The single-input frequency response for the lateral designs indicate that the stability properties improve with airspeed as shown in Tables 13 and 14. The minimum singular values in Table 10 for the multi-input sigma plots indicate that the stability properties degrade with airspeed. The single-loop frequency response is considered to be a better indication of actual control system performance for the lateral outer-loop control designs. The LAT1 control system stability properties in Table 13 are better than the LAT2 control system stability properties in Table 14.

VI. CURVED TRAJECTORY SIMULATION

The performance of the 3D RNAV control system described in the previous chapters is evaluated in this chapter along a complex curved trajectory in the terminal area. Two versions of the nonlinear six degree of freedom simulation along the curved trajectory are presented. The first version has all external noise and disturbances deactivated. The second version has all noise and disturbances (except for wind shear) activated. The noise and disturbances include a steady wind of 10 kt moving east to west, the sensor noise and bias errors shown in Table 3 and wind gusts from a Dryden model with a standard deviation of 0.3 m/s (1.0 fps). The waypoints and the aircraft's initial trim conditions are shown in Table 15. The horizontal curved trajectory generated by the waypoints and the steady wind direction are shown in Fig. 23.

The curved trajectory begins with the aircraft flying straight and level with the flaps fully extended at 40 deg. The aircraft rolls left, flys level for a short time, then rolls right and enters a circular turn with a 233 deg change in heading. During the first roll to the left, the aircraft begins to descend at a steep rate, 7.2 m/s (23.6 ft/sec). The trajectory of the aircraft is a descending spiral during the circular turn part of the trajectory. After completing the 233 deg change in heading, the aircraft, still descending, flys level for a short time, then rolls left to line up with the runway center line. During the final turn, the aircraft decreases the descent rate to 3.7 m/s (12.3 ft/sec). The simulation is terminated at the point where an automatic landing control system could complete the descent and land. The latitude and longitude values in Table 15 correspond to Earth coordinates near the NASA Wallops Flight Center.

A. LONGITUDINAL DYNAMICS

The disturbance free simulations for the longitudinal dynamics are shown in Figs. 24 to 26. The simulation begins with an initial condition mismatch in commanded and actual CAS. The descent path is begun 25 seconds into the simulation. The command model limits the vertical deceleration and the aircraft descends to capture the path using aircraft accelerations which ensure passenger comfort. The value used to limit $\ddot{h}$ is an adjustable input to the flight control system and has no effect on closed-loop stability. Increasing the maximum allowed value of $\ddot{h}$ decreases the height error. The maximum value of $\ddot{h}_{min}$ in the command model is 0.457 m/s^2 (1.5 ft/sec^2), The purposeful increase in height error caused by the acceleration limit grows to between 70 and 80 m in Figs. 24 to 26. The error between commanded and actual vertical velocity decreases to zero as the simulation progresses. There is a slight error of less than 10 m in the height response because of the control system's Type 1 response. The control system decreases throttle during the descent to keep airspeed from increasing.

The changes in height and vertical velocity after 180 sec into the simulation are caused by the rolling motions of the aircraft. A cross-axis term which feeds back roll angle squared to elevator is used in the control design and aids in decreasing height error during turns.

A comparison of the simulations indicate LON2 and LON3 are almost identical in performance. LON1 has larger errors and less damping but overall, has a smoother response. The 20 sps and 5 sps longitudinal control system designs have similiar simulation performance. The 20 sps simulations are not presented.

In contrast, the 20 sps and 5 sps lateral designs exhibit a noticeable difference as shown in Figs. 27 and 28. The 20 sps design is better damped and has less cross track error (6 m vrs. 22 m). The commanded bank angle changes to the desired value required in a turn 5 seconds before the turn commences as discussed in Chapter III D. The turns are well coordinated, i.e., steady-state sideslip is zero and steady turn cross track error is zero. The maximum sideslip at turn entry is ~1.0 deg.

The longitudinal curved trajectory simulations with all disturbances activated are shown in Figs. 29 to 33. Elevator activity is kept at a reasonable level. Throttle activity is low and nonoscillatory. Stochastic performance, which is most clearly evident in the HDOT response, improves from LON1 to LON2 and further improves in LON3. The bias in the CAS response is caused by the fact that the true aircraft CAS is plotted. The control system causes measured CAS, which contains a bias, to follow commanded CAS. Throttle activity for LON1 is lower than either LON2 or LON3.

The simulations for LON1 and LON2 operating at 20 sps are shown in Figs. 32 and 33. Stochastic performance is improved when comparisons are made with the 5 sps designs. Throttle activity is smoother and height error is relatively flat during the descent. The aircraft response is quicker as evidenced by the sharper pitch angle changes. It remains to be determined if passengers can detect a difference between the same type of control system operating at different rates.

B. LATERAL DYNAMICS

The lateral control design responses along the curved trajectory with disturbances are shown in Figs. 34, 35 and 36. The steady wind causes the aircraft dynamics in the simulation to initially trim the aircraft with a nonzero track angle error but with a zero cross track error. The 20 sps LAT1 design quickly drives the track angle error to zero. The steady wind and gusts have little effect on the excellent simulation performance of the LAT1 design at 20 sps.

The 5 sps design simulations for LAT1 and LAT2 in Figs. 34 and 36 have a slower response than the 20 sps LAT1 design and develop a larger cross track error, (60 m vers. 15 m). Differences between the 5 sps LAT1 and 5 sps LAT2 outer-loop control designs are noticeable in the roll response

and slideslip response. LAT1 has slightly larger slideslip excursions, while LAT2 has a slightly larger roll overshoot. The cross track error and track angle error simulations for LAT1 and LAT2 are essentially identical. Increasing the cross track error gain in the lateral integrator for LAT2 does not reduce the cross track error response in transients. It remains to be determined if aircraft passengers can detect differences between the two lateral control systems.

From the simulation runs, it is seen that the overall performance of the outer-loop control systems starting from level flight to near the runway is satisfactory. The simultaneous lateral and longitudinal maneuvers are performed and completed with response consideration given to passenger comfort. There are no detrimental overshoots or oscillations in the presence of steady winds and typical levels of atmospheric turbulence.

VII. CONCLUSIONS AND RECOMMENDATIONS

A. Conclusions

The conclusions of this study are:

- Outer-loop digital flight control systems can be successfully designed and practically implemented using the synthesis theory of optimal limited state feedback.

- Optimal limited state feedback allows a designer to explore a variety of control structures and compensation elements in the control loop.

- Integrated control designs, such as LON3 and LAT1 in the report, have superior performance over the nested decentralized approach, such as LON1, for identical quadratic weights.

- The outer-loop control system can operate at a very slow sample rate (5 sps) with reasonable performance and stability margins. The performance at the fast rate outer-loop designs (20 sps) is better than the slow rate design, as expected, but pilot opinion will have to be used to determine if the difference is noticeable in flight.

- The structure used to form the integral error has a significant effect on control performance. LON3 performed better than LON2 which performed better than LON1 for identical cost functions. The three longitudinal control systems primarily differed in the way the integral error is constructed.

- The control system in simulation flies the airplane successfully through severe wind shears near the terminal area.

- The gain-scheduled control system stabilizes the airplane in simulation for the following individual variations in parameters away from the design flight conditions:

    - 3048 m (10,000 ft) to sea level
    - 59 m/s (115 kt) to 154 m/s (300 kt)
    - 0.2 to 0.3 cg
    - 90,000 lb to 75,000 lb
    - throttle saturated either full forward or zero
    - rudder actuator failed

- The use of multi-input sigma plots for relative evaluation of control performance was unsatisfactory. A better indication of relative control performance was provided by single-loop Bode plots. The sigma plots were considered to be too conservative.

- The control system flies a curved trajectory in the terminal area with high accuracy and good response to measurement noise, gusts and steady winds.

B. Recommendations

- The performance of the lateral control system degrades with bank angle, particularly past 35 deg. The maximum bank angle expected in flight is 25 deg. Improvements could be made by identifying the linear dynamics of the aircraft while the aircraft is banked in the nonlinear simulation using readily available parameter identification programs.

- An interesting use of the lateral command system is for the RNAV/MLS transition problem reported in Ref. 8. The position estimate of the aircraft changes abruptly when the MLS transmitters are in range and the MLS measurements become available to the filters onboard the aircraft. The change is caused by the increased accuracy of MLS versus RNAV. When the change is detected, the control system can be reinitialized and the command model activated to transfer the aircraft to the more highly accurate guidance path.

- A potentially better approach to gain scheduling is to bring the selection of the regression coefficients directly into the control design optimization process. ICS has developed an approach using stochastic optimal limited state feedback which could perform the optimization.

- Dynamic compensation and eigenvalue sensitivity analysis should be incorporated in the cost function.

- Wind shear accommodation using the command generator tracker should be used in the outer-loop control design.

- The energy probe, Ref. 20, should be investigated as a feedback sensor.

- The design of the inner- and outer-loop should be integrated using multirate optimal output feedback theory.

Appendix A GAIN SCHEDULES

This appendix presents the regression coefficients for all the control system gains. The appendix is a printout of the two FORTRAN subroutines used to compute the lateral (LATGAIN) and the longitudinal (LONGSCH) gains. LATGAIN and LONGSCH are called by the subroutines PIFLAT and PIFLON discussed in Appendix B.

A.1 LATGAIN

```
      SUBROUTINE LATGAIN( VGS, ICHOSLA, GAINA )

C   ICHOSLA---------DETERMINES WHICH SCHEDUAL TO USE IN LATGAIN
C                    = 1  0.05 SEC   1.0PHI + 0.5Y DESIGN
C                    = 2  0.20 SEC   1.0PHI + 0.5Y DESIGN
C                    = 3  0.20 SEC   1.0PHI + 1.0Y DESIGN
C   VGS-------------AIRSPEED USED FOR GAIN SCHEDUAL
C   GAINA-----------OUTPUT GAIN VECTOR

      DIMENSION GAINA(1)
      DIMENSION PVL2A(18), PCL2A(18), PVL8A(18), PCL8A(18),
     A          PCL2B(18), PVL8B(18), PVL2B(18), PCL8B(18),
     B          PCL2C(18), PVL8C(18), PVL2C(18), PCL8C(18)

C#############################################################

C   GAIN SET FOR ICHOSLA = 1 : LAT1 20 SPS

C  A1

      DATA PVL2A /0.0000122,  0.0001380, -0.001690,  -0.001060,
     A           -0.01530,    0.00712,   -0.05050,    0.01815,
     B           -0.0000535,  0.0003700,
     C           -0.00003190,-0.00000718,-0.0014610, -0.0004200,
     D            0.004550,   0.000231,   0.10700,    0.01820/

C  A2

      DATA PCL2A /0.9260,     -0.02740,    0.22500,    1.0003,
     A           -1.410,      -1.570,      0.2380,    -1.6580,
     B           -0.166,      -0.01660,
     C            0.003500,  -0.000595,   0.1340,     0.01560,
     D            1.688,      -0.4790,    -10.35,      0.3720/

C  A3

      DATA PVL8A /0.00010860, 0.0000978, -0.001440,  -0.00076700,
     A            0.00513,    0.003520,  -0.02620,    0.01508,
     B            0.0001219, -0.0000221,
     C            0.00001161, 0.00000708,0.0001950,  0.0001518,
     D            0.001370,   0.000231,   0.07008,   -0.002995/

C  A4

      DATA PCL8A /0.0006,     -0.02290,    0.16600,    0.9420,
     A           -4.9080,     -0.89290,  -3.8430,     -0.91880,
     B           -0.2002,      0.05237,
     C           -0.0036800 ,-0.003103,  -0.1575,     -0.09110,
     D            2.101,      -0.479,     1.19600,    4.6/


C#############################################################

C   GAIN SET FOR ICHOSLA = 2 : LAT1  5 SPS

C  A1

      DATA PVL2B /0.00000736, 0.000422,  -0.00265,   -0.00368,
     A           -0.00969,    0.00639,   -0.0509,     0.0123,
     B           -0.000355,   0.000177,
     C           -0.0000418, -0.00000943,-0.00238,   -0.00100,
     D            0.00431,   -0.00428,    0.0864,     0.0164 /
```

```
C  A2

      DATA PCL2B /0.7026,     -0.0904 ,     0.453  ,     0.969 ,
     A           -1.859 ,     -1.328 ,     0.431  ,    -0.889 ,
     B           -0.133 ,      0.000878,
     C            0.00607 ,  -0.00394 ,    0.183 ,      0.00627,
     D            1.617,       0.368 ,    -8.573,       0.536 /

C  A3

      DATA PVL8B /0.00025000, 0.000317  ,-0.00197 ,    0.0,
     A            0.00211,     0.00303 ,  -0.0345 ,     0.00906 ,
     B            0.0000542, -0.0000412,
     C            0.0000297,   0.000033   , 0.0009995, 0.00110  ,
     D            0.00262 ,    0.001188,    0.0621 ,   -0.000962/

C  A4

      DATA PCL8B /0.643 ,     -0.0803 ,     0.319  ,     0.30  ,
     A           -3.86  ,     -0.783  ,    -2.397 ,     -0.149  ,
     B           -0.197,       0.0426,
     C           -0.00613   ,-0.01185 ,   -0.4468,     -0.4125 ,
     D            1.93 ,      -0.565 ,     0.731  ,     3.851 /

C*************************************************************

C   GAIN SET FOR ICHOSLA = 3 : LAT2  5 SPS

C  A1

      DATA PVL2C /-.00006347,  .00052460, -.00445020, -.00387860,
     A            -.01454307,  .00696107, -.05593540,  .01714920,
     B            -.00036427,  .00027847,
     C            -.00006600, -.00001620, -.00347640, -.00114100,
     D             .00625027, -.00570140,  .10954627,  .01698967/



C  A2

      DATA PCL2C / .71257900, -.10296300,  .66837100,  .99597300,
     A           -1.36775800,-1.42958700,  .56022700,-1.56585600,
     B            -.15631200, -.00579400,
     C             .00682000, -.00271400,  .27671700,  .01472500,
     D            1.35425200,  .67990200,-11.23503800,  .23233500/

C  A3

      DATA PVL8C / .00047339,  .00024057,  .00052169, -.00038889,
     A             .00400966,  .00266535, -.04970220,  .00361226,
     B            -.00019993, -.00017509,
     C             .00006924,  .00004200,  .00274026,  .00154682,
     D             .00522494,  .00236178,  .05518912, -.00396304/

C  A4

      DATA PCL8C / .57379086, -.06181143, -.34302971,  .36824171,
     A           -4.62242514, -.66170971,-1.07118800, 1.21282886,
     B            -.20716400,  .08338371,
     C            -.01615143, -.01326000, -.88210114, -.48773771,
     D            1.37765914, -.83018829, 3.63572686, 4.10506943/


C   ICHOSLA = 1

      IF( ICHOSLA .NE. 1 ) GO TO 30

          IF( VGS .GE. 180. ) GO TO 15

C   VGS IS LESS THAN 180.0

              DO 10 I=1,18
                  GAINA(I) = PVL2A(I) * VGS + PCL2A(I)
   10         CONTINUE
              GO TO 100

C   VGS IS GREATER THAN 180.0

   15     CONTINUE

              DO 20 I=1,18
                  GAINA(I) = PVL8A(I) * VGS + PCL8A(I)
   20         CONTINUE
              GO TO 100
```

```
C    ICHOSLA = 2


   30 CONTINUE

      IF( ICHOSLA .NE. 2 ) GO TO 70

          IF( VGS .GE. 180. ) GO TO 50

C    VGS IS LESS THAN 180.0

               DO 40 I = 1,18
                   GAINA(I) = PVL2B(I)*VGS + PCL2B(I)
   40          CONTINUE
               GO TO 100

   50      CONTINUE

C    VGS IS GREATER THAN 180.0

               DO 60 I = 1,18
                   GAINA(I) = PVL8B(I)*VGS + PCL8B(I)
   60          CONTINUE

           GO TO 100

C    ICHOSLA = 3 (DATA FROM LATDAT1 - 9/22/82 **J. BROUSSARD'S ACCOUNT**)

   70 CONTINUE

      IF( ICHOSLA .NE. 3 ) GO TO 90

          IF( VGS .GE. 180 ) GO TO 80

C    VGS IS LESS THAN 180.0

               DO 75 I = 1,18
                   GAINA(I) = PVL2C(I)*VGS + PCL2C(I)
   75          CONTINUE
               GO TO 100

   80      CONTINUE

C    VGS IS GREATER THAN 180.0

               DO 85 I = 1,18
                   GAINA(I) = PVL8C(I)*VGS + PCL8C(I)
   85          CONTINUE
               GO TO 100

   90 CONTINUE


      PRINT *," ERROR IN LATGAIN - ICHOSLA = ",ICHOSLA," THIS IS NOT AN
     APTION"
      STOP "ERROR IN LATGAIN NO OPTION ICHOSLA"

  100 CONTINUE

      RETURN
      END
```

A.2 LONGSCH

```
      SUBROUTINE LONGSCH( VGS, ICHOSLO, GAINA )

C    ICHOSLO---------DETERMINES WHICH SCHEDUAL TO USE IN LONGSCH
C                     = 1  NESTED  0.05 SEC  1.0Z + 0.1ZDOT DESIGN
C                     = 2  NESTED  0.20 SEC  1.0Z + 0.1ZDOT DESIGN
C                     = 3  COUPLED 0.20 SEC  1.0Z + 20ZDOT + 0.1V2 DESIGN
C                     = 4  COUPLED 0.20 SEC  1.0Z + 20ZDOT + 1.0V2 DESIGN
C                     = 5  COUPLED 0.20 SEC  1.0Z + 10ZDOT DESIGN
C                     = 6  COUPLED 0.05 SEC  1.0Z + 10ZDOT DESIGN
C    VGS-------------AIRSPEED USED FOR GAIN SCHEDUAL
C    GAINA-----------OUTPUT GAIN VECTOR
```

```
      DIMENSION GAINA(1)
      DIMENSION PVLO2A(22), PVLO8A(22), PCLO2A(22), PCLO8A(22),
     A          PVLO2C(22), PVLO8C(22), PCLO2C(22), PCLO8C(22),
     B          PVLO2D(22), PVLO8D(22), PCLO2D(22), PCLO8D(22),
     C          PVLO2E(22), PVLO8E(22), PCLO2E(22), PCLO8E(22),
     D          PVLO2F(22), PVLO8F(22), PCLO2F(22), PCLO8F(22),
     E          PVLO2G(22), PVLO8G(22), PCLO2G(22), PCLO8G(22)

C#####################################################################

C    GAIN SET FOR ICHOSLO = 1 : LON1 20 SPS

C  A1

      DATA PVLO2A/-0.000000,  0.0000000,   0.000000,    0.0001570,
     A             0.0000386,-0.000000,   -0.00570,     0.000000,
     B            -0.00000,    0.00826,    -0.000000,   0.0020600,
     C            -0.00000,    0.002430,
     D            -0.0000000, 0.00002348,  0.00000000,  0.0000000,
     E            -0.000000,   0.000000,   -0.000000,   -0.0000000/

C  A2

      DATA PCLO2A/ 0.970,     -0.00000,    -0.00000,     0.901,
     A            -0.4180,    -0.0000,     1.7240,      7.520,
     B            -0.000000, -2.290000,    0.00000,    -0.4930,
     C            -0.0000,    -0.520300,
     D             0.00000,   -0.004740,   -0.000544,   -0.00000,
     E            -0.0000,     1.1000,      0.1800,      0.000/

C  A3

      DATA PVLO8A/ 0.0000000, 0.0,          0.0,         0.0002390,
     A            -0.000449, -0.000000,    0.04160,     0.0157,
     B             0.000000,  0.00569,     0.00000,     0.00000,
     C             0.0,       0.00466,
     D             0.0000000,-0.00000889,  0.00000000,  0.0000000,

     E             0.00000,   -0.012000,   -0.000476,    0.000000/

C  A4

      DATA PCLO8A/ 0.9690,     0.0,         0.000,       0.896,
     A            -0.3190,     0.0000,     -2.523,       4.326,
     B            -0.000,     -1.609,      -0.0000,     -0.463,
     C             0.00,      -2.135,
     D             0.00000,    0.0004466, -0.001080,    -0.000000,
     E            -0.00,       1.63,        0.304,       0.000/

C#####################################################################

C    GAIN SET FOR ICHOSLO = 2 : LON1  5 SPS

C  A1

      DATA PVLO2C/ 0.000181,   0.0000000,   0.000000,    0.0011900,
     A            -0.0000348,-0.000000,    -0.00533,     0.009140,
     B            -0.00000,    0.00675,    -0.000000,    0.0003610,
     C            -0.00000,    0.002235,
     D            -0.0000000, 0.00001170, -0.00001160,  0.0000000,
     E            -0.000000,   0.000000,   -0.000000,   -0.0000000/

C  A2

      DATA PCLO2C/ 0.838000,   0.0000000,   0.000000,    0.5330000,
     A            -0.4430000,-0.000000,     1.58600,     6.030000,
     B            -0.00000,   -2.24300,    -0.000000,   -0.2040000,
     C            -0.00000,   -0.508000,
     D            -0.0000000,-0.00505000, -0.00046400,  0.0000000,
     E            -0.000000,   1.10000,     0.180000,   -0.0000000/

C  A3

      DATA PVLO8C/ 0.0000772,  0.0,         0.0,         0.0005280,
     A            -0.000179,  -0.000000,    0.04820,     0.0311,
     B             0.000000,   0.00317,     0.00000,    -0.00175,
     C             0.0,        0.002354,
     D             0.000000,  -0.00003910,  0.00000352,  0.0000000,
     E             0.00000,   -0.013100,   -0.000476,    0.000000/
```

```
C  A4

      DATA PCL08C/ 0.8720000, 0.0,          0.0,          0.6160000,
     A             -0.343000, -0.000000,   -4.58000,      0.4740,
     B              0.000000, -1.24900,     0.00000,      0.01130,
     C              0.0,      -1.594000,
     D              0.0000000, 0.00256000, -0.00469000,   0.0000000,


     E              0.00000,   4.530000,    0.304000,     0.000000/

C#############################################################

C   GAIN SET FOR ICHOSLO = 3 : LON3  5 SPS

C  A1

      DATA PVL02D / .00068400,  .00003400,  .00002733,  .00061533,
     A              .00236467, -.00530533,  .00411267,  .00540533,
     B             -.00145333,  .00756267, -.00060600,  .00004000,
     C             -.00220800,  .00002800,
     D             -.00000824, -.00000299, -.00000367,  .00002056,
     E              .00683267, -.00349067, -.00197333, -.00491667/

C  A2

      DATA PCL02D /  .86493000,  .01143000, -.00527000,  .57369000,
     A             -.86279000, 1.05291000, -.73503000, 6.40359000,
     B              .26415000,-2.32138000,  .13333000, -.09770000,
     C              .44589000, -.67069000,
     D              .00169770, -.00221090, -.00199250, -.00388680,
     E            -1.69338000, 1.95067000,  .70090000, 1.15825000/

C  A3

      DATA PVL08D /-.00007876, -.00015895,  .00016943, -.00007333,
     A             -.00060886, -.00243019,  .10392314,  .06879019,
     B              .00021933,  .00225229, -.00035238,  .00001248,
     C              .00047057,  .00035114,
     D              .00000225,  .00000122, -.00000192,  .00000057,
     E              .00672657,  .00107133, -.00010324, -.00049171/

C  A4

      DATA PCL08D / .89456857,  .06116571, -.01910857,  .69970000,
     A             -.22378286,  .75389714,-14.8256029,-5.84489714,
     B             -.09696000,-1.57896571,  .07461429, -.10176286,
     C             -.00229143, -.73558286,
     D             -.00029869, -.00285320, -.00263177, -.00020897,
     E            -1.35985143, 1.24982000,  .46065143,  .22197429/

C#############################################################

C   GAIN SET FOR ICHOSLO = 4 (NOT DISCUSSED IN REPORT)

      DATA PVL02E /-.00002733,  .00005200, -.00000400,  .00061733,
     A              .00006800, -.01051133,  .00525333,  .00573133,
     B             -.00155067,  .00843533, -.00041533,  .00026867,


     C             -.00111467,  .00048700,
     D             -.00000663,  .00000080, -.00000095,  .00002026,
     E              .00701200, -.00464533, -.00133133, -.00690200/

      DATA PCL02E / .88727000,  .00604000, -.00318000,  .56533000,
     A             -.42214000, 1.37354000, -.86895000, 6.91521000,
     B              .26317000,-2.53511000,  .09846000, -.14091000,
     C              .17209000, -.71646000,
     D              .00101480, -.00288950, -.00255460, -.00272680,
     E            -1.70516000, 2.29066000,  .51899000, 1.72696000/

      DATA PVL08E /-.00008305, -.00051724, -.00008171, -.00078905,
     A             -.00074000, -.00088646,  .10650143,  .03509333,
     B             -.00063447, -.00075200, -.00036152,  .00029362,
     C              .00048171, -.00033286,
     D              .00000590, -.00000245, -.00000360,  .00001938,
     E              .00672314,  .00107562, -.00010152, -.00049000/

      DATA PCL08E / .89575429,  .16029143,  .05037429,  .89771429,
     A             -.18750000,  .32680286,-15.53892B6, 3.47790000,
     B              .13925800, -.74778000,  .08267714, -.17954571,
     C             -.00537429, -.54634286,
     D             -.00130654, -.00183823, -.00216697, -.00541426,
     E            -1.35890286, 1.24863429,  .46017714,  .22150000/
```

```
C*************************************************************

C   GAIN SET FOR ICHOSLD = 5 : LON2  5 SPS

C  A1

      DATA PVLO2F / .00006333,  .00008267,  .00008267,  .00072600,
     A              .00222933, -.00410133,  .00507533,  .00824400,
     B             -.00226733,  .00813667, -.00087200, -.00014200,
     C             -.00142000,  .00027600,
     D             -.00001061, -.00000795, -.00000644,  .00002184,
     E              .00792133, -.00523200, -.00238867, -.01026000/

C  A2

      DATA PCLO2F / .86825000, -.00038000, -.01728000,  .58062000,
     A             -.86933000,  .90229000,-1.07116000, 6.13488000,
     B              .42792000,-2.43505000,  .19546000, -.10319000,
     C              .28365000, -.35593000,
     D              .00222270, -.00139840, -.00149530, -.00442770,
     E            -1.89854000, 2.14586000,  .74386000, 1.98925000/

C  A3


      DATA PVLO8F /-.00008010, -.00009010,  .00019162, -.00017390,
     A             -.00044000, -.00171990,  .10039133,  .05010914,
     B              .00009943,  .00189629, -.00034543,  .00001905,
     C              .00073933, -.00005619,
     D              .00000441, -.00000008, -.00000232,  .00000146,
     E              .00601571,  .00089181, -.00038095, -.00088762/

C A4

      DATA PCLO8F / .89394857,  .03774857, -.02512571,  .74529143,
     A             -.27210000,  .63995143,-14.11268000,-2.39336286,
     B             -.05810857,-1.49760571,  .08096857, -.12781429,
     C             -.08546000, -.31374286,
     D             -.00063683, -.00262969, -.00256974, -.00057054,
     E            -1.19761429, 1.04497714,  .52878571,  .28488571/

C*************************************************************

C   GAIN SET FOR ICHOSLD = 6 : LON2 20 SPS

C   A1

      DATA PVLO2G / .00001333,  .00001933,  .00002733,  .00018933,
     A              .00153333, -.00438067,  .00467000,  .00692733,
     B             -.00215133,  .00858800, -.00089133, -.00011333,
     C             -.00144667,  .00025400,
     D             -.00000273, -.00000191, -.00000162,  .00000599,
     E              .00852133, -.00713067, -.00262467,  .00643800/

C  A2

      DATA PCLO2G / .96690000,  .00012000, -.00592000,  .89397000,
     A             -.79025000,  .96557000, -.96175000, 6.96783000,
     B              .40574000,-2.56514000,  .19944000, -.11945000,
     C              .28940000, -.37767000,
     D              .00056630, -.00043060, -.00039690, -.00120830,
     E            -2.01369000, 2.58562000,  .79524000, -.01184000/

C  A3

      DATA PVLO8G /-.00002486, -.00002257,  .00009362, -.00009905,
     A             -.00054686, -.00179248,  .10309933,  .05867886,
     B              .00024276,  .00053686, -.00031924, -.00001476,
     C              .00066724,  .00007190,
     D              .00000138, -.00000020, -.00000073,  .00000038,
     E              .00613810,  .00115895, -.00034952, -.00095581/

C  A4


      DATA PCLO8G / .97347714,  .00991143, -.01844571,  .94571429,
     A             -.26510286,  .68076286,-14.44085994,-3.34991714,
     B             -.08400857,-1.33629714,  .07681143, -.13387143,
     C             -.07069143, -.36007143,
     D             -.00021423, -.00069954, -.00064446, -.00014134,
     E            -1.22052857, 1.11313429,  .53945714,  .30436286/

C*************************************************************
```

```
C   ICHOSLO = 1

      IF( ICHOSLO .NE. 1 ) GO TO 30

          IF( VGS .GE. 180. ) GO TO 15

              DO 10 I = 1,22
                  GAINA(I) = PVLO2A(I)*VGS + PCLO2A(I)
10            CONTINUE
              GO TO 200

15        CONTINUE

              DO 20 I = 1,22
                  GAINA(I) = PVLO8A(I)*VGS + PCLO8A(I)
20            CONTINUE
              GO TO 200


C   ICHOSLO = 2

30 CONTINUE

      IF( ICHOSLO .NE. 2 ) GO TO 50

          IF( VGS .GE. 180. ) GO TO 40

              DO 35 I = 1,22
                  GAINA(I) = PVLO2C(I)*VGS + PCLO2C(I)
35            CONTINUE
              GO TO 200

40        CONTINUE

              DO 45 I = 1,22
                  GAINA(I) = PVLO8C(I)*VGS + PCLO8C(I)
45            CONTINUE
              GO TO 200


C   ICHOSLO = 3 (DATA FROM LONDAT1 - 9/22/82 **J. BROUSSARD'S ACCOUNT**)

50 CONTINUE

      IF( ICHOSLO .NE. 3 ) GO TO 70

          IF( VGS .GE. 180. ) GO TO 60

              DO 55 I = 1,22
                  GAINA(I) = PVLO2D(I)*VGS + PCLO2D(I)
55            CONTINUE
              GO TO 200

60        CONTINUE

              DO 65 I = 1,22
                  GAINA(I) = PVLO8D(I)*VGS + PCLO8D(I)
65            CONTINUE
              GO TO 200

C   ICHOSLO = 4 (DATA FROM LONDAT2 - 9/22/82 **J. BROUSSARD'S ACCOUNT**)

70 CONTINUE

      IF( ICHOSLO .NE. 4 ) GO TO 90

          IF( VGS .GE. 180. ) GO TO 80

              DO 75 I = 1,22
                  GAINA(I) = PVLO2E(I)*VGS + PCLO2E(I)
75            CONTINUE
              GO TO 200

80        CONTINUE

              DO 85 I = 1,22
                  GAINA(I) = PVLO8E(I)*VGS + PCLO8E(I)
85            CONTINUE
              GO TO 200

C   ICHOSLO = 5 (DATA FROM LONDAT3 - 9/22/82 **J. BROUSSARD'S ACCOUNT**)
```

```
 90 CONTINUE

    IF( ICHOSLO .NE. 5 ) GO TO 110

        IF( VGS .GE. 180. ) GO TO 100


            DO 95 I = 1,22
                GAINA(I) = PVLO2F(I)*VGS + PCLO2F(I)
 95         CONTINUE
            GO TO 200

100     CONTINUE

            DO 105 I = 1,22
                GAINA(I) = PVLO8F(I)*VGS + PCLO8F(I)
105         CONTINUE
            GO TO 200

C   ICHOSLO = 6 (DATA FROM LONDAT4 - 9/22/82 **J. PROUSSARD'S ACCOUNT**)

110 CONTINUE

    IF( ICHOSLO .NE. 6 ) GO TO 150

        IF( VGS .GE. 180. ) GO TO 120

            DO 115 I = 1,22
                GAINA(I) = PVLO2G(I)*VGS + PCLO2G(I)
115         CONTINUE
            GO TO 200

120     CONTINUE

            DO 125 I = 1,22
                GAINA(I) = PVLO8G(I)*VGS + PCLO8G(I)
125         CONTINUE
            GO TO 200

150 CONTINUE

    PRINT *," ERROR IN LONGSCH - ICHOSLO = ",ICHOSLO," THIS IS NOT AN
   APTION"
    STOP "ERROR IN LONGSCH NO OPTION ICHOSLO"

200 CONTINUE

    RETURN
    END
```

Appendix B LONGITUDINAL AND LATERAL SOFTWARE

This appendix presents the FORTRAN listing of the subroutines PIFLON and PIFLAT. The subroutines are called 20 times per second during the nonlinear simulations in Chapters IV and VI.

B.1 PIFLAT

```
      SUBROUTINE PIFLAT( DACMD,   DRCMD,   RNK,     BNKBAR,  CRTE,
     A                   TAGE,    CAS,     VGS,     DAM,     DRM,
     B                   PHIDOT,  KV,      T,       ICHOSLA, HMAX,
     C                   POLLMAK, ROLLMAX, NMULATI, DEGP1,   RDCMAI,
     D                   DEBUGA                                      )

C    DACMD-------------COMMAND AILERON      - DEG
C    DRCMD-------------COMMAND RUDDER       - DEG
C    RNK---------------BANK ANGLE           - DEG
C    BNKBAR------------COMMAND BANK ANGLE   - DEG
C    CRTE--------------CROSS TRACK ANGLE    - FEET
C    TAGE--------------TRACK ANGLE ERROR    - DEG
C    CAS---------------CALIBRATED AIRSPEED - KT
C    VGS---------------GROUND SPEED         - FT/SEC
C    DAM---------------MEASURED AILERON     - DEG
C    DRM---------------MEASURED RUDDER      - DEG
C    PHIDOT------------MEASURED ROLL RATE   - DEG/SEC
C    KV----------------ELEVATOR CAS SCHEDULED GAIN
C    T-----------------SAMPLE TIME          - SEC
C    ICHOSLA = 1-------DELT = 0.05,   GKY = 0.5
C            = 2-------DELT = 0.20,   GKY = 0.5
C            = 3-------DELT = 0.20,   GKY = 1.0
C    HMAX--------------TRIP POINT IN FEET FOR WHEN CONVERSION OCCURS FOR
C                      RNAV TO MLS SWITCH CRTE(START WITH = 100.0 )
C    POLLMAK-----------MAXIMUM ROLL ANGLE  - DEG
C    ROLLMAX-----------MAXIMUM ROLL ANGLE IF FINDRM IS FALSE
C    DEGP1-------------MAX COMMANDED ROLL RATE OF CHANGE        - DEG/SEC
C    RDCMAI------------MAX ROLL RATE OF CHANGE IN COMMAND MODEL - DEG/SEC
C    NMULATI-----------NUMBER OF 0.05 SEC PERIOD DELAYS BETWEEN RECEIVING
C                      MEASUREMENTS AND RELEASING CONTROL COMMANDS TO ACT
C                      IF DELT=.20 AND NMULATI=1, DELAY=REGULAR 1 PERIOD
C                      DELAY
C                      IF DELT=.20 AND NMULATI=2, DELAY=REGULAR 2 PERIOD
C                      DELAY
C                      IF DELT=.20 AND NMULATI=3, DELAY=REGULAR 3 PERIOD
C                      DELAY
C                      IF DELT=.20 AND NMULATI=4, DELAY=REGULAR 4 PERIOD
C                      DELAY
C                      IF DELT = .05 THEN NMULATI MUST = 1
C    DEBUGA  = .TRUE.--DEBUG PRINTOUT REQUESTED

      DIMENSION PGLA(18), GAINA(18)

      REAL      KV,       KPHIDOT

      LOGICAL   FIRST,    NOPROP,    FINDRM,    DEBUGA

      EQUIVALENCE (PGLA(1),S311),   (PGLA(2),S312),
     A            (PGLA(3),S313),   (PGLA(4),S314),


     B            (PGLA(5),S321),   (PGLA(6),S322),
     C            (PGLA(7),S323),   (PGLA(8),S324),
     F            (PGLA(9),S325),   (PGLA(10),S326),
     D            (PGLA(11),S411),  (PGLA(12),S412),
     E            (PGLA(13),S413),  (PGLA(14),S414),
     F            (PGLA(15),S421),  (PGLA(16),S422),
     G            (PGLA(17),S423),  (PGLA(18),S424)

      DATA FIRST /.TRUE./

    5 CONTINUE
```

```
      IF( .NOT. FIRST ) GO TO 10

C   INITIALIZE STATES

C     CHOOSE DELT AND GKY

      DELT = 0.2
      IF( ICHOSLA .EQ. 1 ) DELT = .05
      GKY = .5
      IF( ICHOSLA .EQ. 3 ) GKY = 1.

C     INITIALIZE GAINS

      CASG = CAS
      IF( CASG .LT. 120. ) CASG = 120.
      IF( CASG .GT. 300. ) CASG = 300.
      CALL LATGAIN( CASG, ICHOSLA, PGLA )

C     SET UP INITIAL VALUES

      ARY     = .03
      ARP     = 1.15
      PP      = 180.
      PP2     = 360.
      GRAV    = 32.174
      RPD     = 0.0174532925
      DACMAX  = 20.
      DRCMAX  = 30.
      ROLL1   = ROLLO   = BNK
      ITIME   = 0
      TAGE1   = TAGEO   = TAGE
      CRTE1   = CRTEO   = CRTE
      ROLLN1  = BNKBAR
      CASS    = CAS
      DRC     = DR1     = DRO     = DRM
      DA1     = DAO     = DAM
      VDA2    = VDA1    = 0.0
      VDR2    = VDR1    = 0.0

C   INITIALZE MODEL STATES

      Y1      = CRTE
      PSI1    = TAGE
      PHI1    = BNK

C   INITIALZE INNER LOOP STATES

      PHIDOTF = PHIDOT
      C1      = EXP(-20.0*T)
      KPHIDOT = -1.5

C   INITIALZE OTHER DATA

C     NOPROP MODEL INDICATES IF TRUE THAT COMMAND NOT BE PROPAGATED
C
C     FINDRM FINDS THE MAXIMUM ROLL ANGLE FOR CAPTURES

      NOPROP  = .FALSE.
      FINDRM  = .TRUE.
      IF( ABS(CRTE) .LT. 3000.0 ) FINDRM  = .FALSE.
      IF( ABS(TAGE) .LT. 30.0 )   FINDRM  = .FALSE.
      ILOOP   = -1
      FIRST   = .FALSE.
      MLOOP   = 1.0/DELT + 0.1
      MULTI   = DELT/T + 0.1
      ACAS    = EXP(-2.0*DELT)
      BCAS    = 1.0-ACAS
      GFEED   = BCAS
      IMULTI  = MULTI -1

      IF( MULTI .EQ. 1 )MMULATI = 1
      DEGPS   = DEGP1*DELT
      RDCMAX  = RDCMA1*DELT

   10 CONTINUE

C   INNER LOOP CALCULATIONS

      PHIDOTF = C1*(PHIDOTF - PHIDOT) + PHIDOT
      X       = PHIDOTF*KPHIDOT

C   CHECK FOR LOOP ITERATION OF CONTROL LOOP
```

```
      IF( IMULTI .GE. MULTI ) IMULTI = 0
      IMULTI   = IMULTI + 1
      IF( IMULTI .NE. MULTI ) GO TO 65
      ROLLNO   = ROLLN1
      BNKE     = BNKBAR - ROLLN1


C     LIMIT RATE OF CHANGE OF ROLLN TO 5DEG/SEC

      IF( ABS(BNKE) .GT. DEGPS ) BNKE = SIGN(1.0,BNKE)*DEGPS
      ROLLN1   = ROLLN1 + BNKE

C     FILTER CAS

      CASS     = ACAS*CASS + BCAS*CAS

C     UPDATE GAINS EVERY 1.0 SECONDS

      IF( ILOOP .GT. MLOOP ) ILOOP = -1
      ILOOP    = ILOOP + 1
      IF( ILOOP .NE. 0 ) GO TO 30
      CASF     = CASS

C     UPDATE CROSS AXIS GAIN

      IF( CASF .GT. 300.0 ) CASF = 300.0
      IF( CASF .LT. 150.0 ) CASF = 150.0
      IF( CASF .GT. 240.0 ) GO TO 20
      AK       = 0.000160425*CASF - 0.05042
      GO TO 25

   20 CONTINUE

      AK       = 0.0000709693*CASF - 0.02894

C     CONSTRUCT GAINS G1-G18

   25 CONTINUE

      CASG     = CASS
      IF( CASG .GT. 300.0 ) CASG = 300.0
      IF( CASG .LT. 120.0 ) CASG = 120.0

C     CONSTRUCT THE LAT GAINS

      CALL LATGAIN( CASG, ICHOSLA, GAINA )

      ATIME    = ITIME/100
      NTIME    = ATIME*100
      IF( NTIME .EQ. ITIME ) WRITE(6,1000) (I,PGLA(I),I=1,18)

C     PROPAGATE COMMAND MODEL

   30 CONTINUE

      IF( NOPROP ) GO TO 40
      IF( ABS(Y1).LT.0.1  .AND.  ABS(PSI1).LT.0.01 ) NOPROP = .TRUE.
      B        = GRAV/VGS
      AK1      = ARY/(MULTI*MULTI)
      AK2      = ARP*VGS/150.0/MULTI
      YO       = Y1
      PSIO     = PSI1
      PHIO     = PHI1
      PHI1     = -AK1*YO - AK2*PSIO
      RDC      = PHI1 - PHIO
      UM       = RDC

C     DO NOT CHANGE HEADING IF ON PATH TO GLIDESLOPE

      IF( PHI1*(PSI1) .GT. 0.0  .AND.  ABS(PSI1) .GT. 30.0 ) RDC    = 0.0

C     FIND MAXIMUM ROLL IF FAR FROM TRACK

      IF( .NOT. FINDRM ) GO TO 35
      ANUM     = (VGS)*(VGS)*(COS(TAGE*RPD)-1.0 )
      ADEN     = -(CRTE-SIGN(1.0,CRTE)*2000.0 )*GRAV
      ADEN     = SIGN(1.0,ADEN)*0.00001 + ADEN
      ROLLMAX  = ABS(ATAN2(ANUM,ADEN)/RPD)
      IF( ROLLMAX .GT. ROLLMAK ) ROLLMAX = ROLLMAK
      IF( UM*(PHIO + SIGN(1.0,PHIO)*0.00001) .LT. 0.0 ) FINDRM=.FALSE.

   35 CONTINUE
```

```
      ROLLMA1 = AMAX1(POLLMAX,ABS(BNKBAR))
      IF( ABS(PHIO ) .GE. ROLLMA1 ) RDC   = 0.0
      IF( UM*(PHIO + SIGN(1.0,PHIO)*0.00001) .LT. 0.0 ) RDC = UM

C     APPLY CONTROL IF DECELERATION IS APPLICABLE

      IF( ABS(RDC) .GE. RDCMAX ) RDC   = SIGN(1.0,RDC)*RDCMAX
      PHI1     = PHIO + RDC
      PSI1     = PSIO + DELT*R*TAN(RPD*PHI1)/PPD
      IF( PSI1 .GT. PP )  PSI1 = PSI1 - PP2
      IF( PSI1 .LT. -PP ) PSI1 = PSI1 + PP2
      Y1       = YO + DELT*VGS*SIN(RPD*PSIO) + DELT*DELT*R*TAN(RPD*PHI1)*
     A           0.5*VGS

      A        = ROLLN1 - ROLLNO +(PHI1 - PHIO)
      C        = ROLLNO + PHIO  + GKY*(CRTE1 - YO)
      G1       = PSI1 - PSIO
      IF( G1 .GT. PP )  G1 = G1 - PP2
      IF( G1 .LT. -PP ) G1 = G1 + PP2
      G2       = TAGEO - TAGE1
      G        = G2 - G1
      H        = CRTEO - CRTE1 -(Y1 - YO )
      GO TO 50


   40 CONTINUE

      A        = ROLLN1 - ROLLNO
      C        = ROLLNO + GKY*CRTE1
      G        = TAGEO - TAGE1
      IF( G .GT. PP) G = G - PP2
      IF( G .LT. -PP) G = G + PP2
      H        = CRTEO - CRTE1

   50 CONTINUE

      B        = 0.0

      D        = ROLL1 - C
      E        = DR1 - AK*C - DRC
      F        = ROLLO - ROLL1

C     DETERMINE IF THERE HAS BEEN A LARGE CHANGE IN CRTE CAUSED BY
C     CHANGING FROM RNAV TO MLS

      IF( ABS(H) .LT. HMAX ) GO TO 55
      FIRST    = .TRUE.
      GO TO 5

   55 CONTINUE

C     EASYON HERE

      DO 60 I = 1,10
          PGLA(I) = PGLA(I) + GFEED*(GAINA(I) - PGLA(I))
   60 CONTINUE

C     COMPUTE CONTROL LAW

      VDA1     = S311*VDA2 + S313*VDR2 +
     1           S321*F    + S323*G    + S325*H +
     2           S411*D    + S413*E    +
     3           S421*A    + S423*B
      VDR1     = S312*VDA2 + S314*VDR2 +
     1           S322*F    + S324*G    + S326*H +
     2           S412*D    + S414*E    +
     3           S422*A    + S424*B

      DAO      = DA1       + DELT*VDA1
      DRO      = DR1       + DELT*VDR1

      IF (ILOOP .NE. 0 ) GO TO 65

C     TIME CHECK

      OPTIM    = SECOND(CP)

C     PRINT OUTPUT FOR DEBUG

      IF( .NOT. DEBUGA ) GO TO 65
```

```
      WRITE(6,2000) PHI1,  ROLLNO, Y1, CRTE, PSI1, NMULATI,
     A              DPTIM, IMULTI, MULTI, MLOOP
C     WRITE(6,3000) A, B, C, D, E, F, G, H, DACMD, DRCMD

   65 CONTINUE

      IF( IMULTI .NE. NMULATI ) GO TO 70

C   DOWNLOAD DATA

      ROLL1   = ROLLO
      ROLLO   = BNK
      TAGE1   = TAGEO
      TAGEO   = TAGE
      CRTE1   = CRTEO
      CRTEO   = CRTE

   70 CONTINUE

      DACMD   = KV*(DAO + X)
      DRCMD   = DRO

C   PROCESS CONTROL COMMANDS FOR CONTROL LIMITS

      IF ( ABS(DACMD) .LT. DACMAX ) GO TO 75
      DACMD   = SIGN(1.0,DACMD)*DACMAX
      DAO     = (DACMD/KV) - X
      VDA1    = 0.0

   75 CONTINUE

      VDA2    = VDA1
      DA1     = DAO

      IF( ABS(DRCMD) .LT. DRCMAX ) GO TO 80
      DRCMD   = SIGN(1.0,DRCMD)*DRCMAX
      VDR1    = 0.0
      DRO     = DRCMD

   80 CONTINUE

      VDR2    = VDR1
      DR1     = DRO


      ITIME   = ITIME + 1
C
C     FORMAT STATEMENTS

 1000 FORMAT(1X,/,1X,6(I3,F15.8),/,1X,6(I3,F15.8),
     A          /,1X,6(I3,F15.8),/,1X,6(I3,F15.8))
 2000 FORMAT(1X, "PHI1    ROLLNO  Y1      CRETE   PSI1    ",
     A       5(2X,F10.5),/,1X,
     A           "DPTIM   NMULATI  IMULTI  MULTI   MLOOP  ",
     A            1(2X,F10.5),4(2X,I10 ) )
 3000 FORMAT(1X, "A       B       C       D       E       ",
     A       5(2X,F10.5),/,1X,
     A           "F       G       H       DACMD   DRCMD   ",
     A           5(2X,F10.5))

      RETURN
      END
```

B.2 PIFLON

```
      SUBROUTINE PIFLON( DTCMD,   DECMD,   PITCH,   TAS,     CAS,
     A                   EPR,     ROLL,    ZBARO,   HVSI,    ACC,
     B                   Q,       HCWP,    HDCWP,   CASWP,   DTM,
     C                   DEM,     FLAPC,   KV,      T,       KTOFPS,
     D                   ICHOSLO, DMAX,    FLAPON,  ZFILT,   AMAZ,
     E                   AMAZD,   DZMAX2,  AOAMAX,  AOAMIN,  NMULDTI,
     F                   CASMA1,  DDZMA1,  ADZEP1,  DEBUGO             )
```

```
C   PITCH-------------MEASURED PITCH ANGLE                - DEG
C   TAS---------------TRUE AIRSPEED                       - FT/SEC
C   CAS---------------CALIBRATED AIRSPEED                 - KT
C   EPR---------------ENGINE PRESSURE RATIO
C   ROLL--------------MEASURED ROLL ANGLE                 - DEG
C   VGS---------------GROUNDSPEED                         - FT/SEC
C   ZBARO-------------BAROMETRIC HEIGHT MEASUREMENT       - FT          + UP
C   HVSI--------------VERTICAL VELOCITY MEASUREMENT       - FT          + UP
C   ACC---------------VERTICAL ACCELERATION MEASUREMENT   - FT/SEC**2  + UP
C   HCMP--------------HEIGHT COMMAND                      - FT          + UP
C   HDCMP-------------VERTICAL VELOCITY COMMAND           - FT/SEC      + UP
C   CASMP-------------AIRSPEED COMMAND                    - FT/SEC
C   DTCMD-------------THROTTLE COMMAND                    - 1000 LBS
C   DECMD-------------ELEVATOR COMMAND                    - DEG
C   DTM---------------MEASURED THROTTLE                   - 1000 LBS
C   DEM---------------MEASURED ELEVATOR                   - DEG
C   FLAPC-------------COMMANDED FLAP                      - DEG
C   Q-----------------PITCH RATE                          - DEG/SEC
C   ICHOSLO = 1-------NESTED  0.05 1.0Z + 0.10ZDOT
C           = 2-------NESTED  0.20 1.0Z + 0.10ZDOT
C           = 3-------COUPLED 0.20 1.0Z + 20.0ZDOT + 0.1V**2
C           = 4-------COUPLED 0.20 1.0Z + 20.0ZDOT + 1.0V**2
C                     (VALID FOR CAS = 120 TO 180 ONLY)
C           = 5-------COUPLED 0.20 1.0Z + 10.0ZDOT
C           = 6-------COUPLED 0.05 1.0Z + 10.0ZDOT
C   DMAX--------------MAXIMUM CHANGE IN HEIGHT ALLOWED BEFORE TRIPPOINT
C                     FOR TRANSITION BETWEEN RNAV AND MLS
C   FLAPON  = .TRUE.--THE FLAP SCHEDULE IN THIS PROGRAM IS USED TO COMMA
C                     THE FLAPS
C           = .FALSE.-FLAP COMMAND IS INPUT
C   ZFILT   = .TRUE.--THE Z COMPLEMENTARY FILTER IN THIS PROGRAM IS USED
C           = .FALSE.-THE AMAZ FILTER IS USED.  DATA IS PASSED THROUGH
C                     AMAZ, AMAZD
C   DZMAX2------------MAXIMUM VALUE FOR ZDOT               - FT/SEC
C   NMULATI-----------NUMBER OF 0.05 SEC PERIOD DELAYS BETWEEN RECEIVING
C                     MEASUREMENTS AND RELEASING CONTROL COMMANDS TO ACT
C                     IF DELT=.20 AND NMULATI=1, DELAY=REGULAR 1 PERIOD
C                     DELAY
C                     IF DELT=.20 AND NMULATI=2, DELAY=REGULAR 2 PERIOD
C                     DELAY
C                     IF DELT=.20 AND NMULATI=3, DELAY=REGULAR 3 PERIOD


C                     DELAY
C                     IF DELT=.20 AND NMULATI=4, DELAY=REGULAR 4 PERIOD
C                     DELAY
C                     IF DELT = .05 THEN NMULATI MUST = 1
C   CASMA1------------MAXIMUM RATE OF CHANGE OF CAS COMMAND - FT/SEC
C   DDZMA1------------MAXIMUM RATE OF CHANGE OF ZDOT COMMAND - FT/SEC**2
C   ADZEP1------------PARAMETER IN ZDOT - HIGH ALPHA REDUCTION - FT/SEC
C   DEBUGO  = .TRUE.--DEBUG PRINTOUT

      DIMENSION PGLO(22), GAINA(22)

      REAL      KV,       KTOFPS,   LOCASM

      LOGICAL   FIRST,    FLAPON,   ZFILT,   ZALP,   DEBUGO

      EQUIVALENCE (PGLO(1),S311),   (PGLO(2),S312),
     A            (PGLO(3),S313),   (PGLO(4),S314),
     B            (PGLO(5),S321),   (PGLO(6),S322),
     C            (PGLO(7),S323),   (PGLO(8),S324),
     E            (PGLO(9),S325),   (PGLO(10),S326),
     E            (PGLO(11),S327),  (PGLO(12),S328),
     E            (PGLO(13),S329),  (PGLO(14),S3210),
     D            (PGLO(15),S411),  (PGLO(16),S412),
     E            (PGLO(17),S413),  (PGLO(18),S414),
     F            (PGLO(19),S421),  (PGLO(20),S422),
     G            (PGLO(21),S423),  (PGLO(22),S424)

      DATA FIRST /.TRUE./

    5 CONTINUE

      IF( .NOT. FIRST ) GO TO 10

C   INITIALIZE STATES

      IF( CAS .GT. 170 .AND. ICHOSLO .EQ. 4 ) ICHOSLO = 3

      DELT    = 0.2
      IF( ICHOSLO .EQ. 1  .OR.  ICHOSLO .EQ. 6 ) DELT = 0.05
      GKZ     = 1.
      GKZD    = 0.1
      GKV2    = 0.0
```

```
      IF( ICHOSLO .EQ. 3  .OR.  ICHOSLO .EQ. 4 ) GKZD = 20.
      IF( ICHOSLO .GT. 4 ) GKZD = 10.
      IF( ICHOSLO .EQ. 3 ) GKV2 = 0.1
      IF( ICHOSLO .EQ. 4 ) GKV2 = 1.0

      CASZ    = CAS
      IF( CASZ .LT. 120. ) CASZ = 120.
      IF( CASZ .GT. 300. ) CASZ = 300.
      CALL LONGSCH( CASZ, ICHOSLO, PGLO )

      PPD     = 0.017453293
      GRAV    = 32.174
      RPD     = 0.0174532925
      DECMAX  = 15.
      PITCH1  = PITCHO  = PITCH
      CAS1    = CASO    = CAS*KTOFPS
      HDOFO   = HDOF1   = ACC
      ZPLUS   = ZMINUS  = ZBARO
      ZDPLUS  = ZDMINUS = HVSI
      Z1      = ZO      = -ZBARO
      DZ1     = DZO     = -HVSI
      DT1     = DTO     = DTM
      DE1     = DEO     = DEM
      VDT2    = VDT1    = 0.0
      VDE2    = VDE1    = 0.0
      ZBIASP  = ZBIASM  = ACC
      CASWP1  = CASWPO  = CAS*KTOFPS
      ZALP    = .FALSE.
      MULTI   = DELT/T + 0.1
      IMULTI  = MULTI - 1

      IF( MULTI .EQ. 1 ) NMULOTI = 1
      ACAS    = EXP(-2.0*DELT)
      BCAS    = 1.0-ACAS
      ITIME   = 0
      MLOOP   = 1.0/DELT + 0.1
      CASMAX  = CASMA1*DELT
      DDZMAX  = DDZMA1*DELT
      ADZEPR  = ADZEP1*DELT
      ZDDMAX  = 1.50
      AK1     = 0.6/(MULTI*MULTI)
      AK2     = 2.0/(MULTI)
      HTOH    = 0.80*T
      DHTOH   = 0.320*T
      BTOH    = -0.0095*T
      AKCMAX  = 1.0 - EXP(-0.5*DELT)
      AKCMIN  = 1.0 - EXP(-0.025*DELT)
      A1      = (AKCMAX - AKCMIN)/20.0
      A2      = AKCMIN
      GFEED   = 1.0 - EXP(-2.0*DELT)

C     INITIALZE MODEL STATES

      ZM1     = -ZBARO
      ZMD1    = -HVSI

C     INITIALZE INNER LOOP STATES


      HDOF    = ACC
      C9      = EXP(-10.0*T)
      XN      = 0
      C4      = EXP(-0.0625*T)

C     INITIALZE OTHER DATA

      ILOOP   = -1
      CASF    = CAS
      DZMAX1  = DZMAX2
      FIRST   = .FALSE.

 10   CONTINUE

C     CHECK FOR ICHOSLO = 4 PROBLEM

      IF( CAS .GT. 170  .AND.  ICHOSLO .EQ. 4 ) FIRST = .TRUE.
      IF( FIRST ) GO TO 5

C     CHECK FOR LOOP ITERATION OF CONTROL LAW

C     PERFORM INNER LOOP CALCULATIONS
```

```
      HDDF    = C9*(HDDF - ACC) + ACC
      XN      = C4*(XN   -  Q) + Q
      QF      = Q - XN
      ROLL2   = ROLL**2

C   PERFORM Z COMPLEMENTARY FILTER

      ZPLUS   = AMAZ
      ZDPLUS  = AMAZD
      IF( .NOT. ZFILT ) GO TO 15
      ZERROR  = ZBARO   - ZMINUS
      ZPLUS   = ZMINUS  + HTOH*ZERROR
      ZDPLUS  = ZDMINUS + DHTOH*ZERROR
      ZBIASP  = ZBIASM  + BTOH*ZERROR

C   CORRECT ACCELORMETER FOR GRAVITY

C*****AC      = ACC + GRAV*(1.0 - COS(PITCH*RPD)*COS(BNK*RPD))
      AC      = ACC

C   CORRECT FOR BIAS

      AC      = AC - ZBIASP

C   PROPAGATE

      ZDMINUS = ZDPLUS +  T*AC
      ZMINUS  = ZPLUS  +  T*ZDPLUS +  T*T*0.5*AC
      ZBIASM  = ZBIASP

   15 CONTINUE
      IF( IMULTI .GE. MULTI ) IMULTI = 0
      IMULTI = IMULTI + 1
      IF( IMULTI .NE. MULTI ) GO TO 70

C   BEGIN CONTROL LOOP


C   UPDATE CASWP

      CASER = CASWP - CASWPO
      ACASG = A1*ABS(CASER) + A2
      IF( ACASG .GE. AKCMAX ) ACASG = AKCMAX
      DCAS = ACASG*CASER
      IF( ABS(DCAS) .GT. CASMAX ) DCAS = SIGN(1.0,DCAS)*CASMAX
      CASWPO = CASWPO + DCAS

C   SCHEDULE FLAPC

      CASF    = ACAS*CASF + BCAS*CAS
      IF( .NOT. FLAPON ) GO TO 20
      CASQ    = CASWPO/KTOOPS
      FLAPC   = 0.0
      IF( CASQ .LT. 190.0 ) FLAPC = -0.25*CASQ + 47.5
      IF( CASQ .LT. 170.0 ) FLAPC = -0.50*CASQ + 90.0
      IF( CASQ .LT. 150.0 ) FLAPC = -1.00*CASQ + 165.0
      IF( CASQ .LT. 135.0 ) FLAPC = 30.0

C   COMPUTE FLIGHT PATH ANGLE

   20 CONTINUE

      GAMA    = ASIN(ZDPLUS/TAS)/RPD

C   COMPUTE AOA TO COMPARE TO AOAMAX AND AOAMIN

      ALPHA   =  PITCH  -  GAMA
      IF( ALPHA .LT. AOAMIN ) GO TO 35
      IF( .NOT. ZALP ) DZMAX1 = DZMAX2/2.0
      ZALP    = .TRUE.
      IF( ALPHA .GT. AOAMAX ) GO TO 30
      GO TO 40

C   REDUCE ZDOT COMMAND

   30 CONTINUE


      DZD     = AOZEPR*TAS*SIN((AOAMIN - ALPHA)*RPD)
      DZMAX1  = DZMAX1 + DZD
      IF( DZMAX1 .LT. 0.0 ) DZMAX1 = 0.0
      ZM1     = ACAS*ZM1 - BCAS*ZPLUS
      GO TO 40
```

```
   35 CONTINUE
      IF( DZMAX1 .LT. DZMAX2 ) DZMAX1 = DZMAX1 + DDZMAX
      ZALP    = .FALSE.

   40 CONTINUE

      DZMAX3  = AMAX1(DZMAX2,ABS(HDCWP))
      DZMAX   = DZMAX3
      IF( ZALP )DZMAX = AMIN1(DZMAX1, DZMAX3)

C     CHECK TO SEE IF GAIN UPDATE IS REQUIRED

      IF( ILOOP .GT. MLOOP ) ILOOP = -1
      ILOOP   = ILOOP + 1
      IF( ILOOP .NE. 0 ) GO TO 50
      CASZ    = CASF
      IF( CASZ .LT. 120.0 ) CASZ = 120.0
      IF( CASZ .GT. 300.0 ) CASZ = 300.0

C     CALCULATE THE LON GAINS

      CALL LONGSCH( CASZ, ICHOSLD, GAINA )

   50 CONTINUE

C     PROPAGATE MODEL

      ZMO     = ZM1
      ZMDO    = ZMD1
      DZAAA   = HDCWP
      AMPA    = 1.0
      IF( ZALP ) AMPA  = 0.0
      IF( ZALP ) DZAAA = SIGN(1.,HDCWP)*DZMAX
      UM      = AMPA*AK1*(-HCWP - ZMO) + AK2*(-DZAAA - ZMDO)
      ZDD     = UM
      AMP     = 1.0
      IF( UM*ZMDO .LT. 0.0 ) AMP = 2.5
      IF( ABS(ZDD) .GT. (AMP*ZDDMAX) ) ZDD = SIGN(1.,ZDD)*ZDDMAX*AMP

      ZMD1    = ZMDO + DELT*ZDD
      DZBBB   = AMAX1(ABS(DZAAA),DZMAX)
      IF( ABS(ZMD1) .GE. DZBBB  .AND.  ABS(HDCWP) .LT. 0.1 )
     A                              ZMD1 = SIGN(1.,ZMDO)*DZBBB
      ZDD     = (ZMD1 - ZMDO)/DELT
      IF( ABS(ZDD) .GT. (AMP*ZDDMAX) ) ZDD = SIGN(1.,ZDD)*ZDDMAX*AMP
      ZMD1    = ZMDO + DELT*ZDD
      ZM1     = ZMO + DELT*ZMDO + DELT*DELT*ZDD*.5

C     COMPUTE CONTROL LAW STATE FEEDBACK

      A       = CASO - CAS1
      B       = PITCHO - PITCH1
      C       = HDDFO - HDDF1
      D       = ZO - Z1  -  (ZM1 - ZMO)
      E       = DZO - DZ1

C     COMPUTE INTEGRATOR

      F       = GKZ*(Z1-ZMO) + GKZD*(DZ1-ZMDO) + GKV2*(0.5*
     A          (CAS1*CAS1 - CASWP1*CASWP1)/GRAV)
      G       = CAS1 - CASWP1

C     EASYON CONTROL GAINS

      DO 60 I=1,22
          PGLO(I) = PGLO(I) + GFEED*(GAINA(I) - PGLO(I))
   60 CONTINUE

      H       = ZMD1 - ZMDO
      P       = CASWPO - CASWP1

C     DETERMINE IF THERE HAS BEEN A LARGE CHANGE IN Z CAUSED BY CHANGING
C     RNAV TO MLS OR A BAD DATA POINT HAS OCCURRED

      IF( ABS(D) .LT. DMAX ) GO TO 65
      FIRST   = .TRUE.
      GO TO 5

   65 CONTINUE

C     COMPUTE CONTROL LAW
```

```
      VDT1    = S311*VDT2    + S313*VDE2    +
     1          S321*A       + S323*B       + S325*C      +
     2          S327*D       + S329*E       +
     3          S411*F       + S413*G       +
     4          S421*H       + S423*P
      VDE1    = S312*VDT2    + S314*VDE2    +
     1          S322*A       + S324*B       + S326*C      +
     2          S328*D       + S3210*E      +
     3          S412*F       + S414*G       +
     4          S422*H       + S424*P


      DTO     = DT1          + DELT*VDT1
      DEO     = DE1          + DELT*VDE1

      IF( ILOOP .NE. 0 ) GO TO 70

C     PRINT OUTPUT FOR DEBUG

      IF( .NOT. DEBUGO ) GO TO 70

      IF( NTIME .EQ. ITIME ) WRITE(6,1000) (I, PGLO(I), I=1,22)
      WRITE(6,2000) CASO,  CASWPO,  HCWP,   ZM1,    HDCWP,
     A              ZMD1,  ZPLUS,  ZDPLUS, DE1
      WRITE(6,3000) ZALP, AMPA,DZAAA,DZBBB,HDCWP,ZMD1,ZMDO,AMP,E,D

   70 CONTINUE

      IF( IMULTI .NE. NMULOTI ) GO TO 80

C     DOWNLOAD DATA

      PITCH1  = PITCHO
      PITCHO  = PITCH
      CAS1    = CASO
      CASO    = CAS*KTOFPS
      HDDF1   = HDDFO
      HDDFO   = HDDF

      Z1      = ZO
      ZO      = -ZPLUS
      DZ1     = DZO
      DZO     = -ZDPLUS
      CASWP1  = CASWPO
      ATIME   = ITIME/100
      NTIME   = ATIME*100

C     PROCESS CONTROL COMMAND FOR CONTROL LIMITS

   80 CONTINUE

C     LOWER LIMIT ON THROTTLE

      LOCASM  = 0.2*(222.0 - CAS)

C     UPPER LIMIT ON THROTTLE
C     RELATIONSHIP BETWEEN THROTTLE AND EPR AT EPR = 1.85, THROTMAX = 42.
C                                             EPR = 1.2,  THROTMAX = 60.0
C     IF CAS ERROR IS TOO LARGE INCREASE THROTMAX USING ADHICAS

      ADHICAS = ABS(G) - 8.0
      IF( G .GE. -8.0 ) ADHICAS = 0.0
      HICASM  = -27.69*EPR + 93.2265 + ADHICAS
      IF( HICASM .GT. 60.0 ) HICASM = 60.0
      IF( HICASM .LT. 42.0 ) HICASM = 42.0
      IF( LOCASM .LT. 0.0 )  LOCASM = 0.0
      IF( LOCASM .GT.10.0 )  LOCASM = 10.0
      IF( DTO .GT. HICASM )  VDT1   = 0.0
      IF( DTO .GT. HICASM )  DTO    = HICASM
      IF( DTO .LT. LOCASM )  VDT1   = 0.0
      IF( DTO .LT. LOCASM )  DTO    = LOCASM
      VDT2    = VDT1
      DT1     = DTO
      DTCMD   = DTO

C     COMPUTE INNER LOOP FOR ELEVATOR

      Y       = HDDF  +  2.16*QF   -  0.004*ROLL2
      DECMD   = KV*(DEO + Y)
      IF( ABS(DECMD) .LT. DECMAX ) GO TO 90
      DECMD   = SIGN(1.0,DECMD)*DECMAX
      DEO     = (DECMD/KV) - Y
      VDE1    = 0.0
```

```
   90 CONTINUE

      VDE2    = VDE1
      DE1     = DEO

      ITIME   = ITIME + 1

C     FORMAT STATEMENTS

 1000 FORMAT(1X,/,1X,6(I3,F15.8),/,1X,6(I3,F15.8),
     A          /,1X,6(I3,F15.8),/,1X,6(I3,F15.8))
 2000 FORMAT(1X, "CASO    CASWPO  HCWP     ZM1      HDCWP    ",
N    A        5(2X,F10.4),/,1X,
     A           "ZMD1    ZPLUS   ZDPLUS  DE1               ",
     A        5(2X,F10.4) )
 3000 FORMAT(1X, "ZALP AMPA DZAAA DZBBB HDCWP          ",
     A       11,4(2X,F10.5),/,1X,
     A           "ZMD1, ZMDO, AMP, E, D                ",
     A         5(2X,F10.5))
      RETURN
      END
```

REFERENCES

1. Halyo, N. and Broussard, J. R.: "A Convergent Algorithm for the Stochastic Limited State Feedback Optimal Control Problem", 1981 Joint Automatic Control Conference, Charlottesville, VA, June 1981.

2. Roskam, J.: Airplane Flight Dynamics and Automatic Flight Controls, Parts I and II, Second Edition, Roskam Aviation Engineering Corp., Lawrence, KS, 1979.

3. White, W. F., compiler: "Flight Demonstrations of Curved, Descending Approaches and Automatic Landings Using Time Reference Scanning Beam Guidance." NASA TM-78745, 1978.

4. Broussard, J. R.: "Design, Implementation and Flight Testing of PIF Autopilots for General Aviation Aircarft", NASA CR-3709, July 1983.

5. Downing, D. R., Bryant, W. H. and Ostroff, A. J.: "Flight Test of a VTOL Digital Autoland System Along Complex Trajectories", Proc. of the 1979 AIAA Guidance and Control Conference, Boulder, CO, August 1979.

6. Halyo, N.: "Development of a Digital Guidance and Control Law for Steep Approach Automatic Landings Using Modern Control Techniques", NASA CR-3074, February 1979.

7. Broussard, J. R. and O'Brien, M. J.: "Feedforward Control to Track the Output of a Forced Model", IEEE Trans. Auto. Control, Vol. AC-25, August 1980, pp. 851-852.

8. Maybeck, P. S.: Stochastic Models, Estimation and Control, Vol. 3, Academic Press, New York, NY, 1982.

9. Pines, S.: "Terminal Area Automatic Navigation, Guidance, and Control Research Using the Microwave Landing System (MLS) Part 2 - RNAV/MLS Transition Problems for Aircraft", NASA CR-3511, January 1982.

10. Doyle, J. C. and Stein, G.: "Multivariable Feedback Design: Concepts for a Classical Modern Synthesis", IEEE Trans. Auto. Control, Vol. AC-26, February 1981, pp. 4-16.

11. Broussard, J. R. and Stallman, S. T.: "Modification and Verification of an ACSL Simulation of the ATOPS B-737 Research Aircraft", NASA CR-166049, February 1983.

12. Broussard, J. R.: "ATOPS B-737 Inner-Loop Control System Linear Model Construction and Verification", NASA CR-166055, February 1983.

13. Broussard, J. R. and Glasson, D. P.: "Optimal Multirate Flight Control System Design", 1980 Joint Automatic Control Conference, San Francisco, CA, August 1980.

14. Broussard, J. R. and Halyo, N.: "Active Flutter Suppression Using Optimal Output Feedback Digital Controllers", NASA CR-165939, May 1982.

15. Etkin, B.: Dynamics of Atmospheric Flight, John Wiley & Sons, Inc., New York, NY, 1972.

16. Miller, G. K.: "A Decoupled Control System for Improved Flight Performance in Wind Shear", 1981 Joint Automatic Control Conference, Charlottesville, VA, June 1981.

17. Dieudonne, J. E.: "Comments on a Proposed Standard Wind Hazard Environment and Its Use in Real Time Aircraft Simulation", AIAA 17th Aerospace Science Meeting, New Orleans, LA, January 1979, AIAA paper 79-0324.

18. Barrett, M. F.: "Conservatism with Robustness Tests for Linear Feedback Control Systems", Proc. of the 19th Conference on Decision and Control, Albuquerque, NM, December 1980.

19. Mukhopadhyay, V. and Newsom, J. R.: "Application of Matrix Singular Value Properties for Evaluating Gain and Phase Margins of Multiloop Systems", Proc. of the AIAA Guidance and Control Conference, San Diego, CA, August 1982.

20. Safonov, M. G.: Stability and Robustness of Multivariable Feedback Systems, MIT Press, Cambridge, MA, 1980.

21. Ostroff, A. J., Hueschen, R. M., Hellbaum, R. F. and Creedon, J. F.: "Flight Evaluation of a Simple Total Energy-Rate System with Potential Wind-Shear Application", NASA TP-1854, May 1981.

LIST OF SYMBOLS

In general, matrices are represented by capital letters and vectors are underscored; exceptions to these rules are only made when they are contradicted by standard aerodynamic notation.

VARIABLE	DESCRIPTION
A	Discrete time feedforward matrix Fundamental matrix (continuous-time system)
a	Acceleration Roll to rudder crossfeed gain Inverse of gain schedule time constant
a_h	Component of the vehicle acceleration normal to the local level plane
B	Control effect matrix (continuous-time system)
b	Bias estimate
C	Control law feedback gains
c	Cross track error
D	Control observation matrix
E	Disturbance effect matrix (continuous-time system)
e	2.71828 ...
$\underline{e}$	Vector error
$\underline{f}$	Vector-valued nonlinear function
G(s)	Plant transfer function
g	Magnitude of gravitational acceleration vector
H	Command observation matrix
H_1^2	Euler angle transformation form Frame 1 axes to Frame 2 axes
h	Distance from the aircraft's cg to the Earth's surface, positive down

VARIABLE	DESCRIPTION
I	Identity matrix
i	Index integer
J	Cost functional matrix
j	$\sqrt{-1}$
K	Gain value
$K(s)$	Control transfer function
k	Index integer
L_u, L_v, L_w	Scales of turbulence
ℓ	Number of commands
$\hat{M}$	Cross weighting matrix in Linear Quadratic Regulator cost function
m	Mass of the vehicle Number of controls Meters
N	Number of time steps
n	Number of states
P	Riccati matrix in the optimal limited state feedback regulator problem
p	Rotational rate about the body x-axis
$\hat{Q}$	State weighting matrix
q	Rotational rate about the body y-axis
$\bar{q}$	Free stream dynamic pressure ($=\frac{1}{2}\rho V^2$)
R	Control weighting matrix
R_L	Distance-to-go to an end of segment
r	Rotational rate about the body z-axis
S	Covariance matrix in the optimal limited state feedback regulator problem
s	Laplace transform variable

VARIABLE	DESCRIPTION
T	Thrust
T_L	Time-to-go to an end of segment
t	Time
u	Body x-axis velocity component
$\underline{u}$	Control vector
V	Velocity magnitude Measurement noise covariance matrix
v	Body y-axis velocity component Control difference
W	Process noise covariance matrix
w	Body z-axis velocity component
$\underline{w}$	White noise Gaussian vector
X_o	Covariance matrix of state initial conditions
x	Position along the x-axis
$\underline{x}$	State vector
y	Position along the y-axis
z	Position along the z-axis

VARIABLE (GREEK)	DESCRIPTION
α	Wind-body pitch Euler Angle (angle of attack)
β	Negative of wind-body yaw Euler angle (sideslip angle)
Γ	Discrete time control effect matrix
γ	Inertial-velocity axis pitch Euler angle (flight-path angle)
δ	Delta function latitude
δ_A	Aileron deflection

VARIABLE (GREEK)	DESCRIPTION
δ_{AC}	Aileron command
δ_{a}	Aileron state
δ_{E}	Elevator deflection
δ_{EC}	Elevator command
δ_{e}	Elevator state
δ_{F}	Flap deflection
δ_{R}	Rudder deflection
δ_{RC}	Rudder command
δ_{r}	Rudder state
δ_{SPL}	Left spoiler deflection
δ_{SPR}	Right spoiler deflection
δ_{S}	Spoiler state
δ_{T}	Throttle deflection
δ_{TC}	Throttle command
ζ	Damping ratio Track angle error
η	Gaussian noise
θ	Inertial-body pitch Euler angle
λ	Eigenvalue Longitude
ν	Measurement Gaussian noise
ξ	Integrator state
ρ	Air density
Σ	Summation
σ	Real part of an eigenvalue in radians/sec Standard deviation Singular value

VARIABLE (GREEK)	DESCRIPTION
Φ	Discrete-time system matrix
ϕ	Inertial-body axis roll Euler angle
ψ	Inertial-body axis yaw Euler angle
ω	Frequency in radians/sec Imaginary part of an eigenvalue

SUBSCRIPTS	DESCRIPTION
B	Body axis
b	Bias
C	Command value
CL	Closed-loop
E	Earth-relative axis
e	Error quantity
f	Full state feedback
GS	Ground speed
g	Gust
H	Horizontal
IL	Inner-loop
i	Element index for vectors and matrices
j	Element index for vectors and matrices
k	Sampling instant index
m	Model variable
o	Nominal value
s	Static pressure Stochastic
t	Transient

SUBSCRIPTS	DESCRIPTION
u	Velocity component along body x-axis
v	Velocity component along body y-axis
w	Velocity component along body z-axis
x	Horizontal perpendicular to y and z
y	Horizontal perpendicular to x and z
z	Vertical perpendicular to x and y

SUPERSCRIPTS	DESCRIPTION
E	Earth (inertial) axis
T	Transpose of matrix
-1	Inverse of matrix

PUNCTUATION	DESCRIPTION
$(\dot{})$	Derivative of quantity with respect to time
$(\bar{})$	Combined variable
$(\underline{})$	Vector quantity
$\partial(\ )/\partial(\ )$	Partial derivative of one variable with respect to another
$E\{\ \}$	Expected value
$\mid_{\forall}$	For all
$\Delta(\ )$	Perturbation variable
$(\ )^*$	Star trajectory
$(\hat{})$	Estimated quantity Discrete cost function weighting matrix
∞	Infinity
$\int$	Integral
$(\tilde{})$	Difference between variable and star trajectory

ACRONYM	CORRESPONDING PHRASE
ATOPS	Advanced Transport Operating Systems
CAS	Calibrated Airspeed
DIALS	Digital Integrated Automatic Landing System
DOF	Degrees of Freedom
dB	Decibels
EPR	Engine Pressure Ratio
IL	Inner-loop
kt	Knot
lim	Limit
lb	Pound
LQR	Linear Quadratic Regulator
MAX	Maximum
MEAS	Measurement
MLS	Microwave Landing System
MIN	Minimum
MXEPR	Maximum Engine Pressure Ratio
NASA	National Aeronautics and Space Administration
PIF	Proportional Integral Filter
rad	Radians
RNAV	Area Navigation
sec	Seconds
SIGN	The positive or negative sign
SPL	Left Spoiler
SPR	Right Spoiler
TAS	True Airspeed
tr	Trace
WO	Wash-out

TABLE 1. SCALES AND VARIANCE FOR GUST MODELS

	ALTITUDE (m)			
	18.3	18.3-100	100-533.4	>533.4
σ_u (m/sec)	4.88	$12.65h^{-0.32}$	3.05	3.05
σ_v (m/sec)	3.88	$6.52h^{-0.18}$	3.05	3.05
σ_w (m/sec)	2.83	2.83	2.83	2.85
L_u (m)	171.0	171.0	$7.42h^{0.68}$	533.4
L_v (m)	97.5	$43.43h^{0.28}$	$6.85h^{0.68}$	533.4
L_w (m)	53.0	$8.25h^{0.64}$	$6.85h^{0.68}$	533.4

TABLE 2. COMMAND MODEL PARAMETERS

LONGITUDINAL MODEL OPERATING AT 20 sps	
k_h	0.6 sec^{-2}
$k_{\dot{h}}$	2.0 sec^{-1}
k_{CAS}	Min $(0.00117205*(\lvert CAS_c - CAS_m \rvert) + 0.001249, 0.02469)$
$\ddot{h}_{MAX}$	If $\ddot{h}_m * h_m < 0.0$ THEN $\ddot{h}_{MAX}$ = 1.14 m/sec^2 (3.75 ft/sec^2) OTHERWISE $\ddot{h}_{MAX}$ = 0.457 m/sec^2 (1.5 ft/sec^2)
$\dot{CAS}_{MAX}$	0.76 m/s (2.5 ft/sec)
	LATERAL MODEL OPERATING AT 20 sps
k_c	0.0984 deg/sec/m (0.03 deg/sec ft)
k_ζ	3.77 m^{-1} (1.15 ft^{-1})
$\dot{\phi}_{MAX}$	4.0 deg/sec
ϕ_{MAX1}	25.0 deg (ROLLMAX in Appendix B)
ϕ_{MAX3}	30.0 deg (ROLLMAK in Appendix B)

TABLE 3. SENSOR PARAMETERS

Sensor	Noise standard deviation	Bias	Comments
Attitude gyro	0.23 deg	0.23 deg	
Rate gyro	0.02 deg/sec	0.	
Body mounted accelerometers	1% of g	1% of g	0.2, -0.2, 0.25 deg misalignment and 0.25% scaling error modeled
MLS-azimuth	0.01 deg	0.01 deg	
MLS-elevation	0.01 deg	0.01 deg	
MLS-DME	2.3 m	2.3 m	
Barometric altimeter	0.91 m	12.2 m	
Airspeed indicator	1 m/sec	1.5 m/s	
EPR measurement	0.01	0.02	Used for limit check
δ_A measurement	0.1 deg	0.2 deg	Used to initialize $\underline{u}_k$
δ_R measurement	0.1 deg	0.15 deg	"
δ_T measurement	0.2 deg	0.4 deg	"
δ_E measurement	0.1 deg	0.2 deg	"

TABLE 4. SQUARE ROOT OF MATRIX DIAGONAL FOR LONGITUDINAL CONTROL SYSTEMS

UNITS	Q	X_o	R
Δu (m/s)	1.22	0.61	
Δw (m/s)	1.52	1.52	
Δq (deg/sec)	0.0	1.0	
$\Delta\theta$ (deg)	65.0	2.0	
Δz (m)	0.244	3.05	
$\Delta\delta_e$ (deg)	0.0	0.0	
ΔEPR	0.0	0.0	
$\Delta\hat{a}_h$ (m/s^2)	0.0	0.0	
$\Delta\hat{q}$ (deg)	0.0	0.0	
Δu_e (deg)	0.0	7.0	
Δu_t (deg)	6.0	4.0	
$\Delta\xi_{z1}$ -	0.2 LON1	1.0 LON1	
$\Delta\xi_{z2}$ -	0.2 LON2	1.0 LON2	
$\Delta\xi_{z3}$ -	0.2 LON3	1.0 LON3	
$\Delta\xi_{CAS1}$ -	0.2 LON1	4.0 LON1	
$\Delta\xi_{CAS2}$ -	0.2 LON2	4.0 LON2	
$\Delta\xi_{CAS3}$ -	0.2 LON3	4.0 LON3	
Δh (m)	0.0	0.0	
$\Delta\hat{h}$ (m/s)	0.0	0.0	
$\Delta\mu_g$(m/s)	0.0	0.0	
Δw_{g1} (m/s)	0.0	0.0	
Δw_{g2} -	0.0	0.0	
Δv_e (deg/sec)			9.0
Δv_t (deg/sec)			12.0

TABLE 5. SQUARE ROOT OF MATRIX DIAGONAL FOR LATERAL CONTROL SYSTEMS

UNITS	Q	X_o	R
Δv (m/s)	30.5	0.61	
Δp (deg/sec)	0.0	0.0	
Δr (deg/sec)	0.0	0.0	
$\Delta\phi$ (deg)	70.0	2.0	
$\Delta\zeta$ (deg)	0.0	2.0	
Δc (m)	1.5	3.05	
$\Delta\delta_a$ (deg)	0.0	1.32	
$\Delta\delta_r$ (deg)	0.0	0.5	
$\Delta\hat{p}$ (deg/sec)	0.0	0.0	
Δr_{WO} (deg/sec)	0.0	0.0	
$\Delta\hat{r}$ (deg/sec)	0.0	0.0	
Δu_a (deg)	0.1	4.	
Δu_r (deg)	0.2	2.	
$\Delta\xi_{c1}$ -	1.5 LAT1	0.1 LAT1	
$\Delta\xi_{c2}$ -	1.5 LAT2	0.1 LAT2	
$\Delta\xi_{r1}$ -	0.8 LAT1	0.1 LAT1	
$\Delta\xi_{r2}$ -	0.8 LAT2	0.1 LAT2	
Δv_{g1} (m/s)	0.0	0.0	
Δv_{g2} -	0.0	0.0	
Δv_a (deg/sec)			30
Δv_r (deg/sec)			70

TABLE 6. CLOSED-LOOP MAPPED EIGENVALUES

LON1 CLOSED-LOOP EIGENVALUES AT 77 m/s (150 kt)

MODE	INNER-LOOP	OPTIMAL 20 sps	SCHEDULED 20 sps
$\Delta\delta_e$	-23.4	-23.8	-23.8
$\Delta\hat{a}_h$	- 6.93	- 6.1	- 6.1
SHORT PERIOD	- 2.1 ±j2.8	- 2.2 ±j2.5	- 2.1 ±j2.5
$\Delta u_e - \Delta z$	0.0 ±j0.0	- 0.68 ±j0.67	- 1.26
COMP. FILTER	- 0.40 ±j0.40	- 0.40 ±j0.40	- 0.40 ±j0.40
ΔEPR	- 0.50	- 0.81	- 0.64
Δu_t	0.0	- 0.30	- 0.78
PHUGOID	- 0.0004±j0.067	- 0.074±j0.11	- 0.20 ±j0.04
$\Delta\xi_{h1}$	0.0	- 0.064±j0.025	- 0.048±j0.10
$\Delta\hat{q}_{WO}$	- 0.060	- 0.060	- 0.064
$\Delta\xi_{CAS1}$	0.0	---	- 0.034

TABLE 6. CLOSED-LOOP MAPPED EIGENVALUES (CONTINUED)

LON1 CLOSED-LOOP EIGENVALUES AT 77 m/s (150 kt)

MODE	INNER-LOOP	OPTIMAL 5 sps	SCHEDULED 5 sps
$\Delta\delta_e$	-23.4	-20.0	-20.3
$\Delta\hat{a}_h$	- 6.93	- 4.4	- 4.4
SHORT PERIOD	- 2.1 ±j2.8	- 2.6 ±j2.9	- 2.6 ±j2.8
$\Delta u_e - \Delta z$	- 0.0 ±j0.0	- 0.71 ±j0.69	- 0.78 ±j0.59
COMP. FILTER	- 0.40 ±j0.40	- 0.40 ±j0.40	- 0.40 ±j0.40
ΔEPR	- 0.50	- 0.88	- 0.83
Δu_t	0.0	- 0.31	- 0.25
PHUGOID	- 0.0004±j0.067	- 0.060±j0.10	- 0.17
$\Delta\xi_{h1}$	0.0	- 0.065±j0.02	- 0.035±j0.077
$\Delta\hat{q}_{WO}$	- 0.060	- 0.059	- 0.064
$\Delta\xi_{CAS1}$	0.0	---	- 0.032

TABLE 6. CLOSED-LOOP MAPPED EIGENVALUES (CONTINUED)

LON2 CLOSED-LOOP EIGENVALUES AT 77 m/s (150 kt)

MODE	INNER-LOOP	OPTIMAL 20 sps	SCHEDULED 20 sps
$\Delta\delta_e$	-23.4	-23.9	-23.9
$\Delta\hat{a}_h$	- 6.93	- 6.0	- 5.0
SHORT PERIOD	- 2.1 ±j2.8	- 2.3 ±j2.5	- 2.3 ±j2.6
Δu_e-Δz	0.0 ±j0.0	- 0.87±j0.42	- 0.85±j0.17
COMP. FILTER	- 0.40 ±j0.40	- 0.40±j0.40	- 0.40±j0.40
ΔEPR	- 0.50	- 0.68	---
Δu_t	0.0	- 0.20	- 0.41±j0.24
PHUGOID	- 0.004±j0.067	- 0.14±j0.055	- 0.18±j0.038
$\Delta\xi_{h2}$	0.0	- 0.075	- 0.046
$\Delta\hat{q}_{WO}$	- 0.060	- 0.065	- 0.065
$\Delta\xi_{CAS2}$	0.0	- 0.033	- 0.026

TABLE 6. CLOSED-LOOP MAPPED EIGENVALUES (CONTINUED)

LON2 CLOSED-LOOP EIGENVALUES AT 77 m/s (150 kt)

MODE	INNER-LOOP	OPTIMAL 5 sps	SCHEDULED 5 sps
$\Delta\delta_e$	-23.4	-20.3	-20.3
$\Delta\hat{a}_h$	- 6.93	- 4.2	- 4.3
SHORT PERIOD	- 2.1 ±j2.8	- 2.6 ±j2.7	- 2.6 ±j2.7
Δu_e-Δz	0.0 ±j0.0	- 0.91±j0.43	- 0.86±j0.48
COMP. FILTER	- 0.40 ±j0.40	- 0.40±j0.40	- 0.40±j0.40
ΔEPR	- 0.50	- 0.68	- 0.70
Δu_t	0.0	- 0.19	- 0.19
PHUGOID	- 0.004±j0.067	- 0.14±j0.057	- 0.14±j0.06
$\Delta\xi_{h2}$	0.0	- 0.074	- 0.076
$\Delta\hat{q}_{WO}$	- 0.060	- 0.065	- 0.064
$\Delta\xi_{CAS2}$	0.0	- 0.033	- 0.034

TABLE 6. CLOSED-LOOP MAPPED EIGENVALUES (CONTINUED)

LON3 CLOSED-LOOP EIGENVALUES AT 77 m/2 (150 kt)

MODE	INNER-LOOP	OPTIMAL 5 sps	SCHEDULED 5 sps
$\Delta\delta_e$	-23.4	-20.4	-20.3
$\Delta\hat{a}_h$	- 6.93	- 4.1	- 4.2
SHORT PERIOD	- 2.1 ±j2.8	- 2.8 ±j2.8	- 2.8 ±j2.8
Δu_e-Δz	0.0 ±j0.0	- 0.82±j0.60	- 0.79±j0.61
COMP. FILTER	- 0.40 ±j0.40	- 0.40±j0.40	- 0.40±j0.40
ΔEPR	- 0.50	- 0.72	- 0.72
Δu_t	0.0	- 0.24	- 0.23
PHUGOID	- 0.0004±j0.067	- 0.20,-0.13	- 0.21,-0.13
$\Delta\xi_{h3}$	0.0	- 0.051	- 0.051
$\Delta\hat{q}_{WO}$	- 0.06	- 0.063	- 0.063
$\Delta\xi_{CAS3}$	0.0	- 0.032	- 0.032

TABLE 6. CLOSED-LOOP MAPPED EIGENVALUES (CONTINUED)

LAT1 CLOSED-LOOP EIGENVALUES AT 77 m/s (150 kt)

MODE	INNER-LOOP	OPTIMAL 20 sps	SCHEDULED 20 sps
$\Delta\delta_a$	-33.0	-33.0	-33.0
$\Delta\delta_r$	-21.1	-22.1	-22.1
$\Delta\hat{r}$-$\Delta\hat{p}$	- 6.8 ±j2.3	- 6.9 ±j2.6	- 6.9 ±j2.5
u_r	0.0	- 3.9	- 3.9
ROLL MODE-$\Delta\hat{r}_{WO}$	- 2.7 ±j0.91	- 2.4 ±j0.84	- 2.3 ±j0.92
DUTCH ROLL	- 0.53±j0.42	- 0.58 ±j0.82	- 0.61 ±j0.68
ϕ-u_a	0.0 ±j0.0	- 0.41 ±j0.30	- 0.44 ±j0.30
ζ-ξ_{r1}	0.0 ±j0.0	- 0.16 ±j0.21	- 0.17 ±j0.23
c-ξ_{c1}	0.0 ±j0.0	- 0.088±j0.084	- 0.085±j0.084

TABLE 6. CLOSED-LOOP MAPPED EIGENVALUES (CONTINUED)

LAT1 CLOSED-LOOP EIGENVALUES AT 77 m/s (150 kt)

MODE	INNER-LOOP	OPTIMAL 5 sps	SCHEDULED 5 sps
$\Delta\delta_r$	-33.0	-30.5	-31.2
$\Delta\delta_a$	-22.1	-22.2	-22.0
$\Delta\hat{r}$-$\Delta\hat{p}$	- 6.8 ±j2.3	- 6.8 ±j3.1	- 6.9 ±j3.1
u_r	0.0	- 4.6	- 4.6
ROLL MODE-$\Delta\hat{r}_{WO}$	- 2.7 ±j0.91	- 2.4 ±j0.87	- 2.4 ±j0.95
DUTCH ROLL	- 0.53±j0.42	- 0.58 ±j0.83	- 0.58 ±j0.67
ϕ-u_a	0.0 ±j0.0	- 0.38 ±j0.28	- 0.41 ±j0.22
ζ-ξ_{r1}	0.0 ±j0.0	- 0.17 ±j0.18	- 0.19 ±j0.20
c-ξ_{c1}	0.0 ±j0.0	- 0.095±j0.086	- 0.095±j0.08

TABLE 6. CLOSED-LOOP MAPPED EIGENVALUES (CONCLUDED)

LAT2 CLOSED-LOOP EIGENVALUES AT 77 m/s (150 kt)

MODE	INNER-LOOP	OPTIMAL 5 sps	SCHEDULED 5 sps
$\Delta\delta_r$	-33.0	-30.8	-31.0
$\Delta\delta_a$	-22.1	-22.0	-22.0
$\Delta\hat{r}$-$\Delta\hat{p}$	- 6.8 ±j2.3	- 6.9 ±j3.1	- 6.9 ±j3.1
u_r	0.0	- 4.6	- 4.6
ROLL MODE-$\Delta\hat{r}_{WO}$	- 2.7 ±j0.91	- 2.5 ±0.84	- 2.4 ±j0.9
DUTCH ROLL	- 0.53±j0.42	- 0.58 ±0.82	- 0.62 ±j0.73
ϕ-u_a	0.0 ±j0.0	- 0.37 ±0.30	- 0.36 ±j0.30
ζ-ξ_{r2}	0.0 ±j0.0	- 0.17 ±0.20	- 0.19 ±j0.21
c-ξ_{c2}	0.0 ±j0.0	- 0.10 ±0.12	- 0.095±j0.12

TABLE 7. SAMPLE OF CLOSED-LOOP EIGENVALUE VARIATIONS WITH AIRSPEED

VELOCITY (m/s)	SHORT PERIOD	PHUGOID	CONTROL SYSTEM
62	-1.7 ±j1.9	-0.009 ±j0.087	INNER-LOOP
69	-1.9 ±j2.6	-0.004 ±j0.082	
77	-2.1 ±j2.8	-0.0004±j0.067	
85	-2.1 ±j3.2	-0.0006±j0.062	
93	-1.7 ±j3.9	0.018 ±j0.049	
124	-1.2 ±j5.3	0.024 ±j0.026	
139	-1.0 ±j5.6	0.030 ±j0.013	
154	-0.95±j5.7	0.029 ±j0.012	
62	-1.06±j1.4	-0.26 ±j0.10	LON1 5 sps SCHEDULED
69	-2.5 ±j2.3	-0.23 ±j0.018	
77	-2.6 ±j2.8	-0.25, -0.17	
85	-2.4 ±j3.3	-0.26, -0.14	
93	-1.9 ±j3.9	-0.28, -0.052+j0.04	
124	-1.2 ±j5.2	-0.36, -0.045+j0.035	
139	-1.0 ±j5.5	-0.42, -0.041+j0.042	
154	-1.0 ±j5.5	-0.50, -0.045+j0.041	
62	-1.1 ±j1.8	-0.15 ±j0.09	LON2 5 sps SCHEDULED
69	-2.6 ±j2.3	-0.14 ±j0.06	
77	-2.6 ±j2.7	-0.14 ±j0.06	
85	-2.5 ±j3.2	-0.14 ±j0.02	
93	-1.7 ±j4.0	-0.25 ±j0.03	
124	-1.0 ±j5.3	-0.33, -0.04 +j0.012	
139	-0.84±j5.5	-0.32, -0.04 +j0.026	
154	-0.81±j5.6	-0.30, -0.04 +j0.026	
62	-1.0 ±j1.3	-0.19 ±j0.072	LON3 5 sps SCHEDULED
69	-2.7 ±j2.3	-0.18 ±j0.008	
77	-2.8 ±j2.8	-0.21, -0.13	
85	-2.6 ±j3.3	-0.23, -0.09	
93	-1.7 ±j4.0	-0.27, -0.046+j0.014	
124	-1.03±j5.3	-0.33, -0.036+j0.011	
139	-0.88±j5.5	-0.32, -0.037+j0.020	
154	-0.84±j5.7	-0.30, -0.037+j0.020	

TABLE 7. SAMPLE OF CLOSED-LOOP EIGENVALUE VARIATIONS WITH AIRSPEED (CONCLUDED)

VELOCITY (m/s)	DUTCH ROLL	CROSS TRACK	CONTROL SYSTEM
62	-0.62±j0.59	0.0 ±j0.0	INNER-LOOP
69	-0.53±j0.42	"	
77	-0.57±j0.36	"	
85	-0.58±j0.37	"	
93	-0.59±j0.42	"	
124	-0.60±j0.38	"	
139	-0.81,-0.70	"	
154	-0.96,-0.62	"	
62	-0.59±j0.97	-0.19 ±j0.21	LAT1 5 sps OPTIMAL
69	-0.56±j0.87	-0.17 ±j0.18	
77	-0.59±j0.78	-0.18 ±j0.17	
85	-0.53±j0.81	-0.15 ±j0.17	
93	-0.64±j0.86	-0.11 ±j0.13	
124	-0.71±j0.86	-0.11 ±j0.15	
139	-0.69±j0.75	-0.093±j0.14	
154	-0.66±j0.75	-0.080±j0.098	
62	-0.56±j1.0	-0.19 ±j0.20	LAT1 5 sps SCHEDULED
69	-0.58±j0.67	-0.19 ±j0.20	
77	-0.57±j0.79	-0.17 ±j0.17	
85	-0.53±j0.85	-0.15 ±j0.16	
93	-0.68±j0.89	-0.16 ±j0.14	
124	-0.55±j0.81	-0.090±j0.15	
139	-0.68±j0.74	-0.090±j0.13	
154	-0.77±j0.78	-0.080±j0.11	

TABLE 8. MINIMUM SINGULAR VALUES FOR LON2, 5 sps, SCHEDULED GAINS

VELOCITY (m/s)	FIRST MINIMUM SINGULAR VALUE (DB)	FREQUENCY (RAD/SEC)	SECOND MINIMUM SINGULAR VALUE (DB)	FREQUENCY (RAD/SEC)
62	-3.6	0.19	-3.2	1.3
69	-3.0	0.21	-3.1	1.2
77	-3.0	0.21	-3.2	1.1
85	-2.8	0.19	-3.2	1.0
93	-1.9	0.17	-3.2	0.91
124	-1.7	0.16	-3.4	1.0
139	-1.9	0.16	-3.5	1.0
154	-1.8	0.16	-3.6	1.0

TABLE 9. MINIMUM SINGULAR VALUES FOR LON2, 20 sps, SCHEDULED GAINS

VELOCITY (m/s)	FIRST MINIMUM SINGULAR VALUE (DB)	FREQUENCY (RAD/SEC)	SECOND MINIMUM SINGULAR VALUE (DB)	FREQUENCY (RAD/SEC)
61	-3.2	0.23	-4.0	1.0
69	-2.5	0.21	-3.8	1.1
77	-2.5	0.20	-3.8	1.1
85	-2.5	0.19	-4.0	1.0
92	-1.8	0.17	-4.0	1.0
123	-1.7	0.17	-4.0	1.0
138	-1.9	0.17	-4.0	1.0
154	-1.0	0.17	-4.0	1.0

TABLE 10. MINIMUM SINGULAR VALUES FOR LAT1, SCHEDULED GAINS

	5 sps		20 sps	
VELOCITY (m/s)	SINGULAR VALUE (DB)	FREQUENCY (RAD/SEC)	SINGULAR VALUE (DB)	FREQUENCY (RAD/SEC)
62	-12.3	0.53	-11.9	0.48
69	-12.6	0.58	-12.3	0.53
77	-17.3	0.44	-17.2	0.44
85	-17.2	0.43	-17.1	0.44
93	-20.1	0.40	-20.1	0.40
124	-23.2	0.53	-23.0	0.44
139	-23.5	0.48	-23.5	0.40
154	-25.9	0.44	-26.2	0.36

TABLE 11. MINIMUM SINGULAR VALUES FOR LON1, 5 sps, SCHEDULED GAINS

VELOCITY (m/s)	FIRST MINIMUM SINGULAR VALUE (DB)	FREQUENCY (RAD/SEC)	SECOND MINIMUM SINGULAR VALUE (DB)	FREQUENCY (RAD/SEC)
62	-6.0	0.08	-3.4	1.4
69	-5.2	0.08	-3.2	1.1
77	-5.2	0.09	-3.2	1.1
85	-4.7	0.10	-3.1	1.1
93	-2.4	0.15	-5.8	1.1
124	-	-	-7.3	0.9
139	-	-	-8.0	0.9
154	-2.6	0.15	-8.2	0.8

TABLE 12. MINIMUM SINGULAR VALUES FOR LON3, 5 sps, SCHEDULED GAINS

VELOCITY (m/s)	FIRST MINIMUM SINGULAR VALUE (DB)	FREQUENCY (RAD/SEC)	SECOND MINIMUM SINGULAR VALUE (DB)	FREQUENCY (RAD/SEC)
62	-2.7	0.21	-3.1	1.6
69	-2.7	0.21	-3.1	1.6
77	-2.9	0.21	-2.6	1.2
85	-2.7	0.19	-2.6	1.1
93	-1.8	0.17	-2.6	1.0
124	-1.6	0.16	-2.8	1.0
139	-1.8	0.16	-2.9	1.0
154	-1.8	0.16	-3.0	1.1

TABLE 13. MINIMUM SINGULAR VALUES FOR LAT1, 5 sps, SCHEDULED GAINS

VELOCITY (m/s)	MINIMUM SINGULAR VALUE (DB)	FREQUENCY (RAD/SEC)	MINIMUM SINGULAR VALUE (DB)	FREQUENCY (RAD/SEC)
62	-6.0	1.1	-3.3	0.56
69	-6.0	1.0	-2.8	0.58
77	-5.0	1.0	-3.5	0.52
85	-5.0	1.0	-2.7	0.58
93	-4.2	1.2	-3.3	0.58
124	-4.7	1.0	-3.3	0.63
139	-4.4	1.0	-2.5	0.58
154	-3.9	1.0	-2.2	0.52

TABLE 14. LAT2 FREQUENCY DOMAIN PROPERTIES, 5 sps, SCHEDULED GAINS, $\Delta\delta_a$ LOOP OPEN, $\Delta\delta_r$ LOOP CLOSED

VELOCITY (m/s)	MINUMUM SINGULAR VALUE (DB)	FREQUENCY (RAD/SEC)	FIRST GAIN MARGIN (DB)	FREQUENCY (RAD/SEC)
62	-6.1	1.1	11.5	0.25
69	-6.1	1.0	10.3	0.25
77	-5.5	1.0	11.6	0.23
85	-5.2	1.0	12.4	0.23
93	-4.5	1.2	25.2	0.22
124	-4.6	1.2	12.2	0.25
139	-4.8	1.2	12.4	0.25
154	-5.1	1.1	12.8	0.27

TABLE 14. LAT2 FREQUENCY DOMAIN PROPERTIES, 5 sps, SCHEDULED GAINS, $\Delta\delta_a$ LOOP OPEN, $\Delta\delta_r$ LOOP CLOSED (CONCLUDED)

VELOCITY (m/s)	PHASE MARGIN (DEG)	FREQUENCY (RAD/SEC)	SECOND GAIN MARGIN (DB)	FREQUENCY (RAD/SEC)
62	38	0.69	-10.0	1.8
69	36	0.69	- 9.5	1.8
77	39	0.63	- 9.8	1.6
85	40	0.63	-10.1	1.7
93	49	.65	-10.2	1.7
124	42	.63	-10.7	1.7
139	41	.61	-11.5	1.7
154	39	.63	-10.8	1.7

TABLE 15. CURVED TRAJECTORY FLIGHT CONDITIONS

WAYPOINT	X (m)	Y (m)	Z (m)	RADIUS (m)
A	-6706.0	2896.0	-1406.0	0
B	-6706.0	- 107.0	-1406.0	2286.0
C	-7209.0	-3048.0	- 829.0	2286.0
D	-4923.0	-2743.0	- 383.5	0
E	-4923.0	0.0	- 256.8	1524.0
F	1000.0	0.0	0.0	0.0
AIRCRAFT STARTING POSITION	-6706.0	1981.0	-1406.0	0

WAYPOINT	LATITUDE (DEG)	LONGITUDE (DEG)	SPEED (m/s)
A	38.01214601	-75.44233621	75.0
B	37.99775995	-75.41336030	75.0
C	37.98749129	-75.38191319	75.0
D	37.97157281	-75.39875636	75.0
E	37.98472385	-75.42522296	69.5
F	37.9449551	-75.45699678	69.5
AIRCRAFT STARTING POSITION	38.00776522	-75.43350985	69.5

AIRCRAFT PARAMETERS	WEIGHT 85000.0 lbs	CG 0.2	FLAPS 40 deg-FIXED
	INITIAL HEADING 122.2 deg	INNER-LOOP SAMPLE RATE 20 sps-ALWAYS	OUTER-LOOP SAMPLE RATE VARIES IN FIGURES

a) DESIGN CONFIGURATION

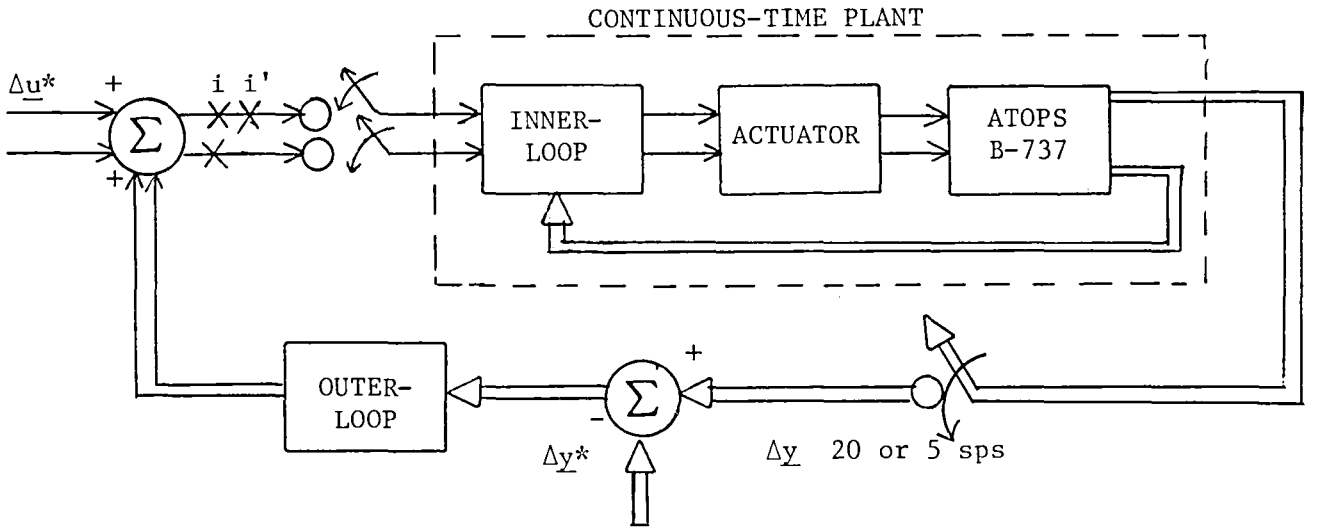

b) IMPLEMENTATION CONFIGURATION

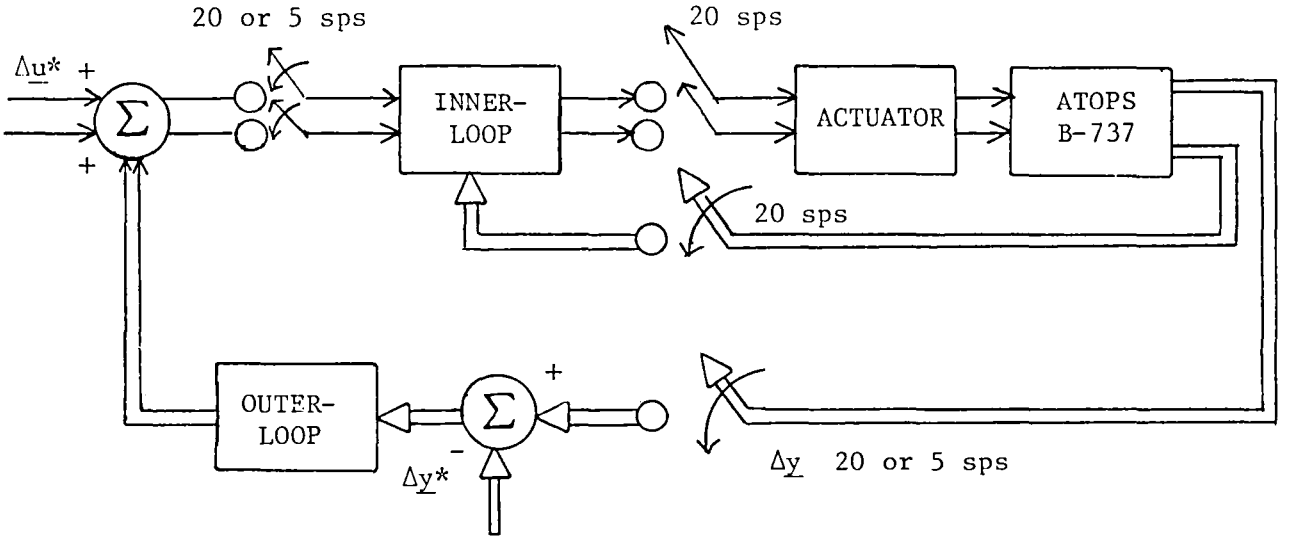

FIGURE 1. INNER-LOOP, OUTER-LOOP CONTROL SYSTEM BLOCK DIAGRAMS

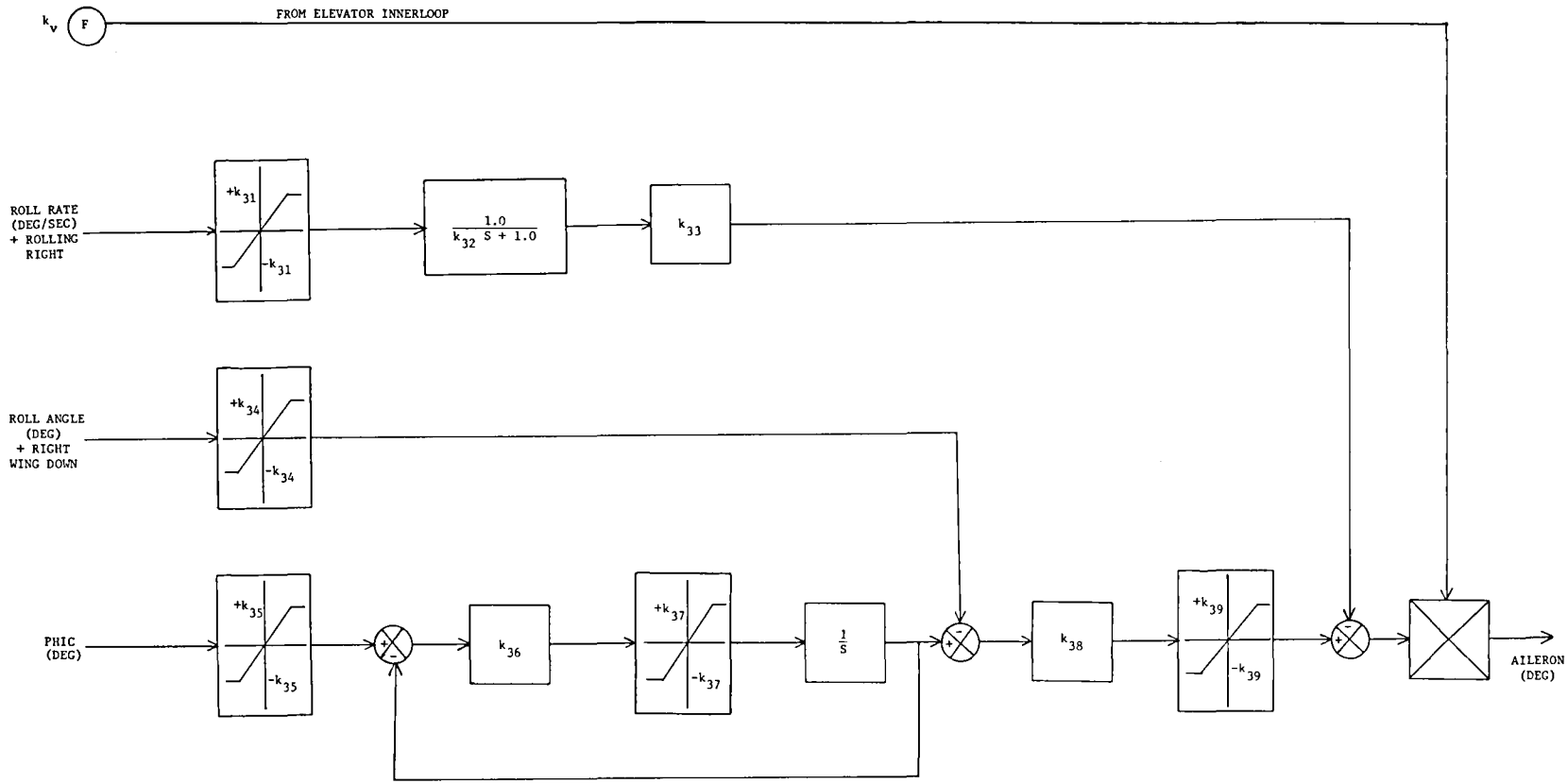

FIGURE 2. AILERON/SPOILER INNER-LOOP CONTROL SYSTEM BLOCK DIAGRAM

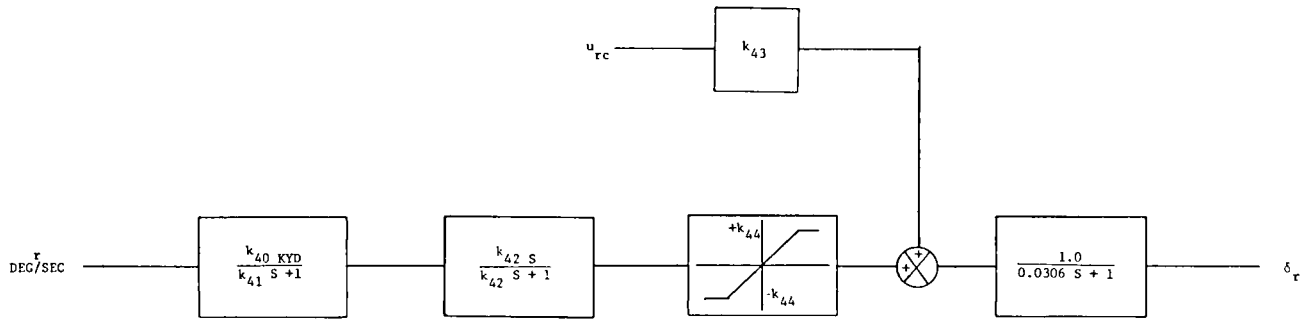

FIGURE 3. YAW DAMPER AND RUDDER ACTUATOR MODEL BLOCK DIAGRAM

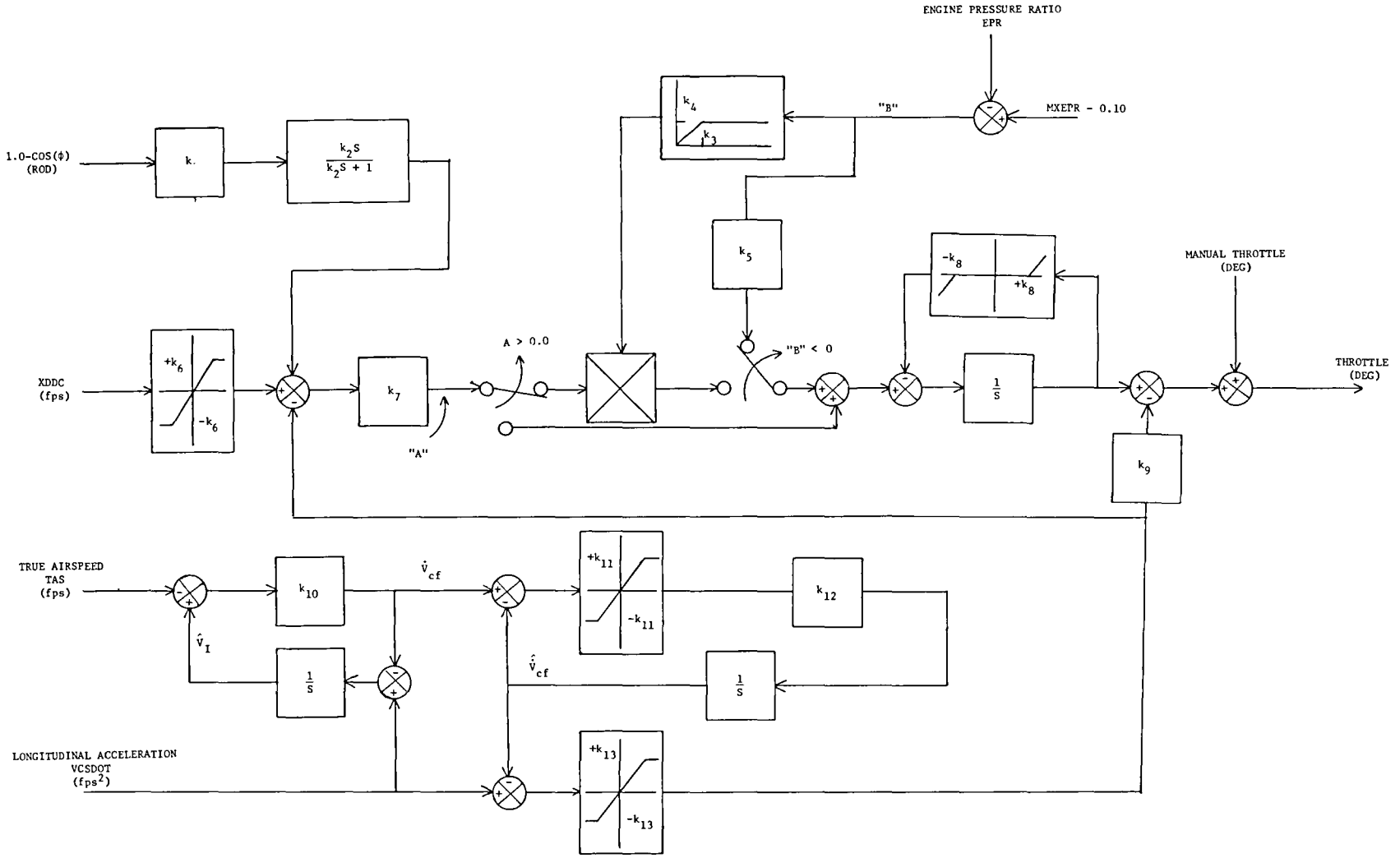

FIGURE 4. AUTOTHROTTLE INNER-LOOP CONTROL SYSTEM BLOCK DIAGRAM

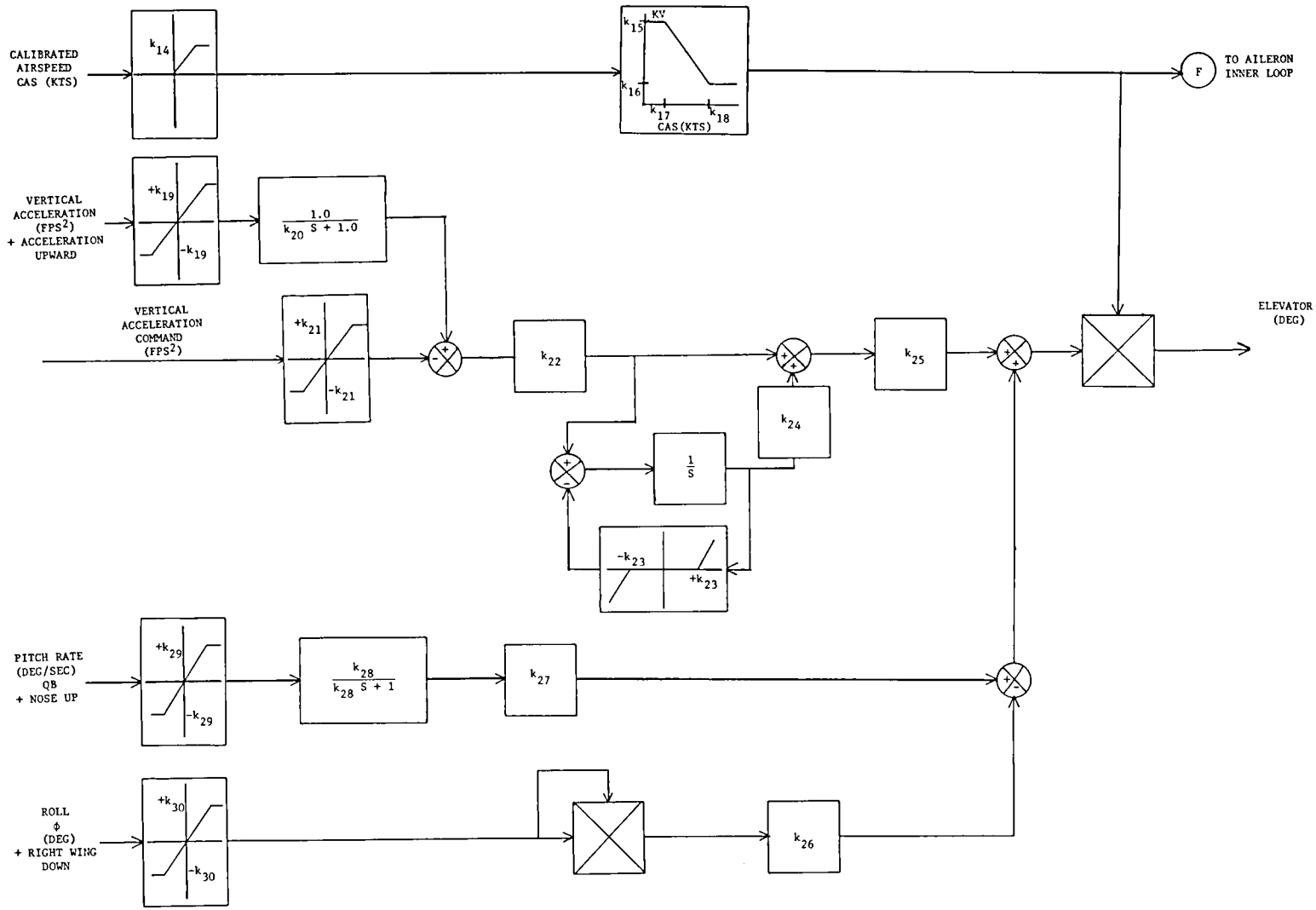

FIGURE 5. ELEVATOR INNER-LOOP CONTROL SYSTEM BLOCK DIAGRAM

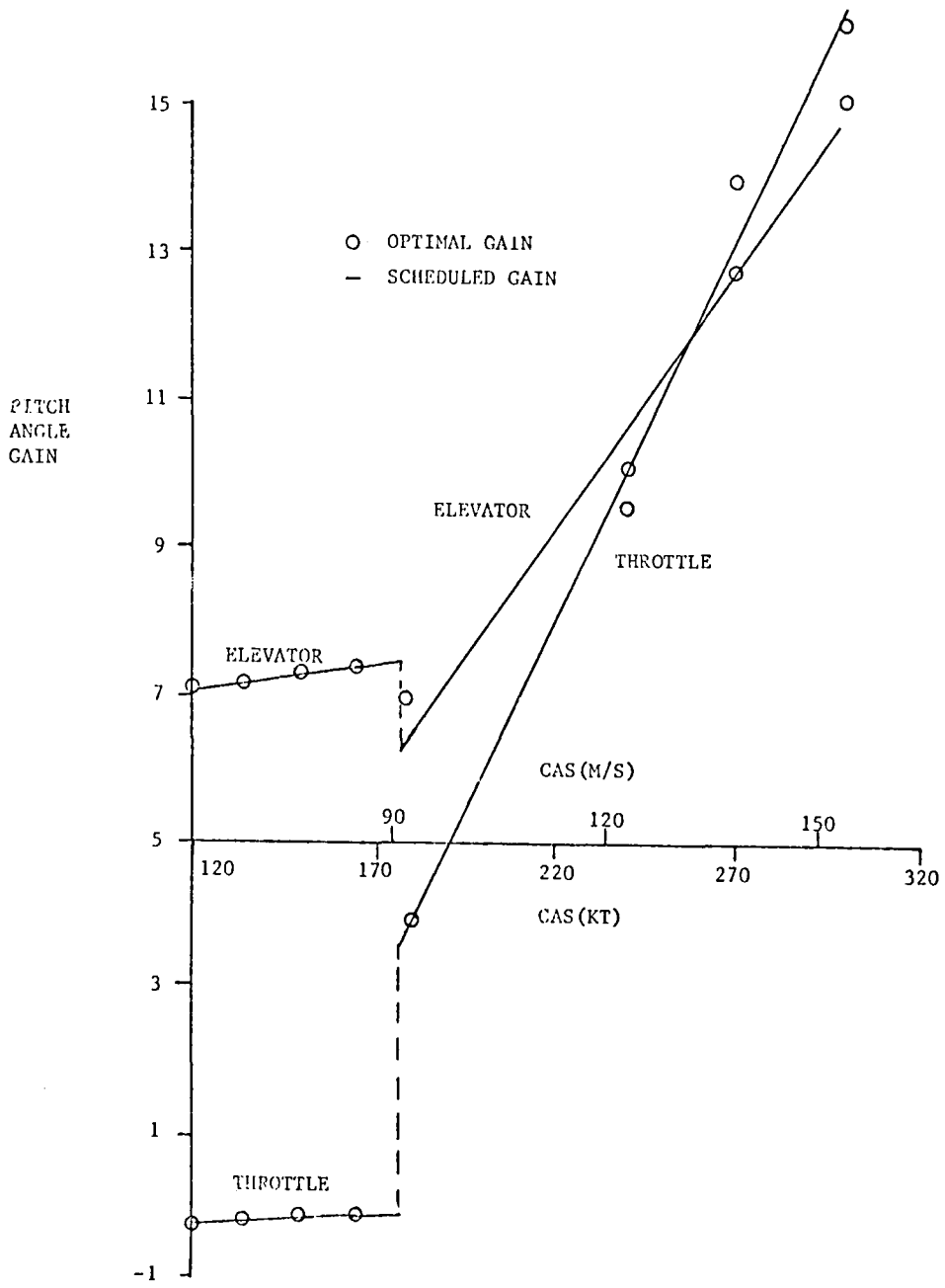

FIGURE 6. COMPARISON OF LON3 OPTIMAL AND GAIN SCHEDULED GAINS

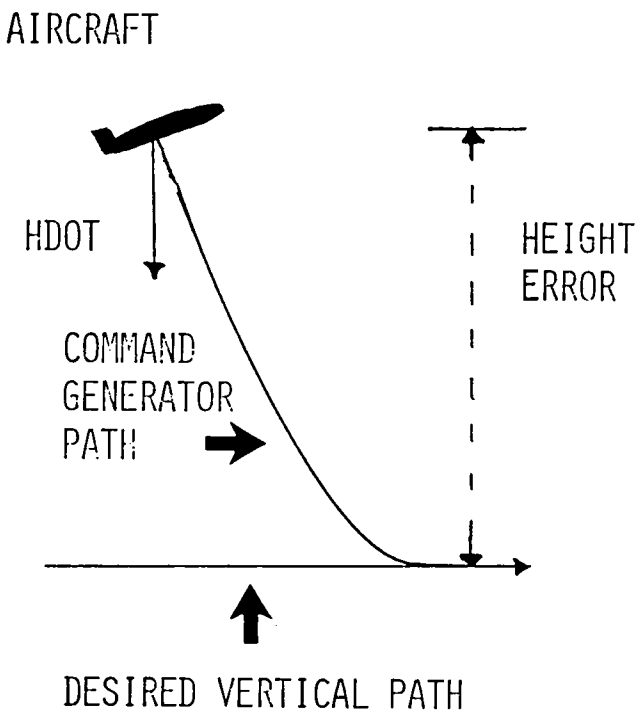

FIGURE 7. ALTITUDE CAPTURE

a) LON1

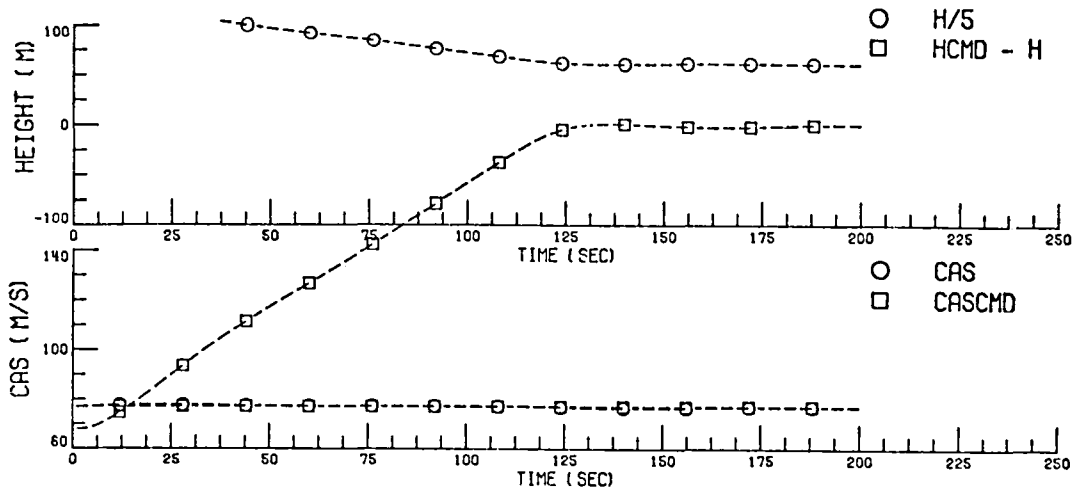

b) LON2

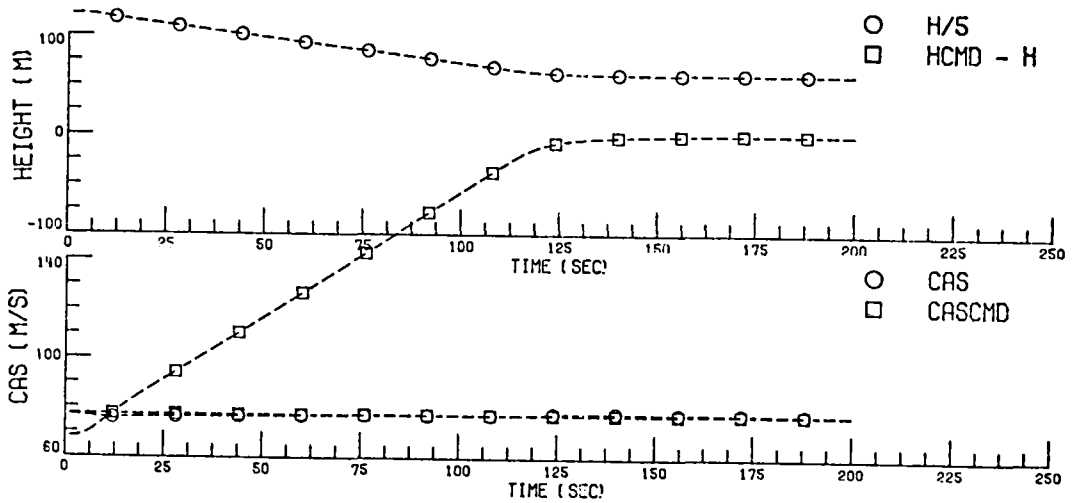

c) LON3

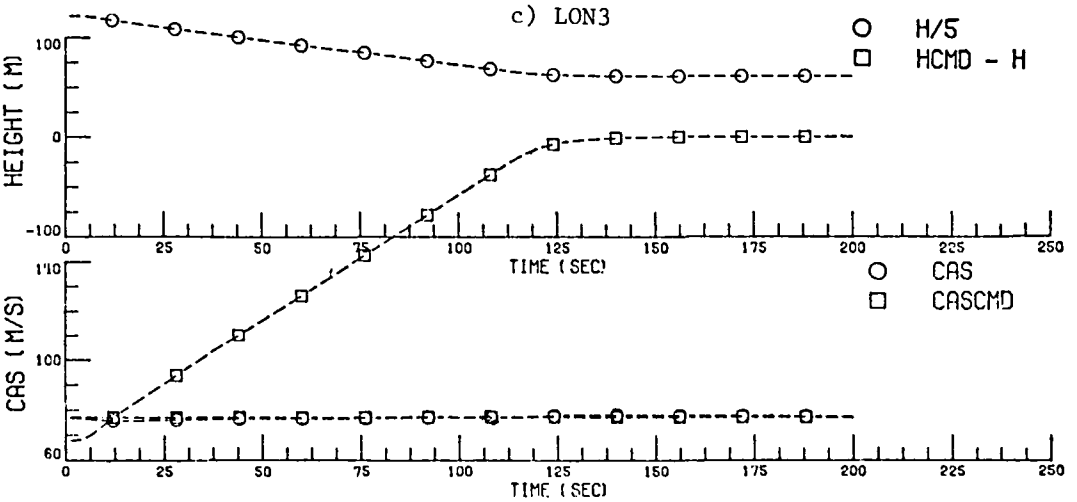

FIGURE 8. ALTITUDE CAPTURE SIMULATION, 5 sps OUTER-LOOP

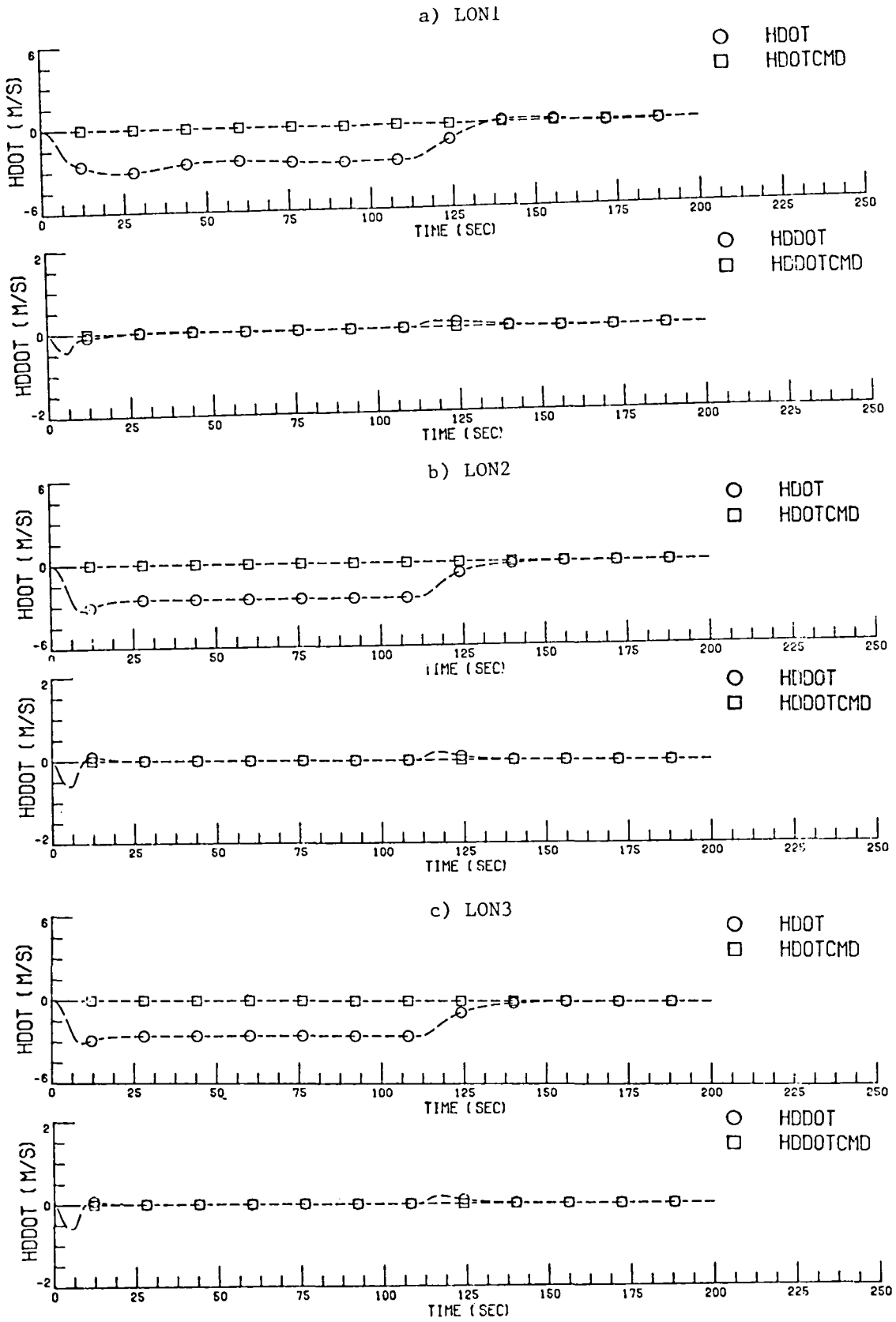

FIGURE 8. ALTITUDE CAPTURE SIMULATION, 5 sps OUTER-LOOP (CONCLUDED)

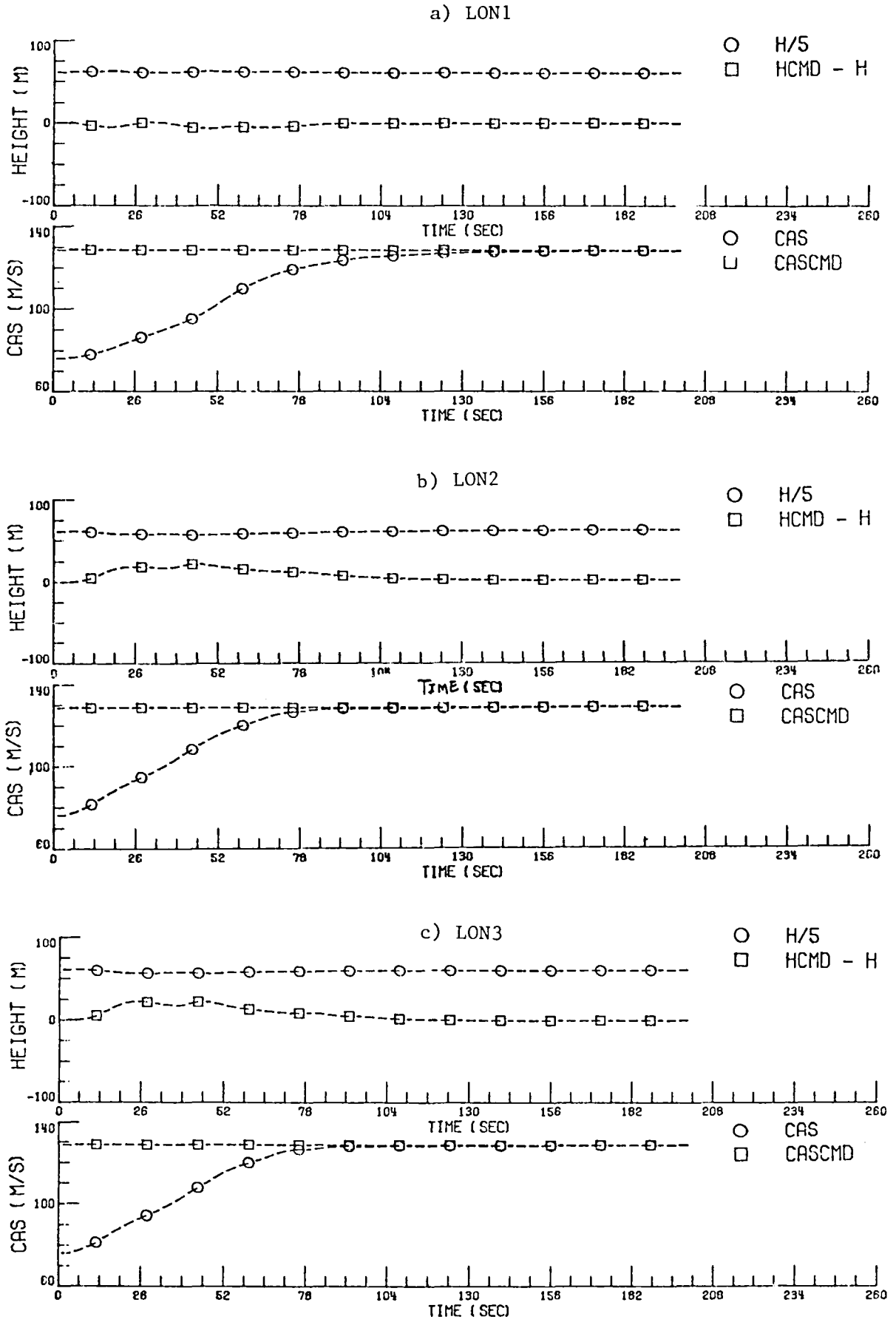

FIGURE 9. CAS CAPTURE SIMULATION, 5 sps OUTER-LOOP

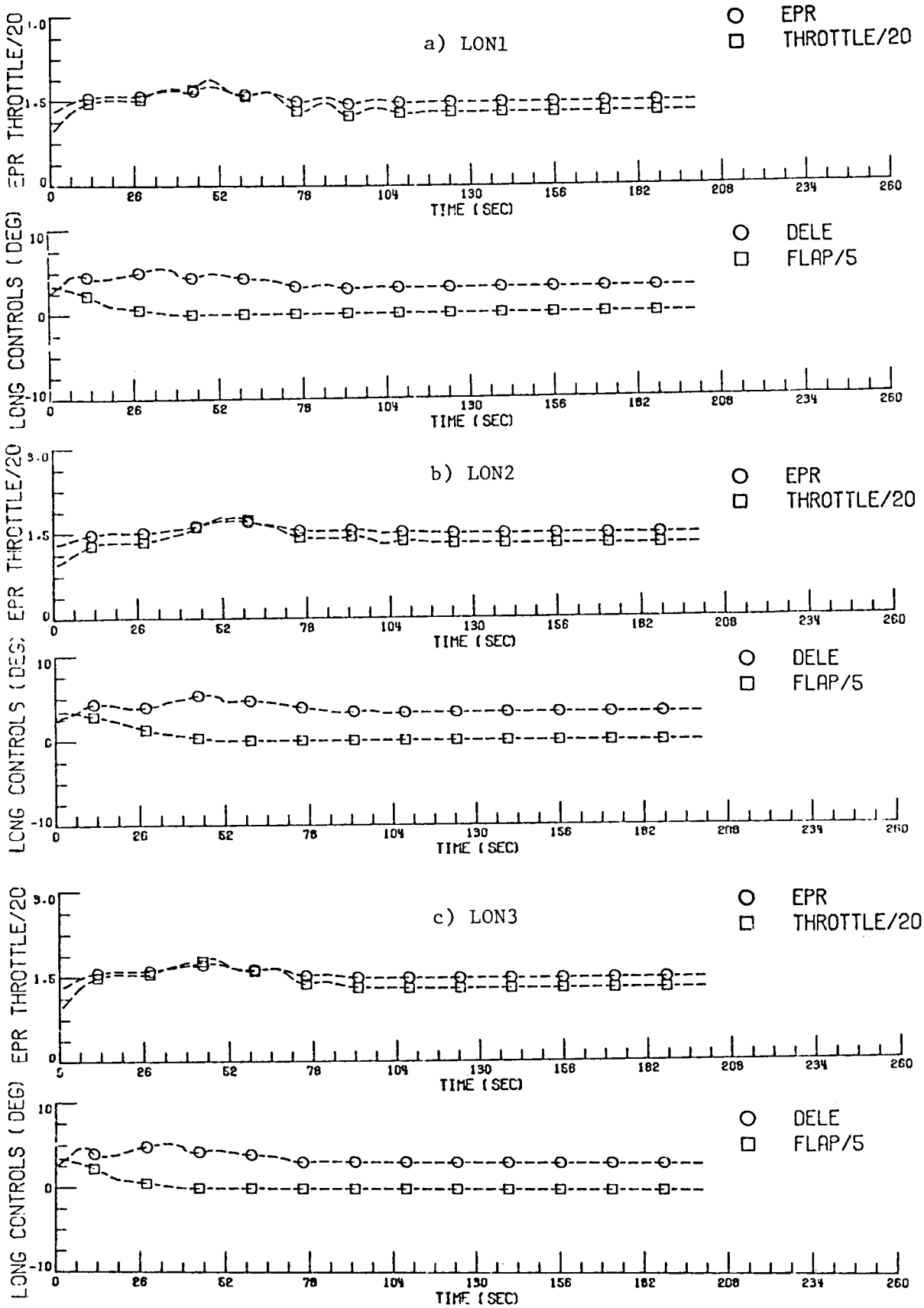

FIGURE 9. CAS CAPTURE SIMULATION, 5 sps OUTER-LOOP (CONCLUDED)

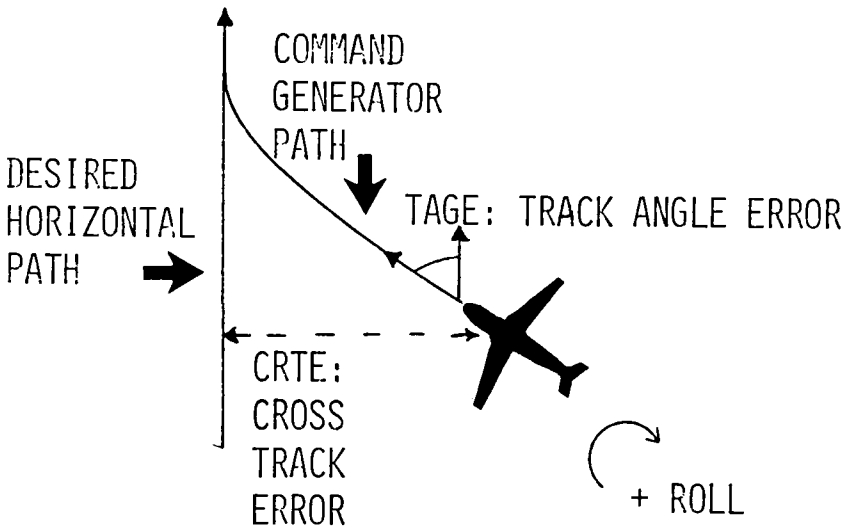

FIGURE 10. HORIZONTAL PATH CAPTURE

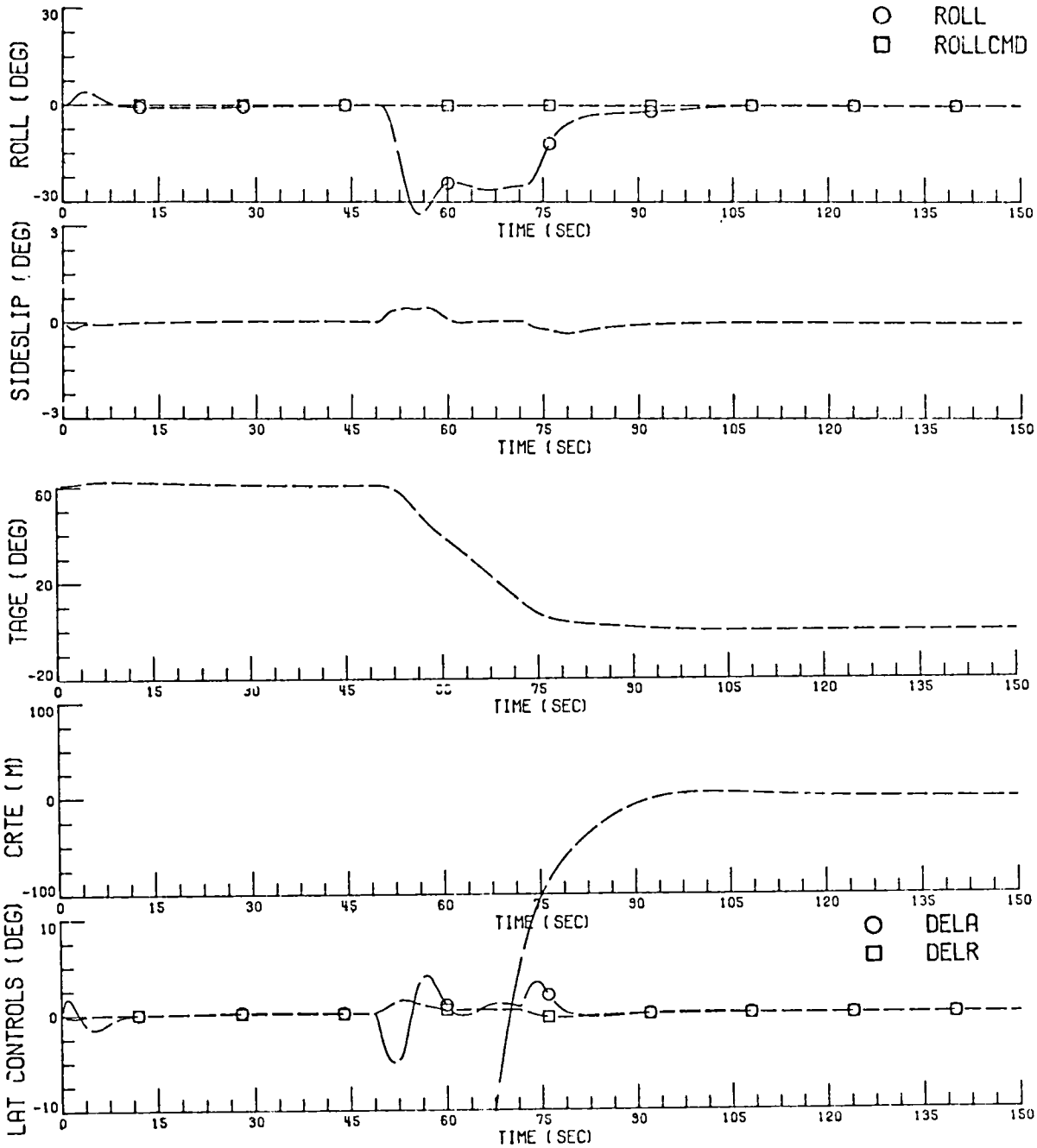

FIGURE 11. LAT1 HORIZONTAL CAPTURE, 5 sps OUTER-LOOP

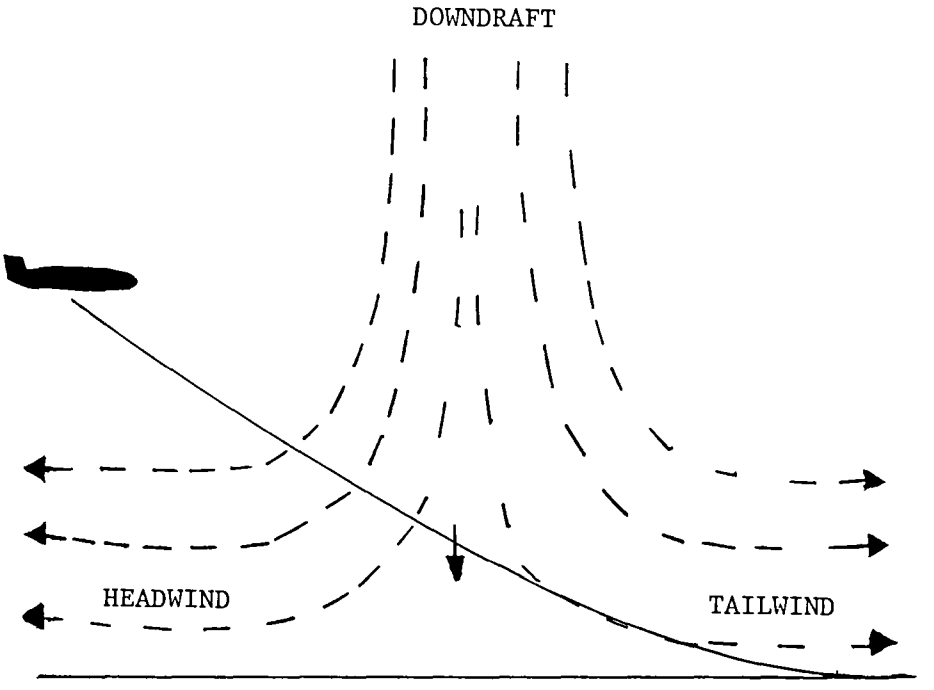

FIGURE 12. WIND SHEAR ENVIRONMENT

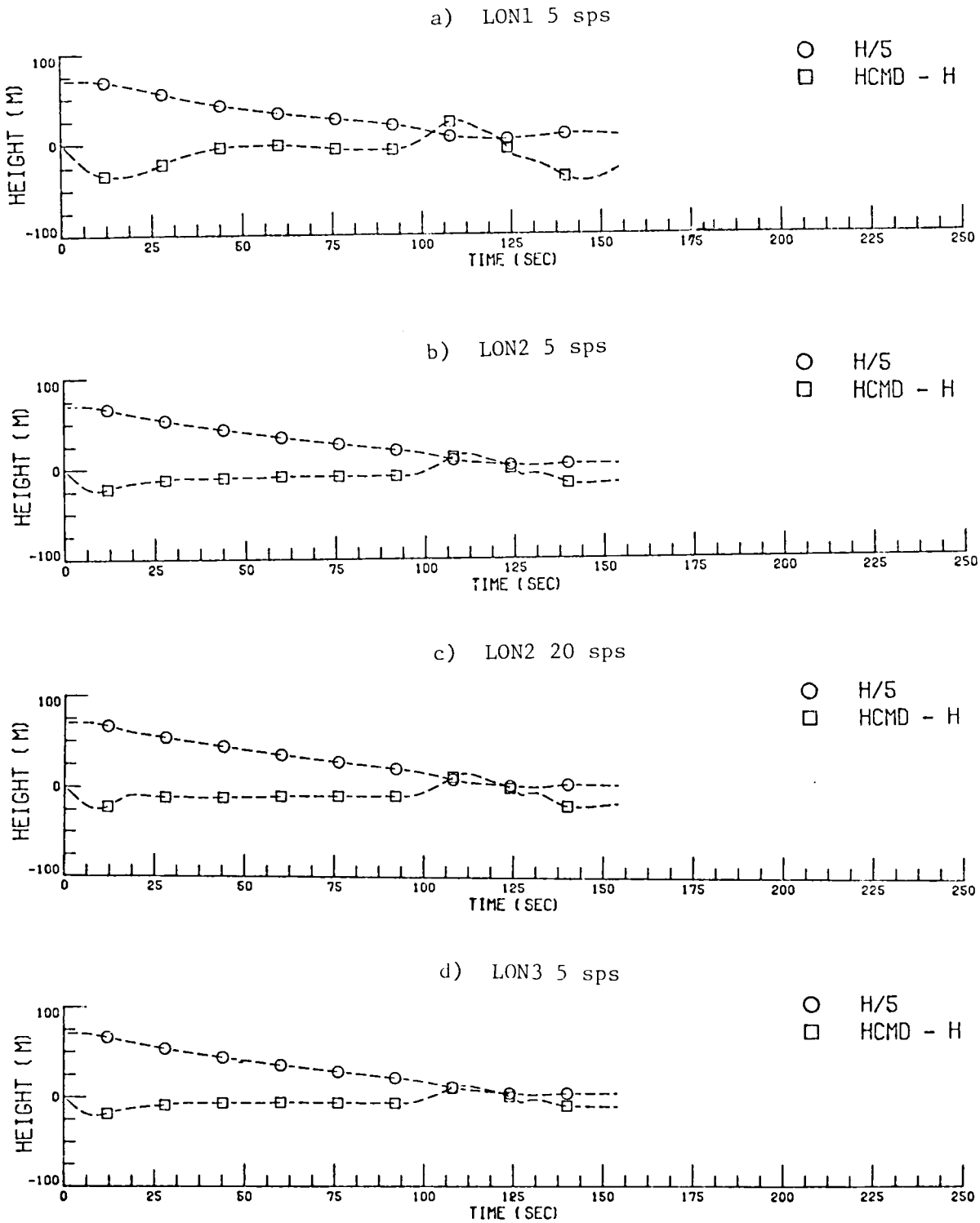

FIGURE 13. WIND SHEAR SIMULATION

a) LON1 5 sps

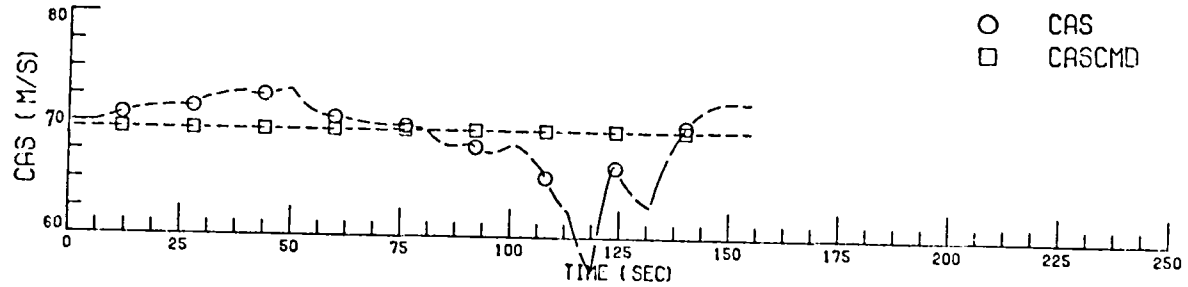

b) LON2 5 sps

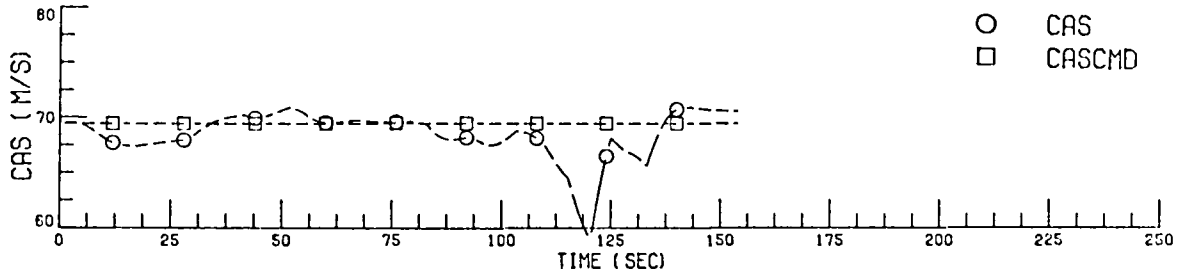

c) LON2 20 sps

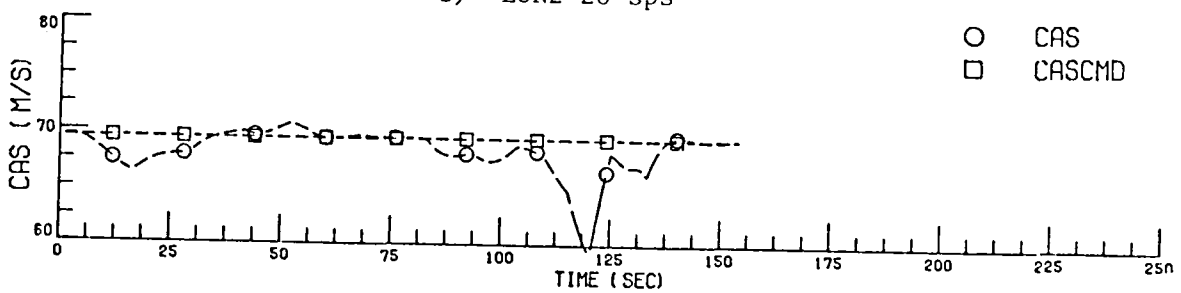

d) LON3 5 sps

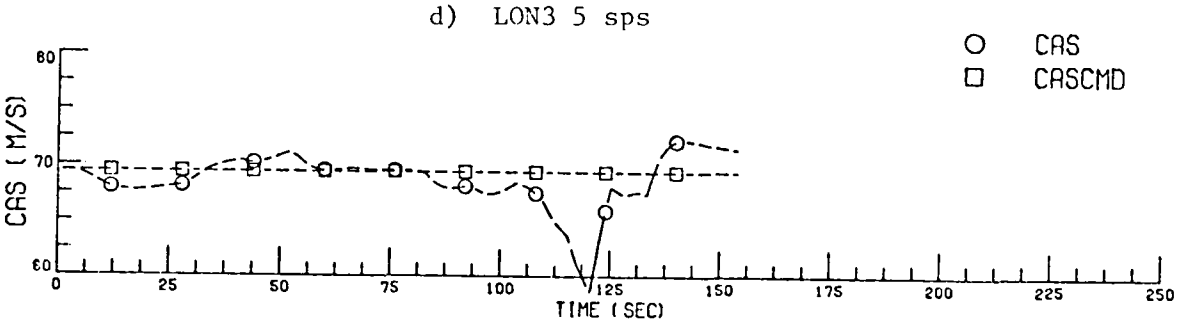

FIGURE 13. WIND SHEAR SIMULATION (CONCLUDED)

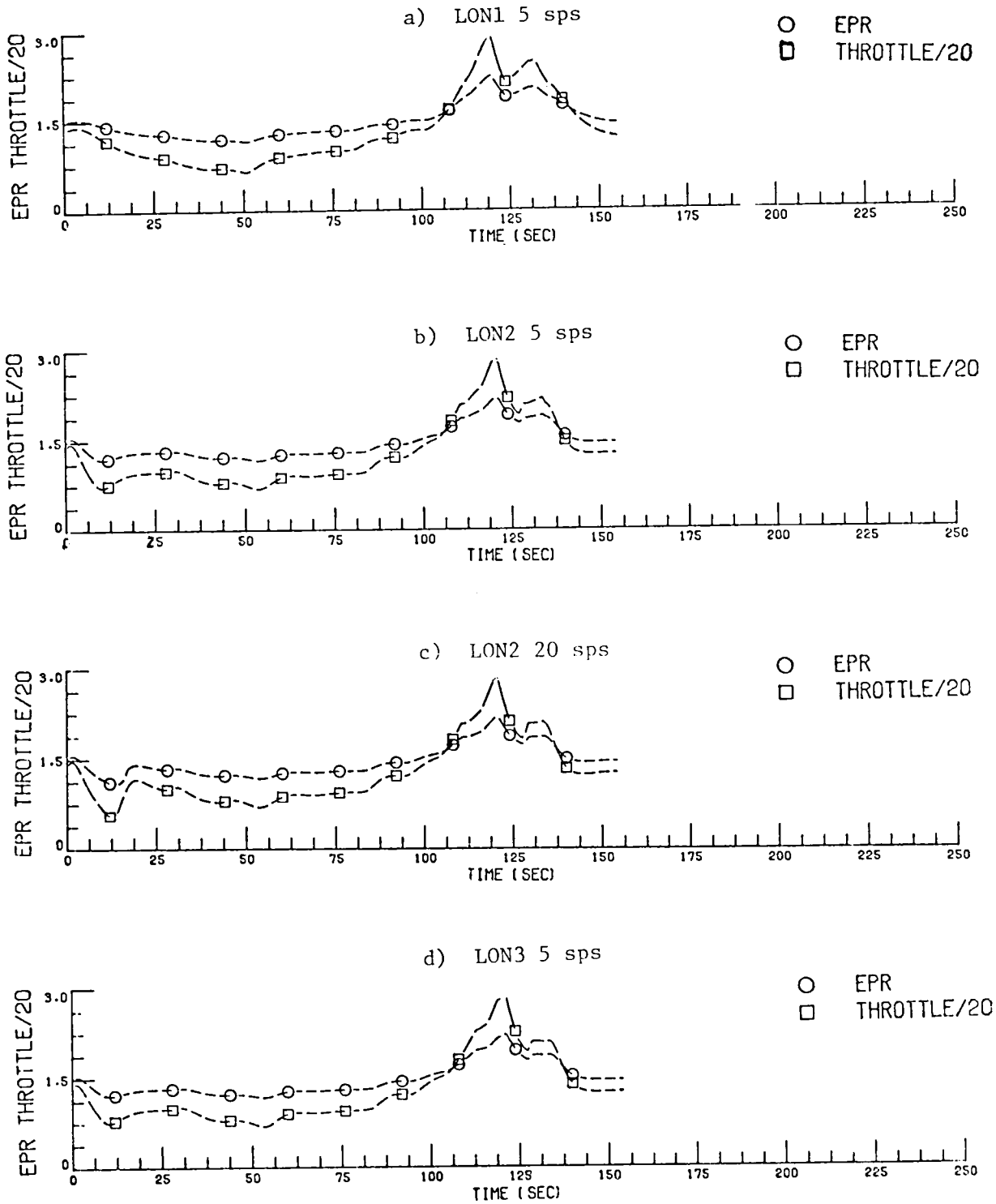

FIGURE 14. WIND SHEAR SIMULATION: THROTTLE RESPONSE

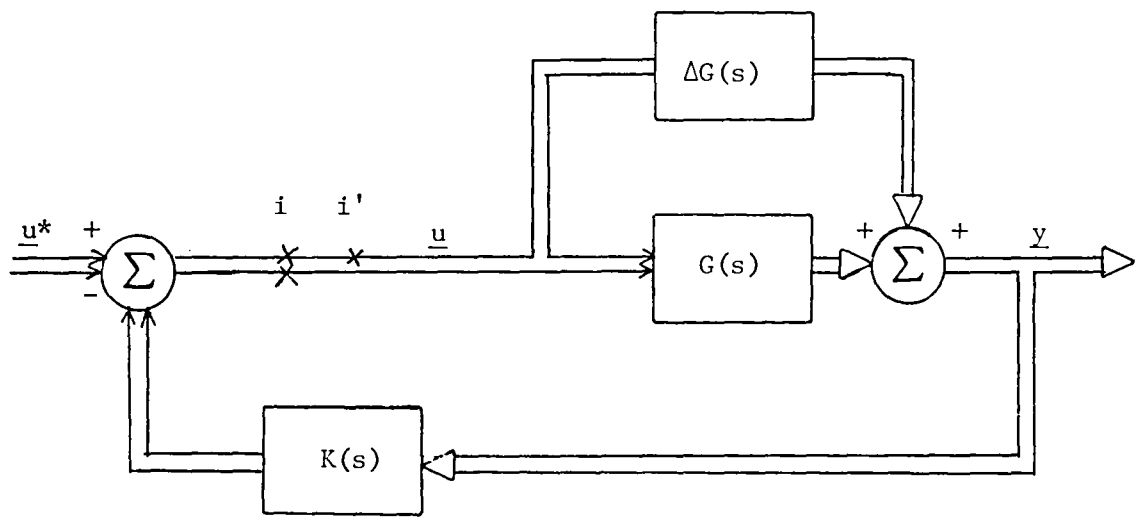

FIGURE 15. CONTROL SYSTEM BLOCK DIAGRAM FOR FREQUENCY DOMAIN EVALUATION

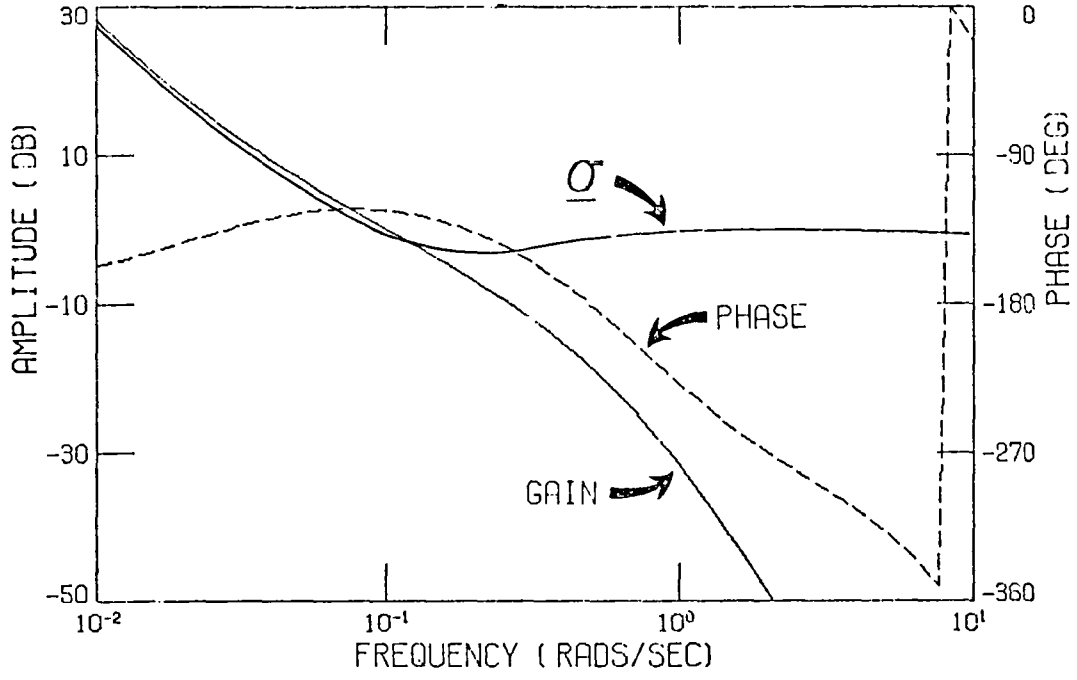

FIGURE 16. LON2 THROTTLE LOOP FREQUENCY RESPONSE USING SCHEDULED GAINS, OUTER-LOOP SAMPLE RATE = 5 sps

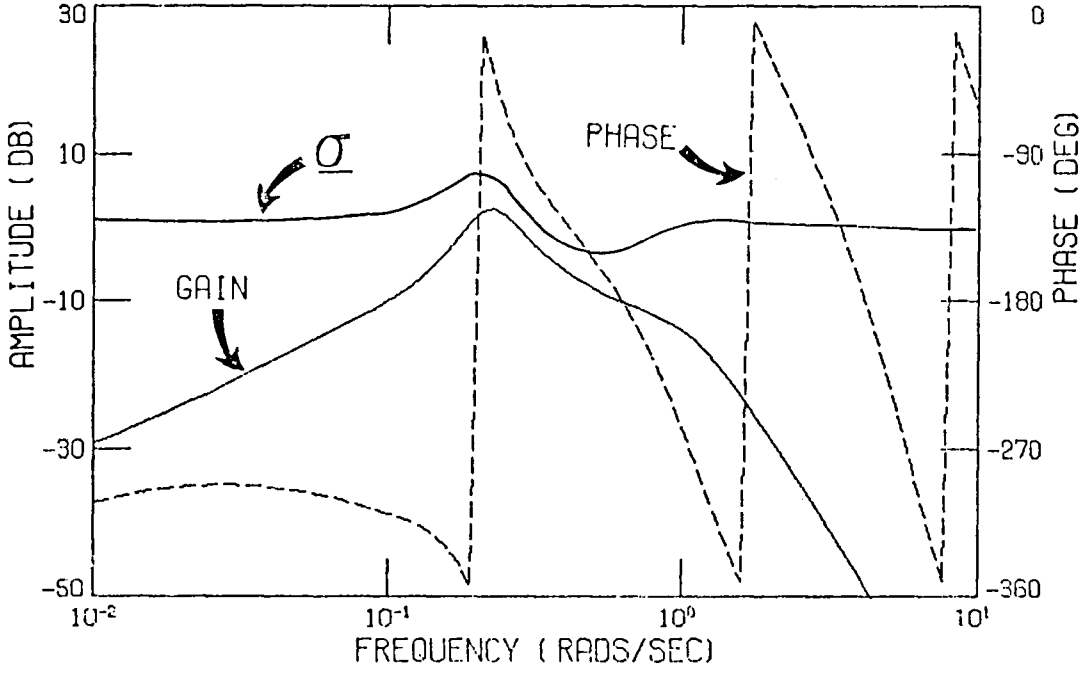

FIGURE 17. LAT1 RUDDER LOOP FREQUENCY RESPONSE USING SCHEDULED GAINS, OUTER-LOOP SAMPLE RATE = 5 sps

a) LON2

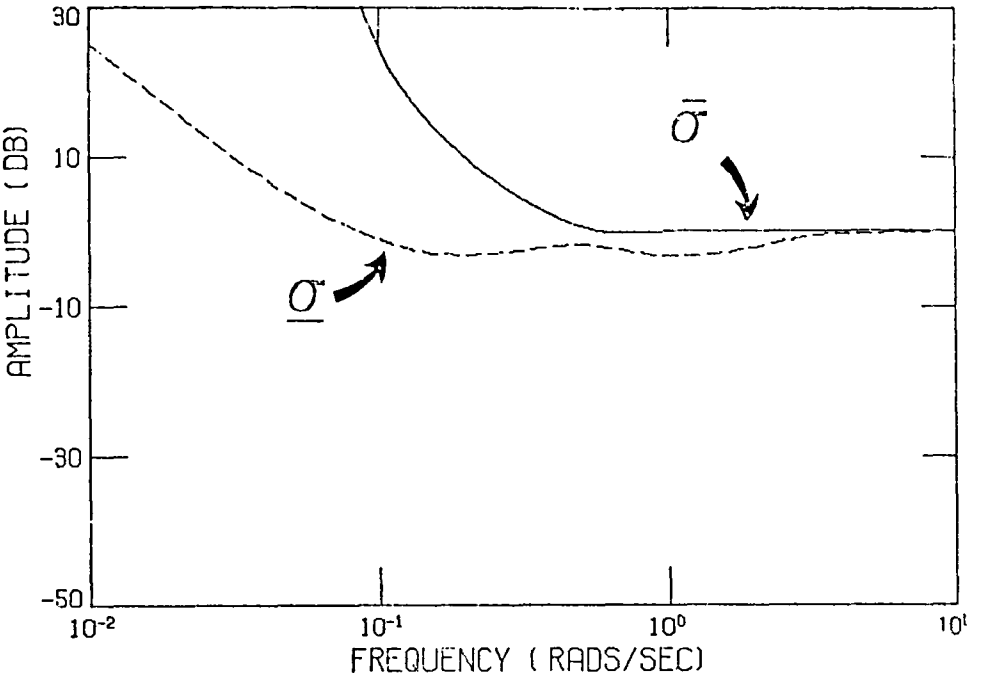

b) LAT1

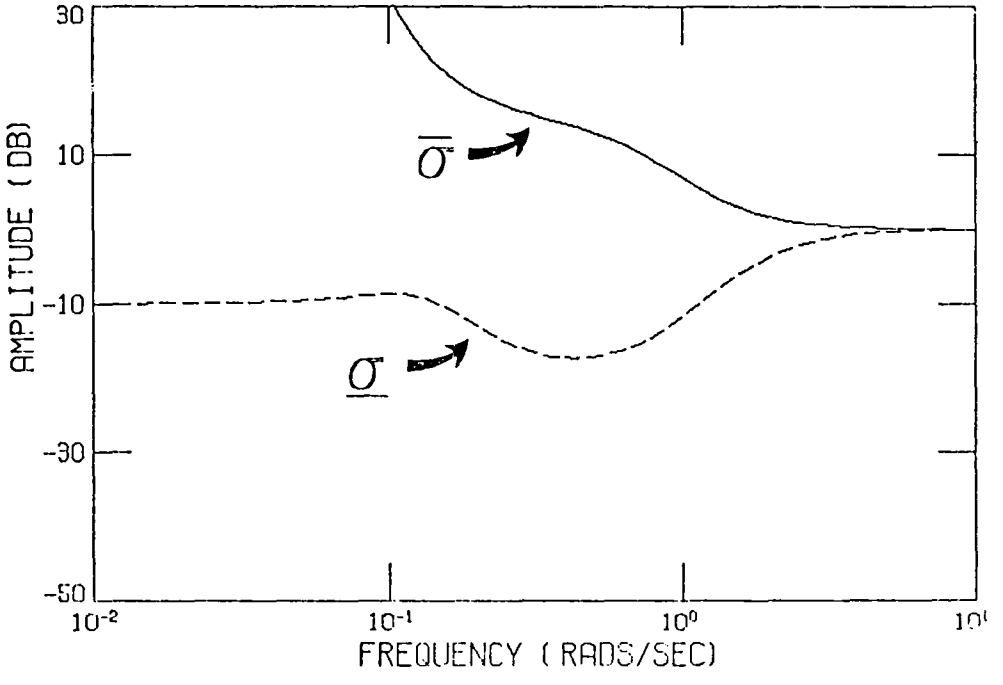

FIGURE 18. LON2 (TOP) AND LAT1 (BOTTOM) SIGMA PLOTS USING SCHEDULED GAINS, OUTER-LOOP SAMPLE RATE = 5 sps

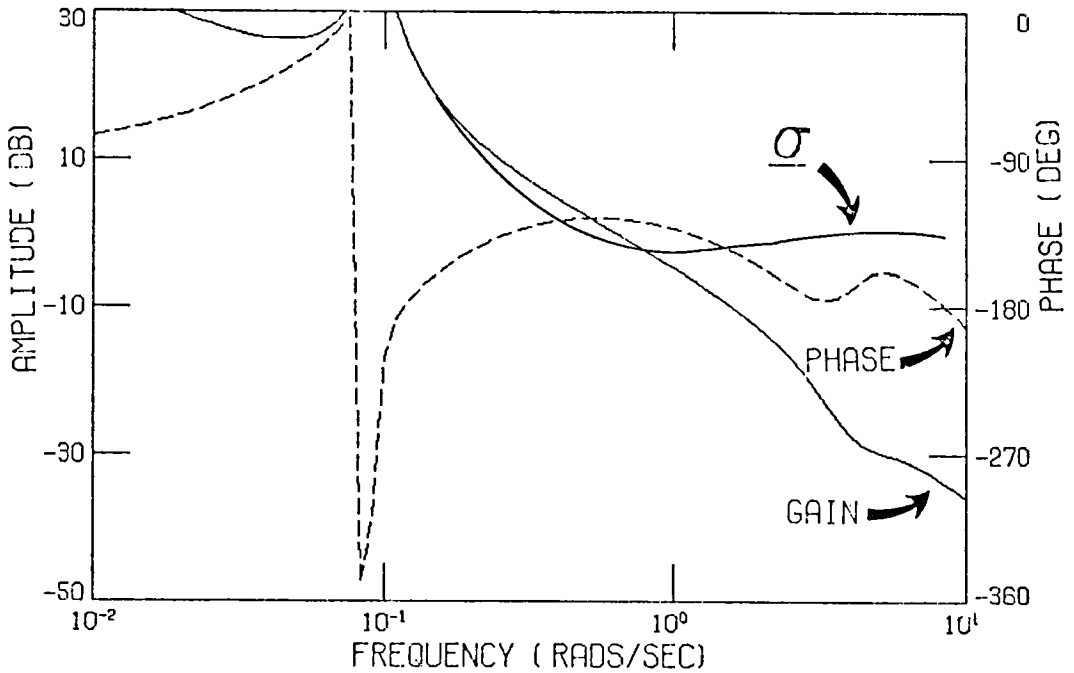

FIGURE 19. LON2 ELEVATOR LOOP FREQUENCY RESPONSE USING SCHEDULED GAINS, OUTER-LOOP SAMPLE RATE = 5 sps

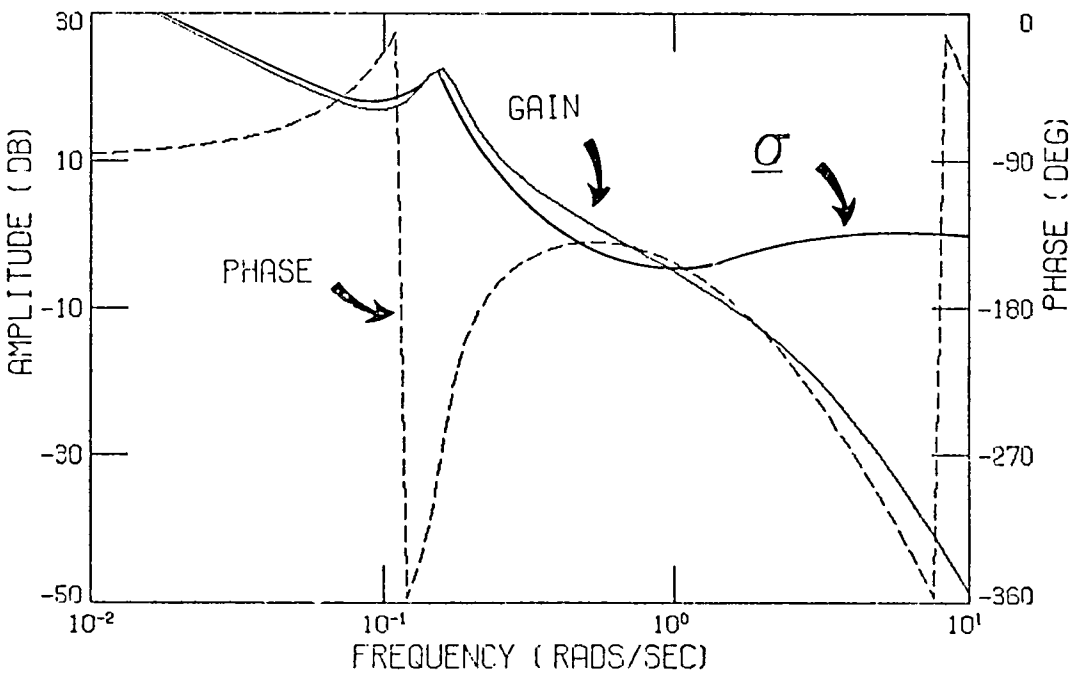

FIGURE 20. LAT1 AILERON LOOP FREQUENCY RESPONSE USING SCHEDULED GAINS, OUTER-LOOP SAMPLE RATE = 5 sps

a) RUDDER LOOP OPEN, AILERON LOOP CLOSED

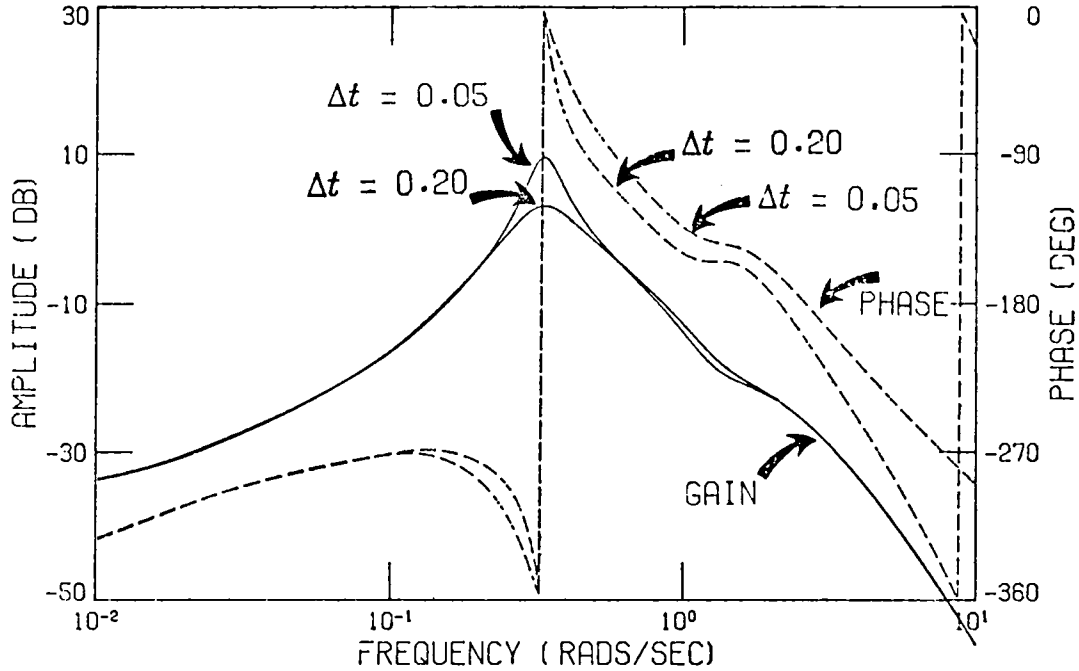

b) AILERON LOOP OPEN, RUDDER LOOP CLOSED

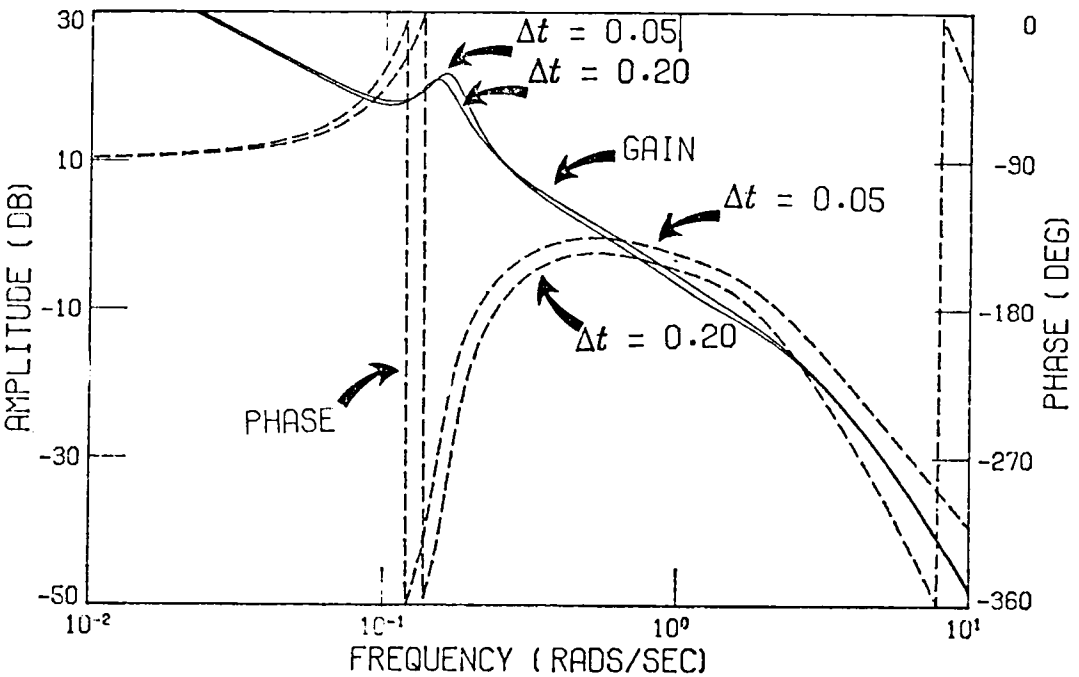

FIGURE 21. LAT1 BODE PLOTS USING OPTIMAL OUTPUT FEEDBACK GAINS

a) THROTTLE LOOP OPEN, ELEVATOR LOOP CLOSED

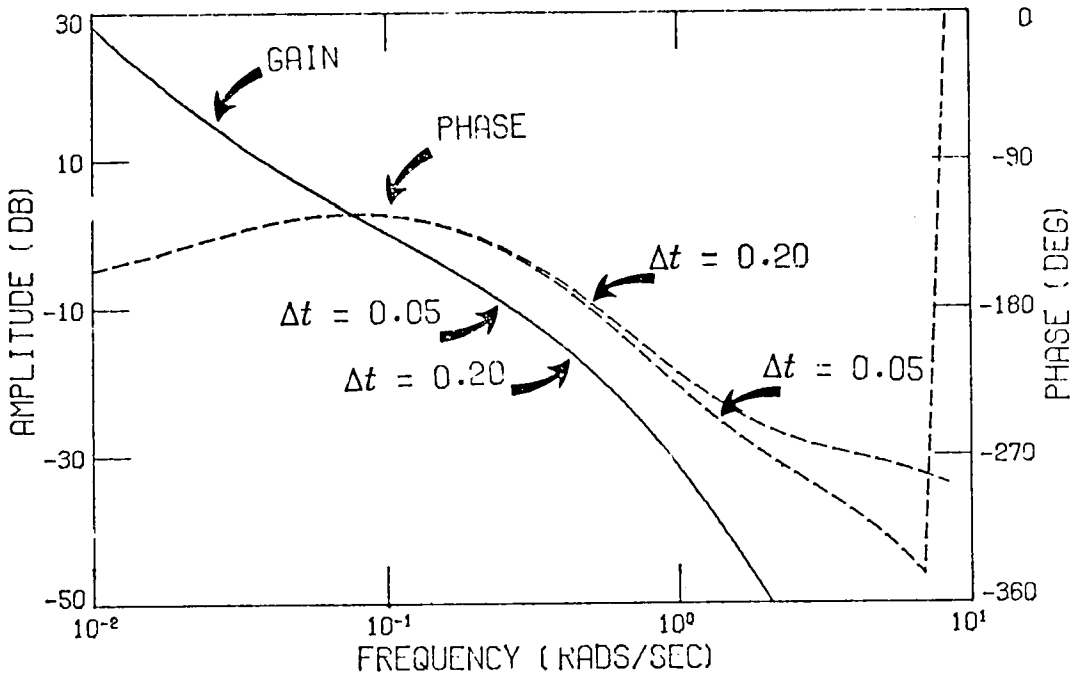

b) ELEVATOR LOOP OPEN, THROTTLE LOOP CLOSED

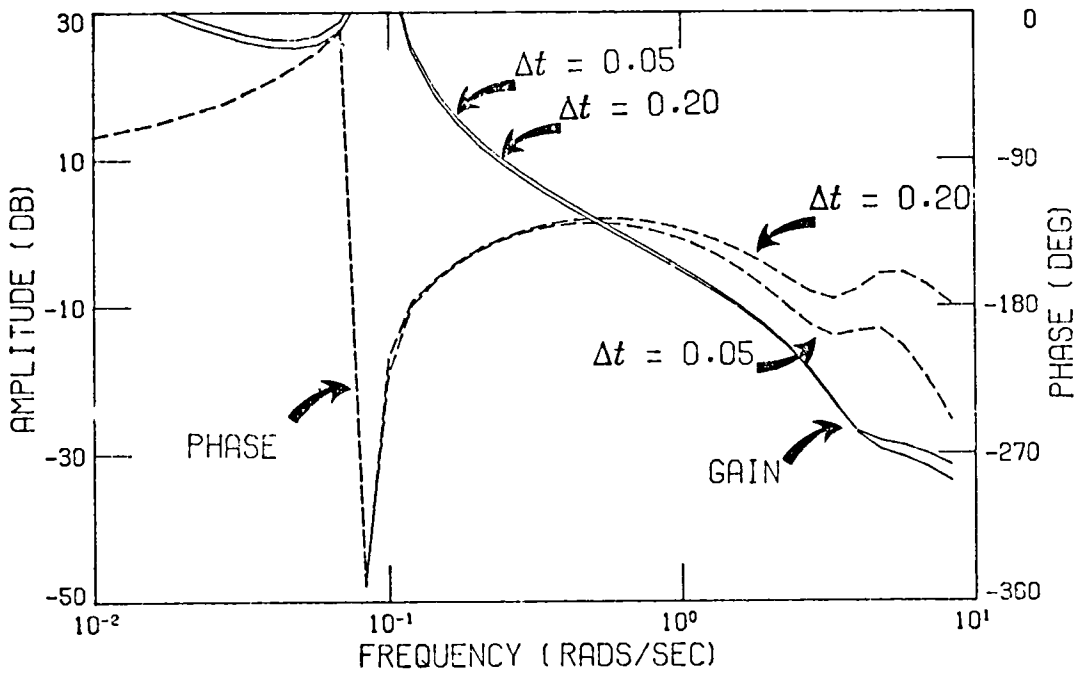

FIGURE 22. LON2 BODE PLOTS USING OPTIMAL OUTPUT FEEDBACK GAINS

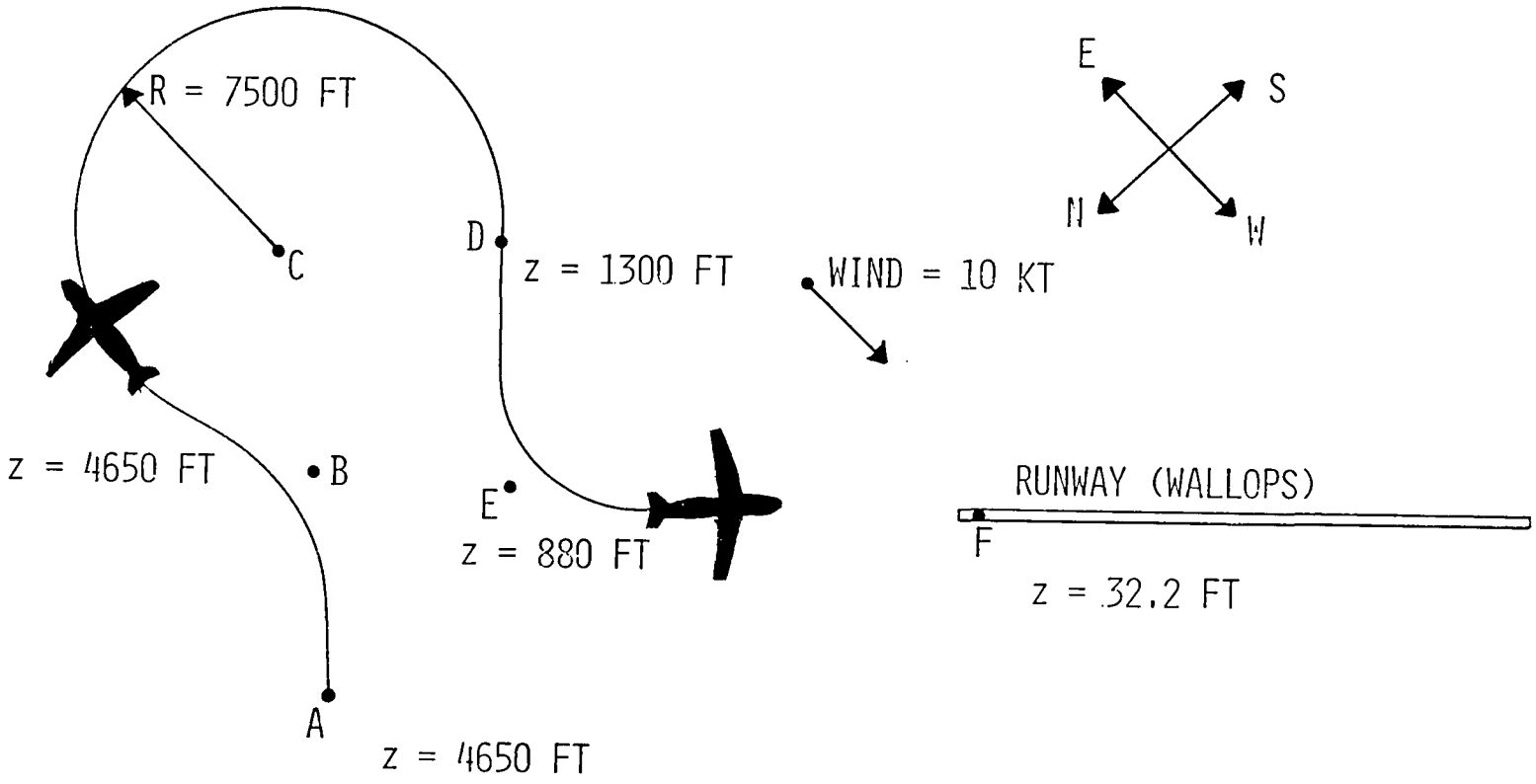

FIGURE 23. HORIZONTAL CURVED TRAJECTORY PROFILE

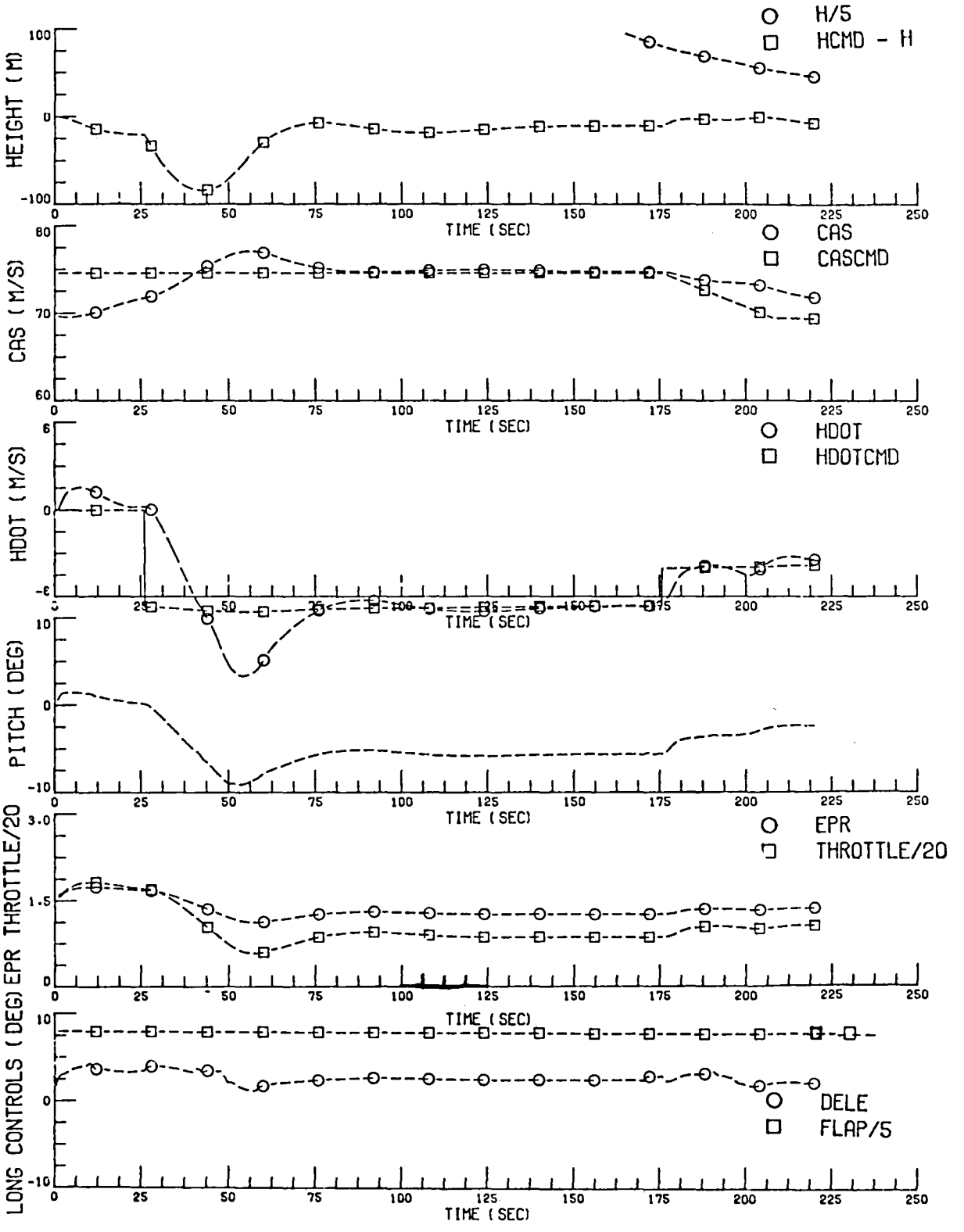

FIGURE 24. LON1 CURVED TRAJECTORY PERFORMANCE, 5 sps

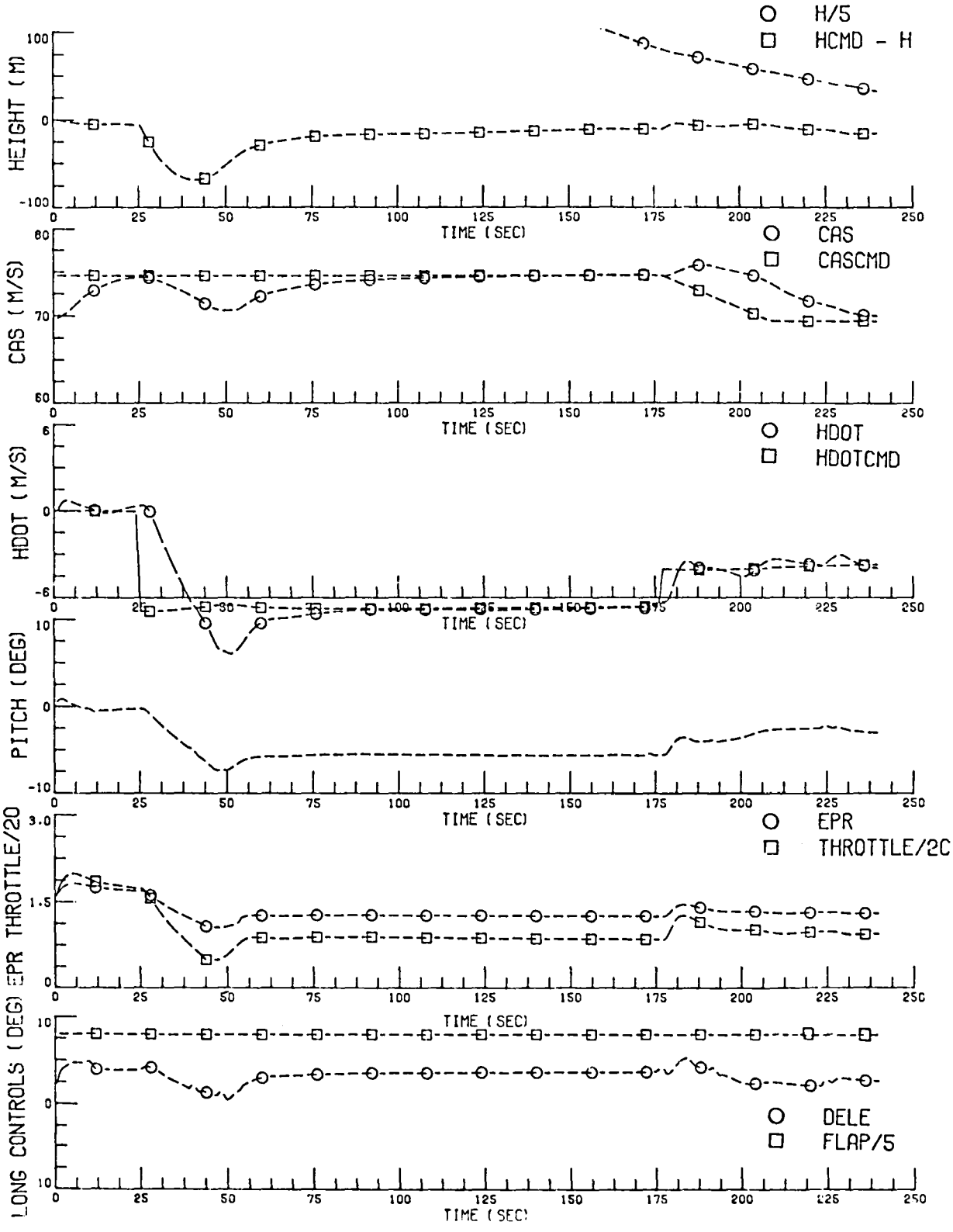

FIGURE 25. LON2 CURVED TRAJECTORY PERFORMANCE, 5 sps

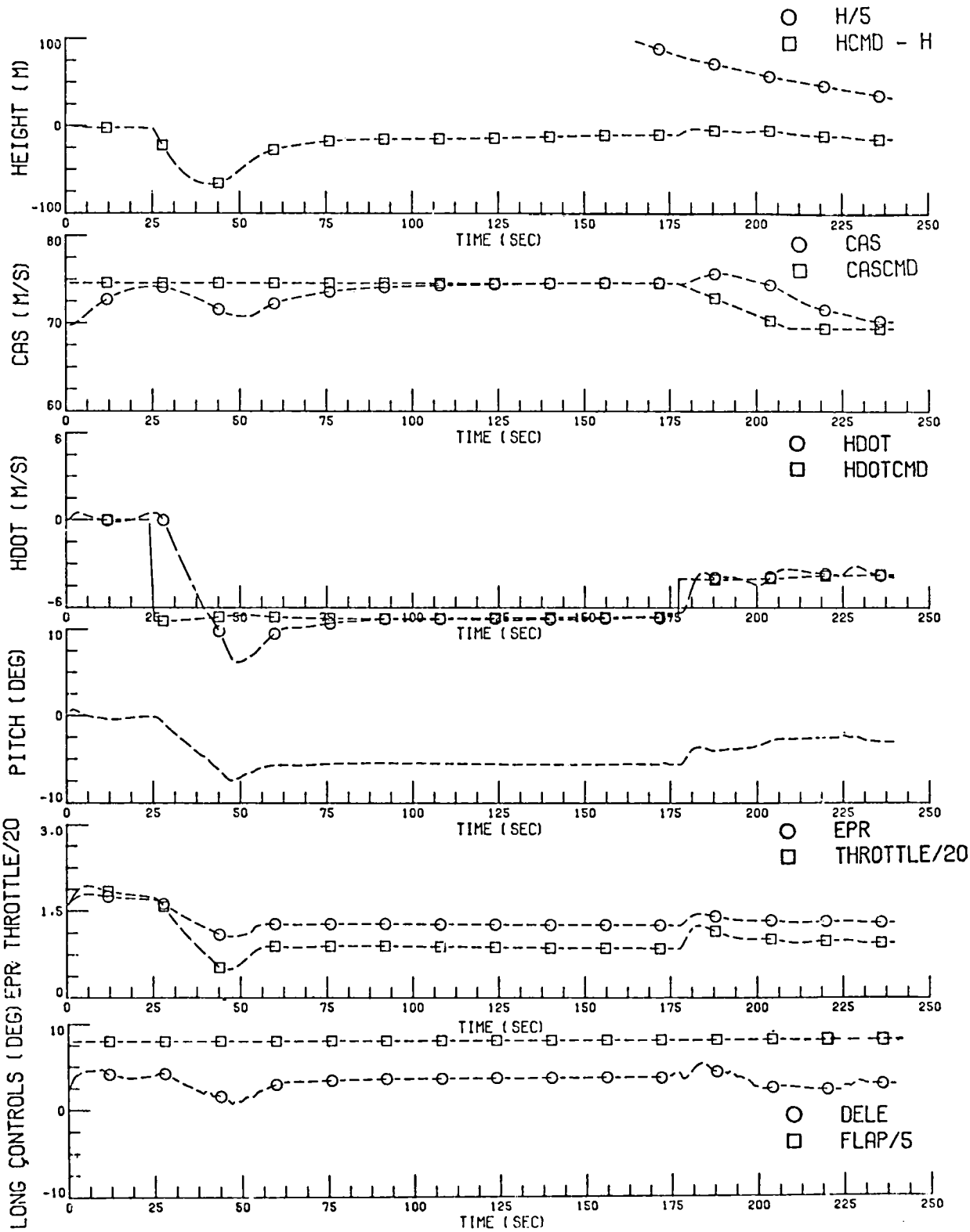

FIGURE 26. LON3 CURVED TRAJECTORY PERFORMANCE, 5 sps

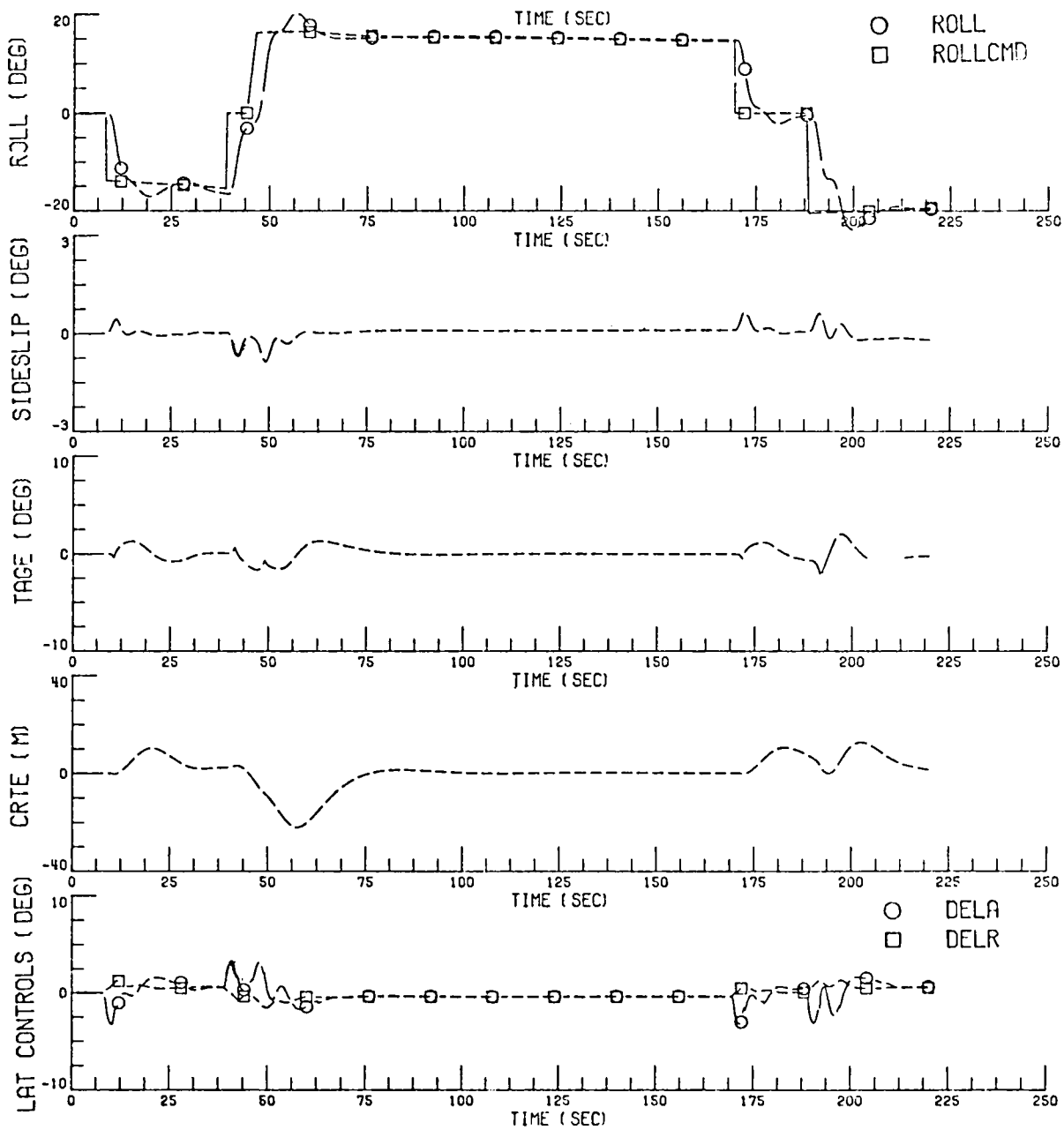

FIGURE 27. LAT1 CURVED TRAJECTORY PERFORMANCE, 5 sps

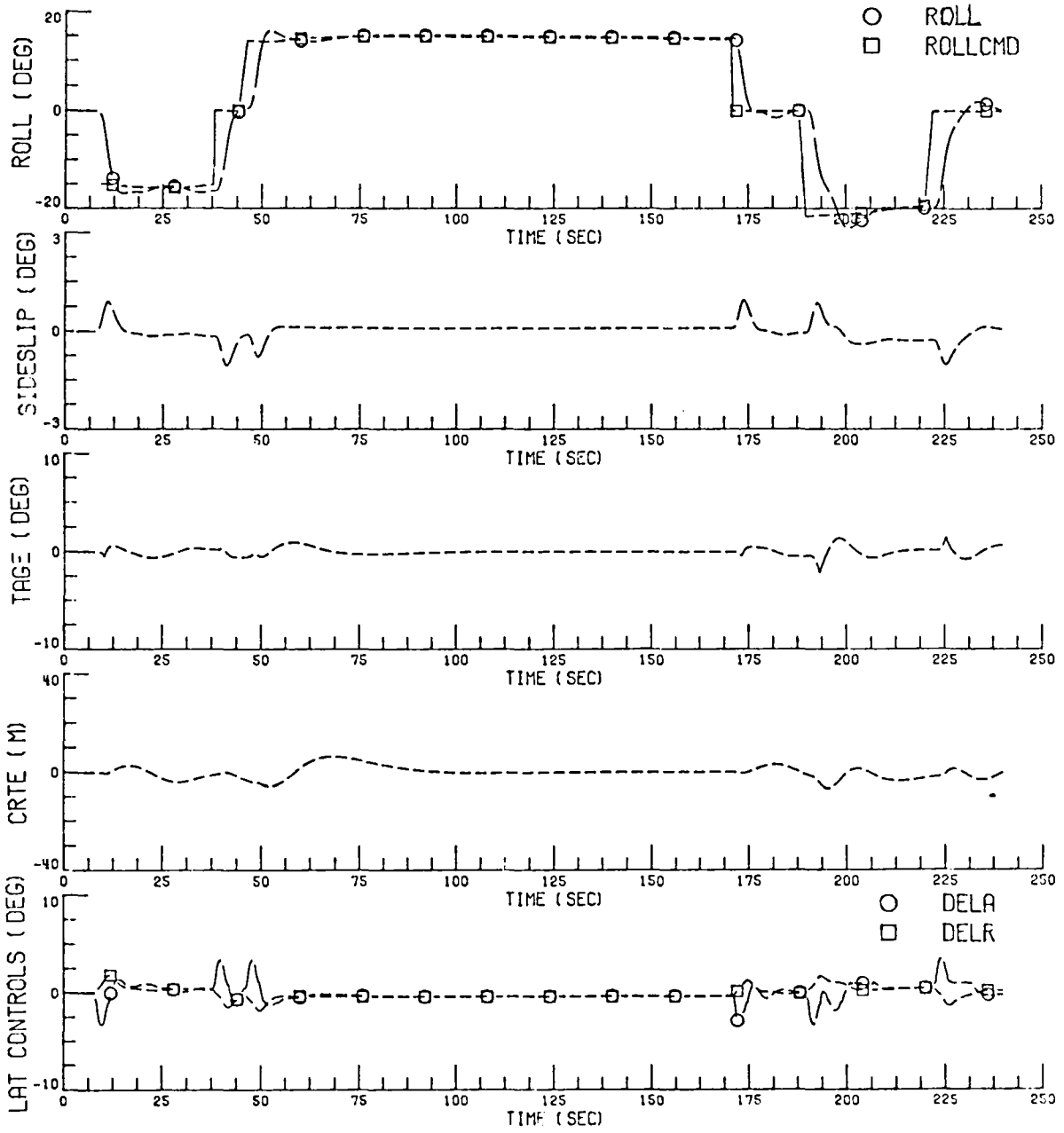

FIGURE 28. LAT1 CURVED TRAJECTORY PERFORMANCE, 20 sps

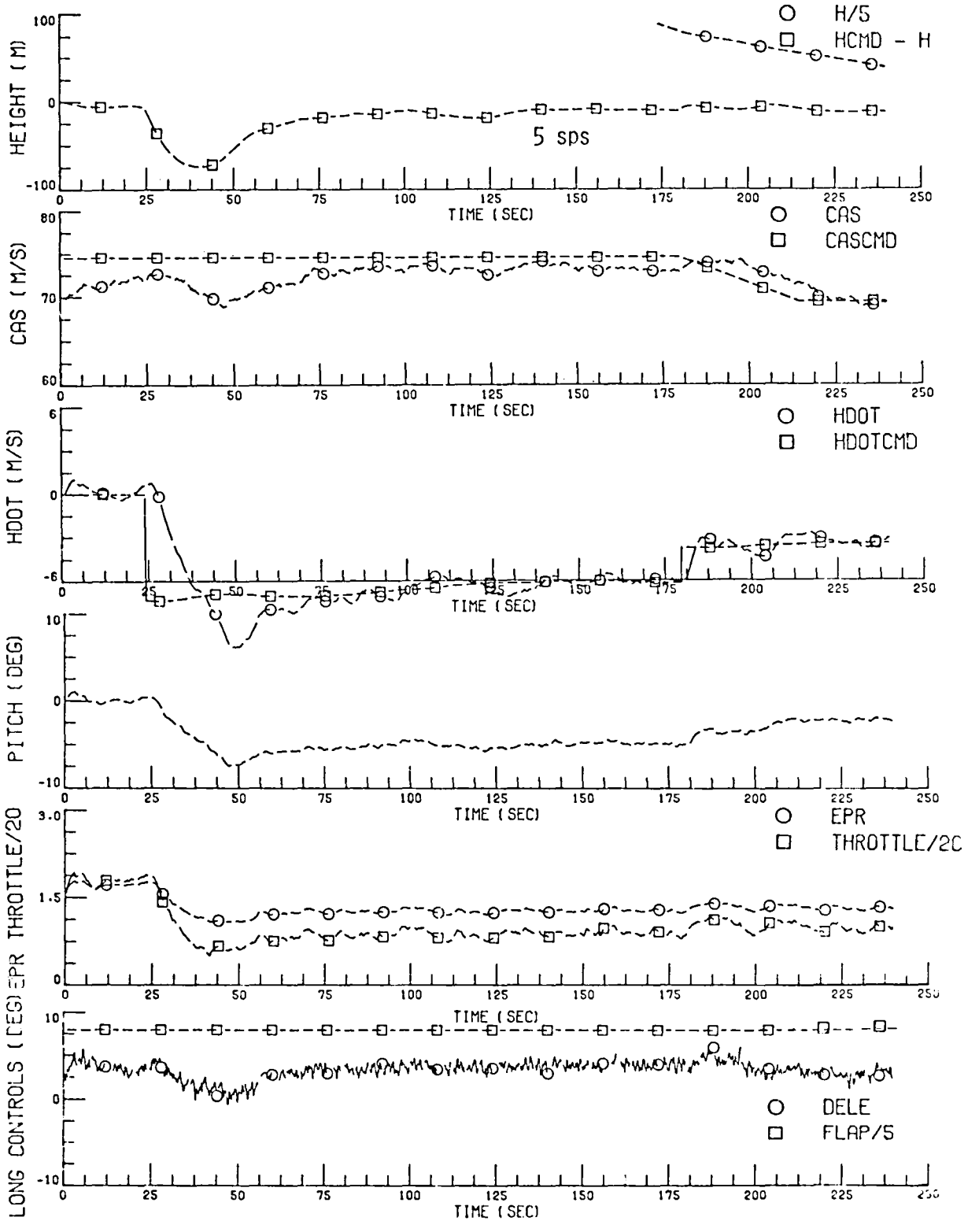

FIGURE 29. LON1 CURVED TRAJECTORY PERFORMANCE WITH DISTURBANCES, 5 sps

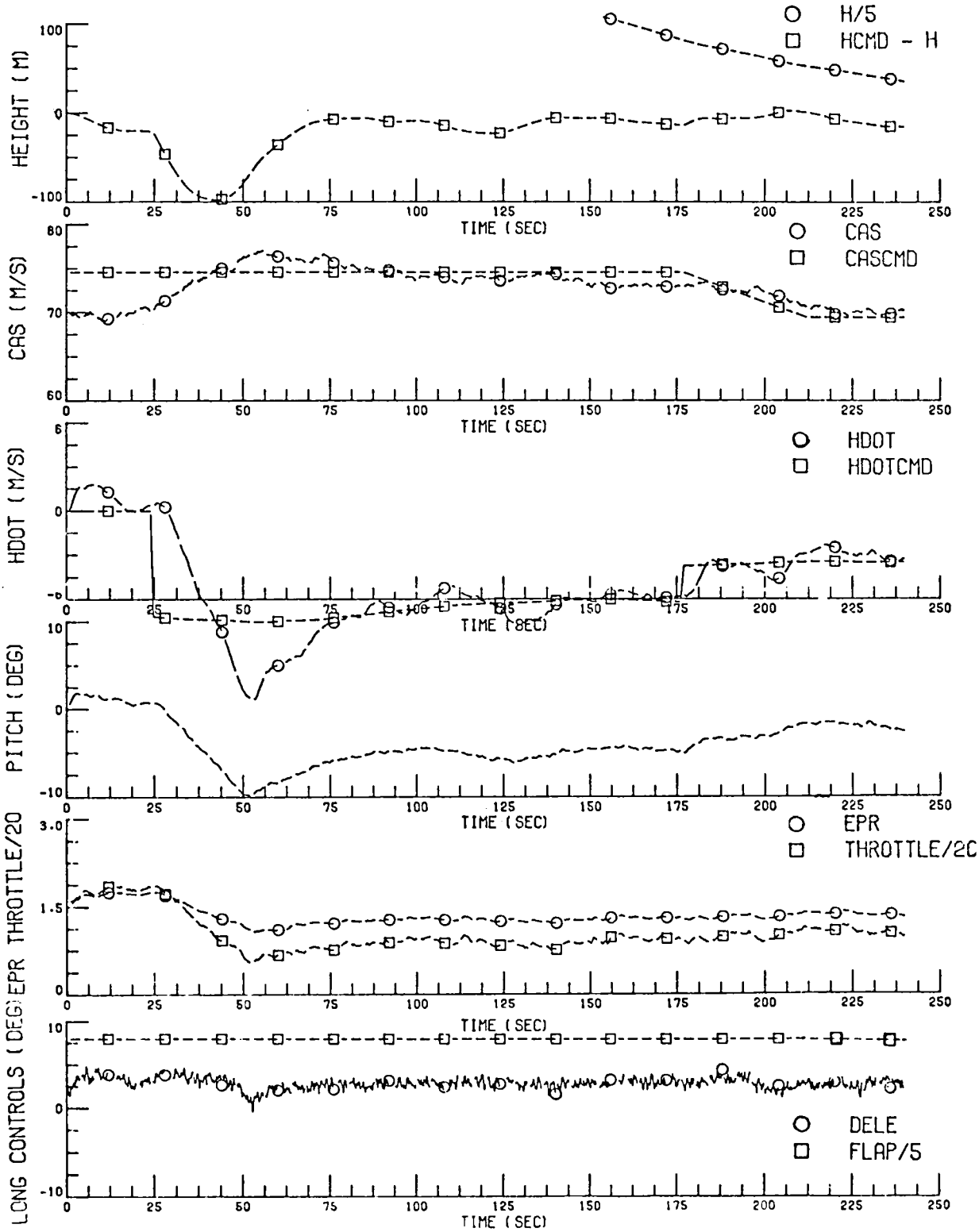

FIGURE 30. LON2 CURVED TRAJECTORY PERFORMANCE WITH DISTURBANCES, 5 sps

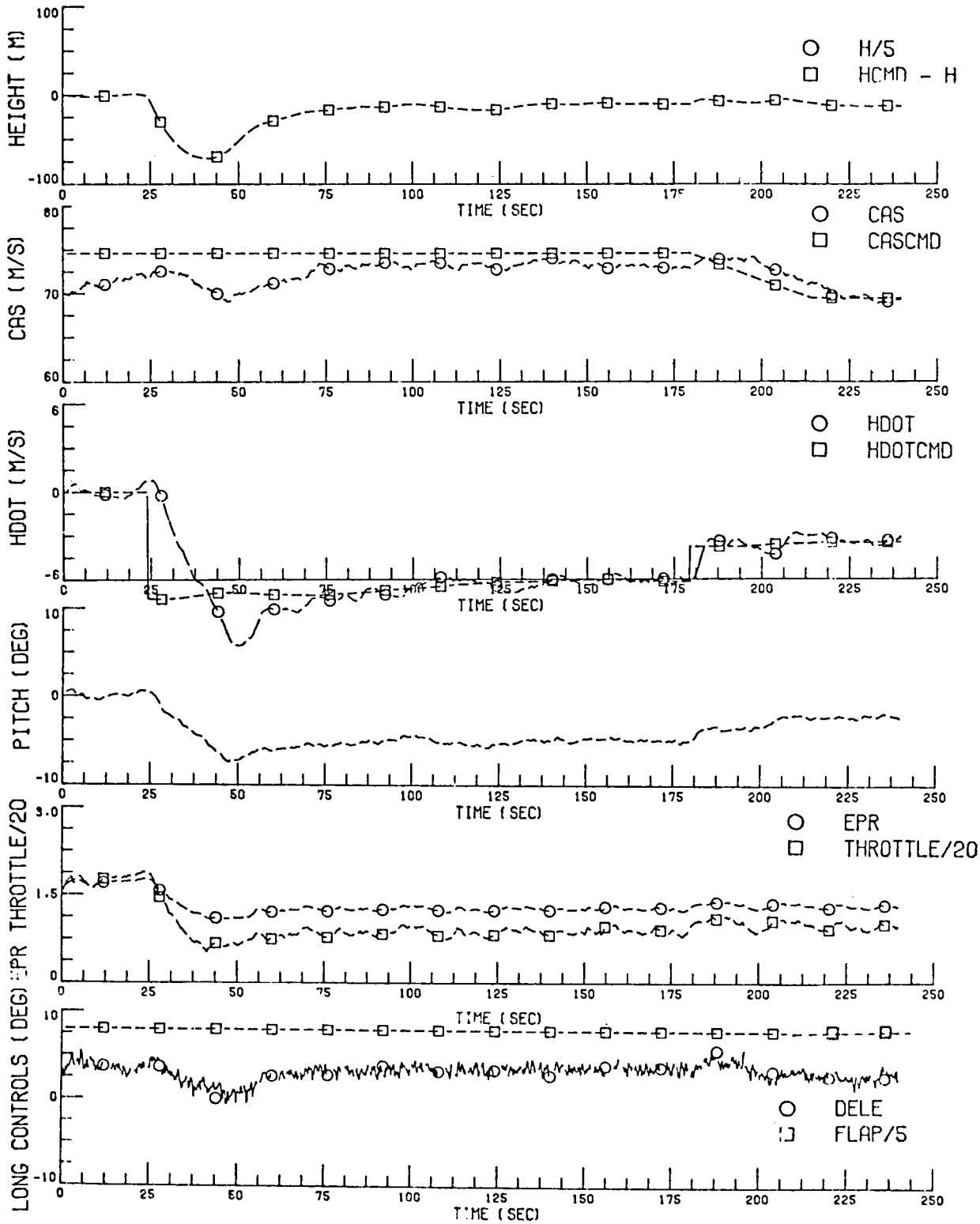

FIGURE 31. LON3 CURVED TRAJECTORY PERFORMANCE WITH DISTURBANCE, 5 sps

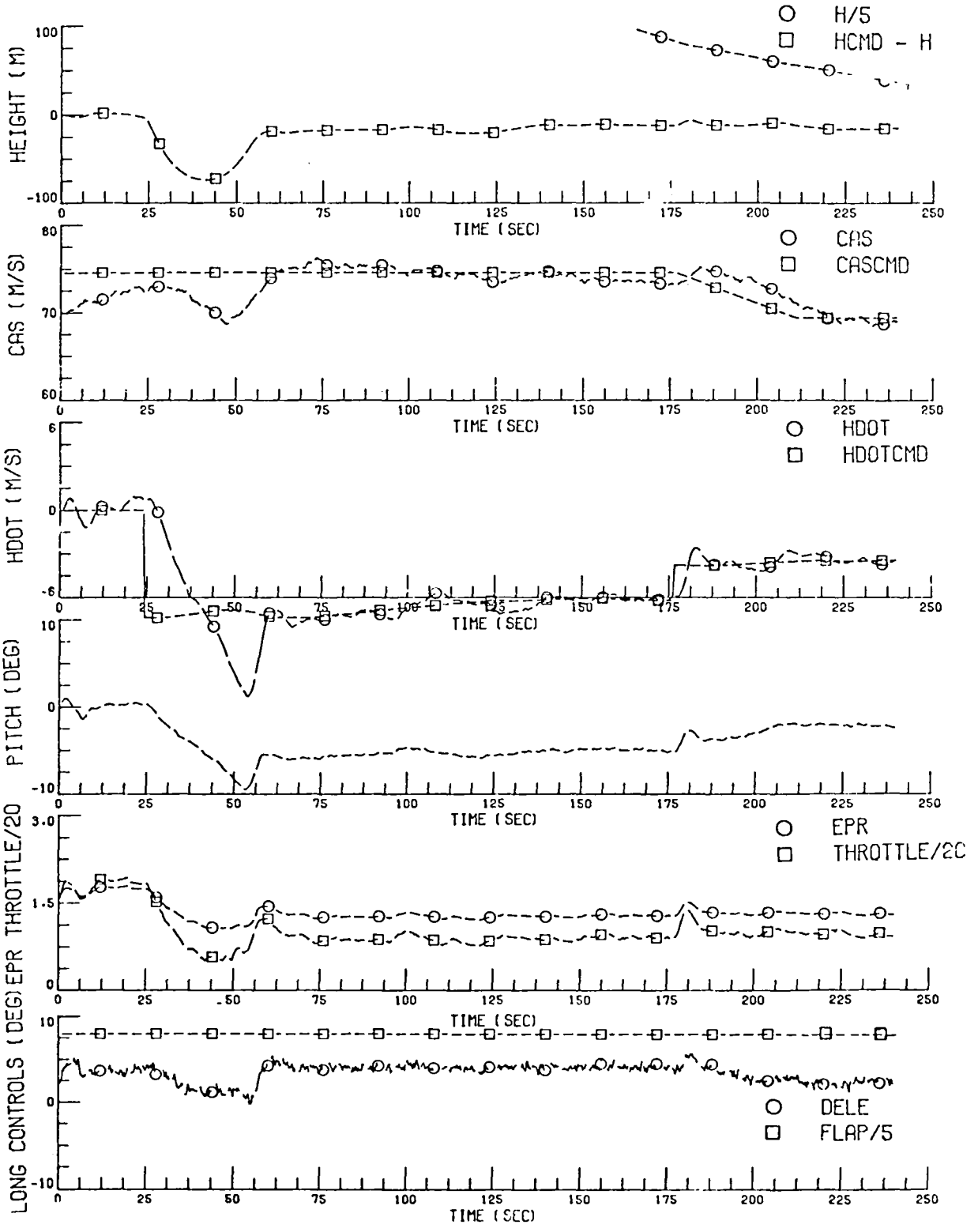

FIGURE 32. LON2 CURVED TRAJECTORY PERFORMANCE WITH DISTURBANCES, 20 sps

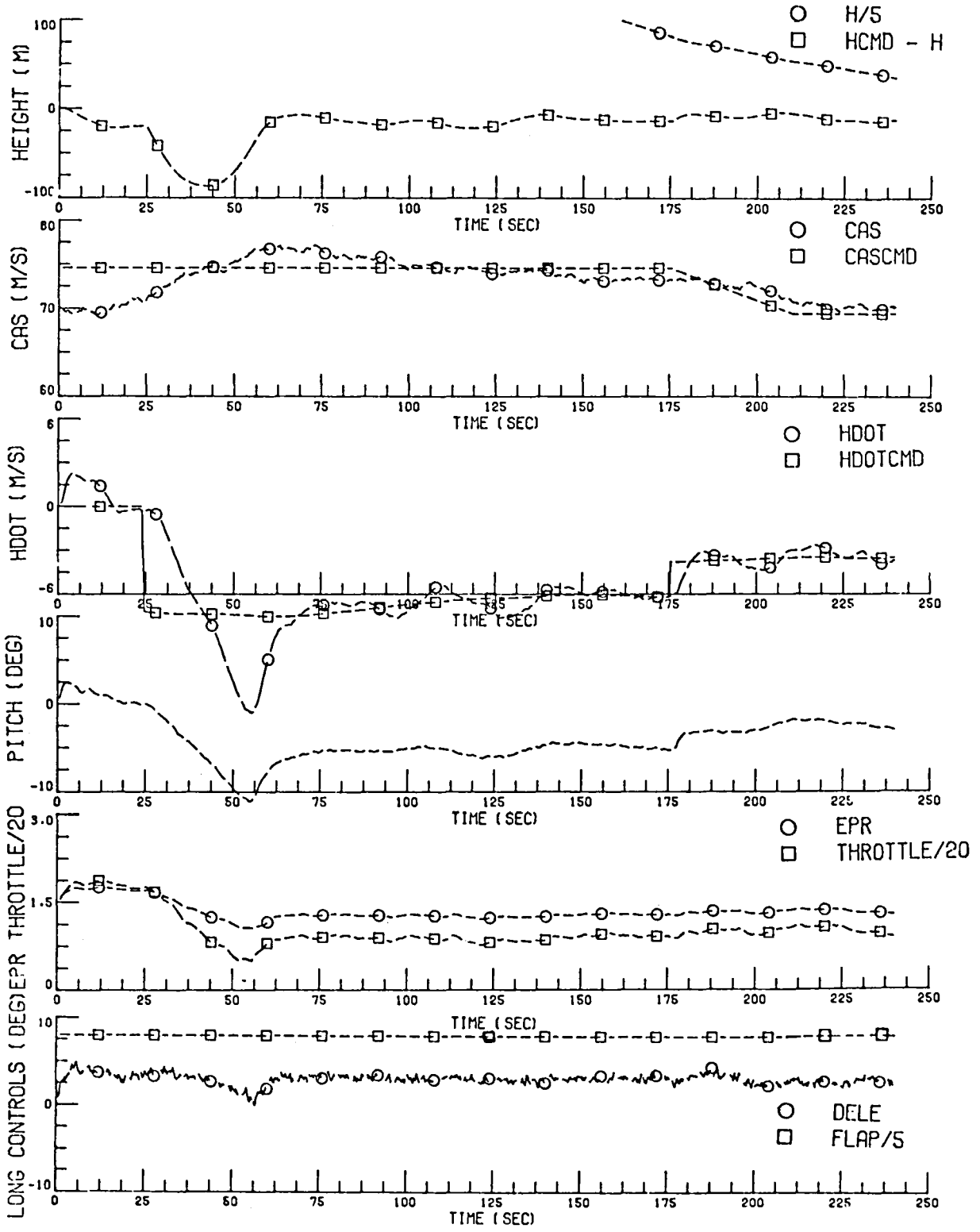

FIGURE 33. LON1 CURVED TRAJECTORY PERFORMANCE WITH DISTURBANCES, 20 sps

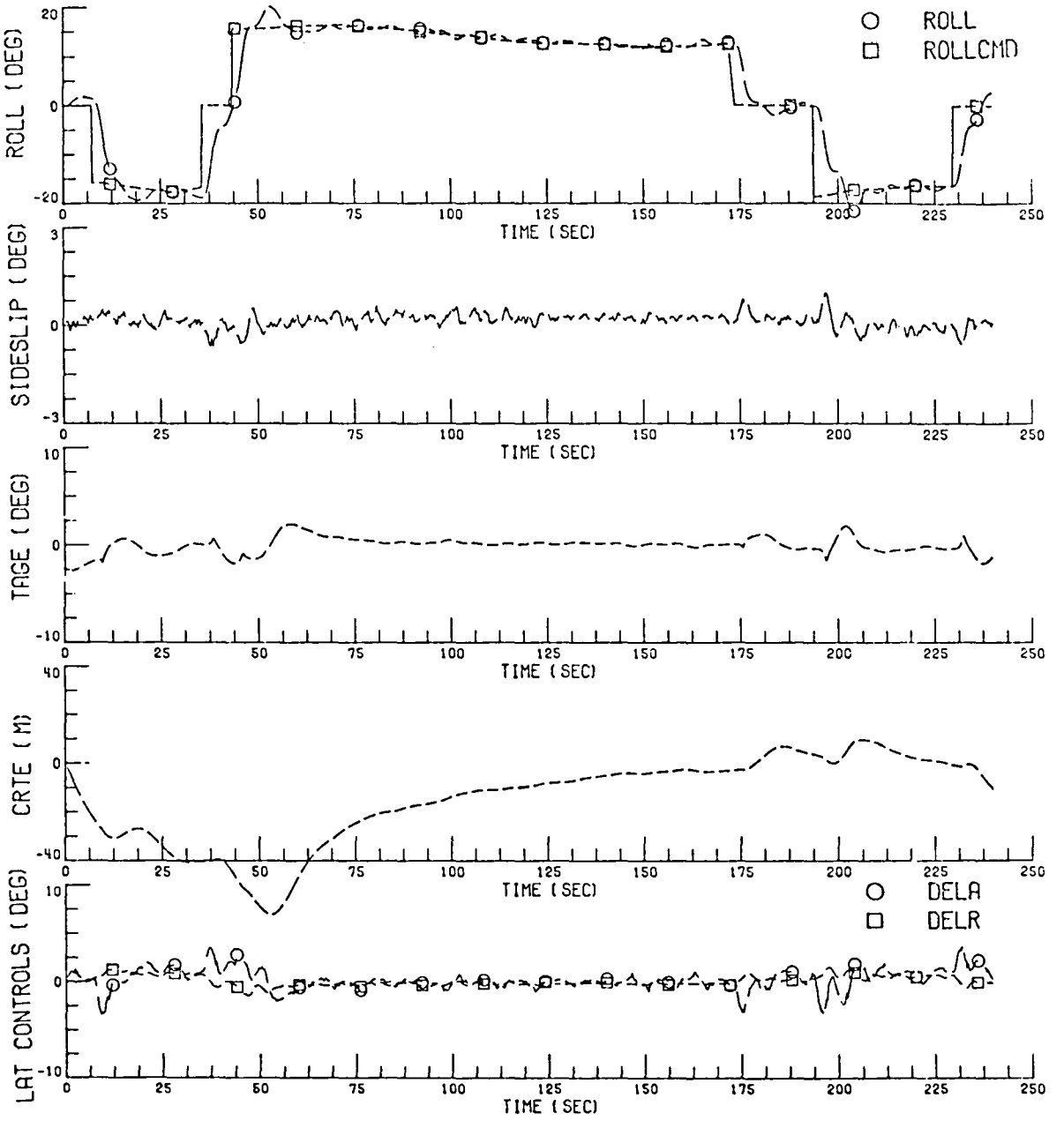

FIGURE 34. LAT1 CURVED TRAJECTORY PERFORMANCE WITH DISTURBANCES, 5 sps

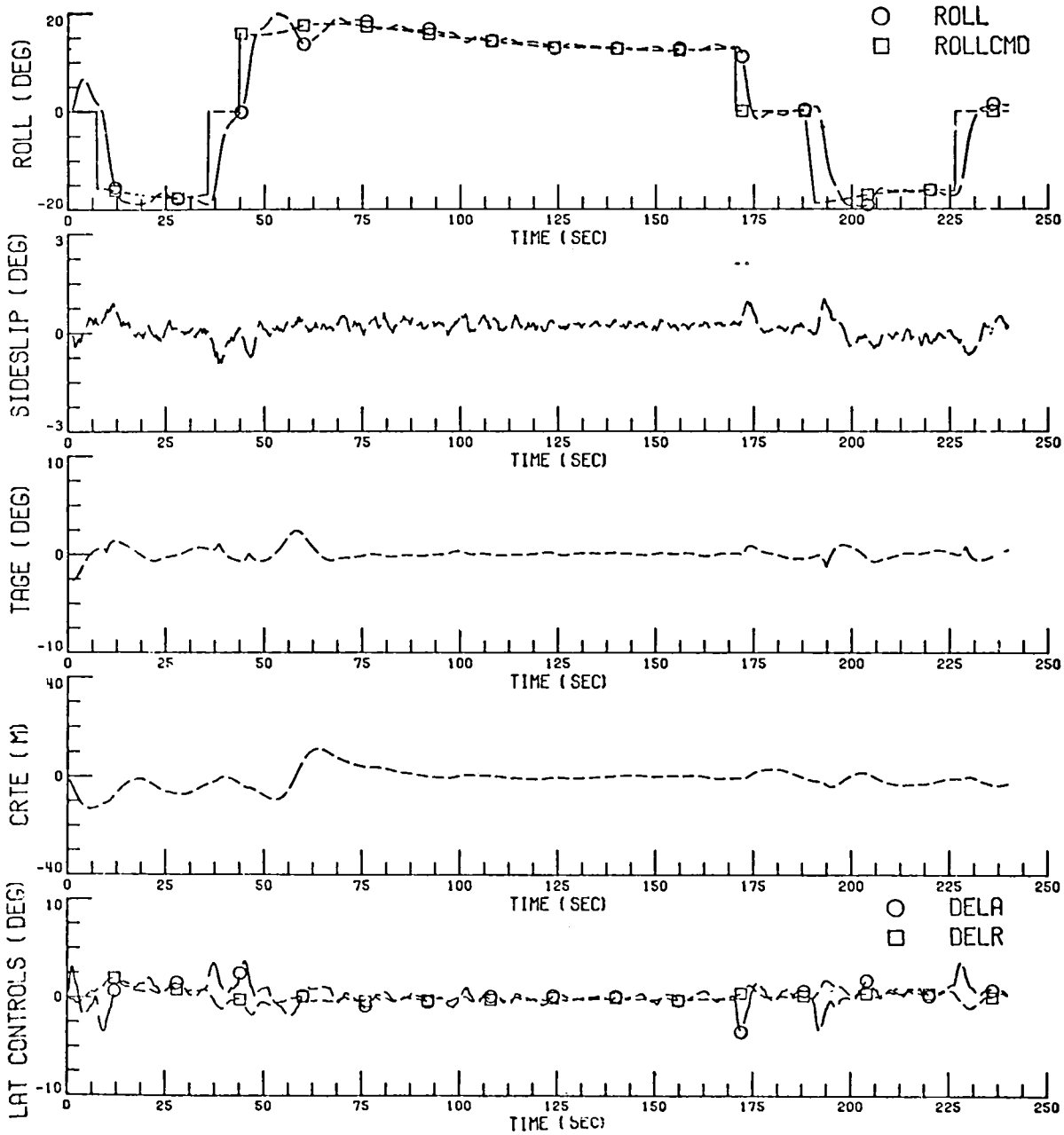

FIGURE 35. LAT1 CURVED TRAJECTORY PERFORMANCE WITH DISTURBANCES, 20 sps

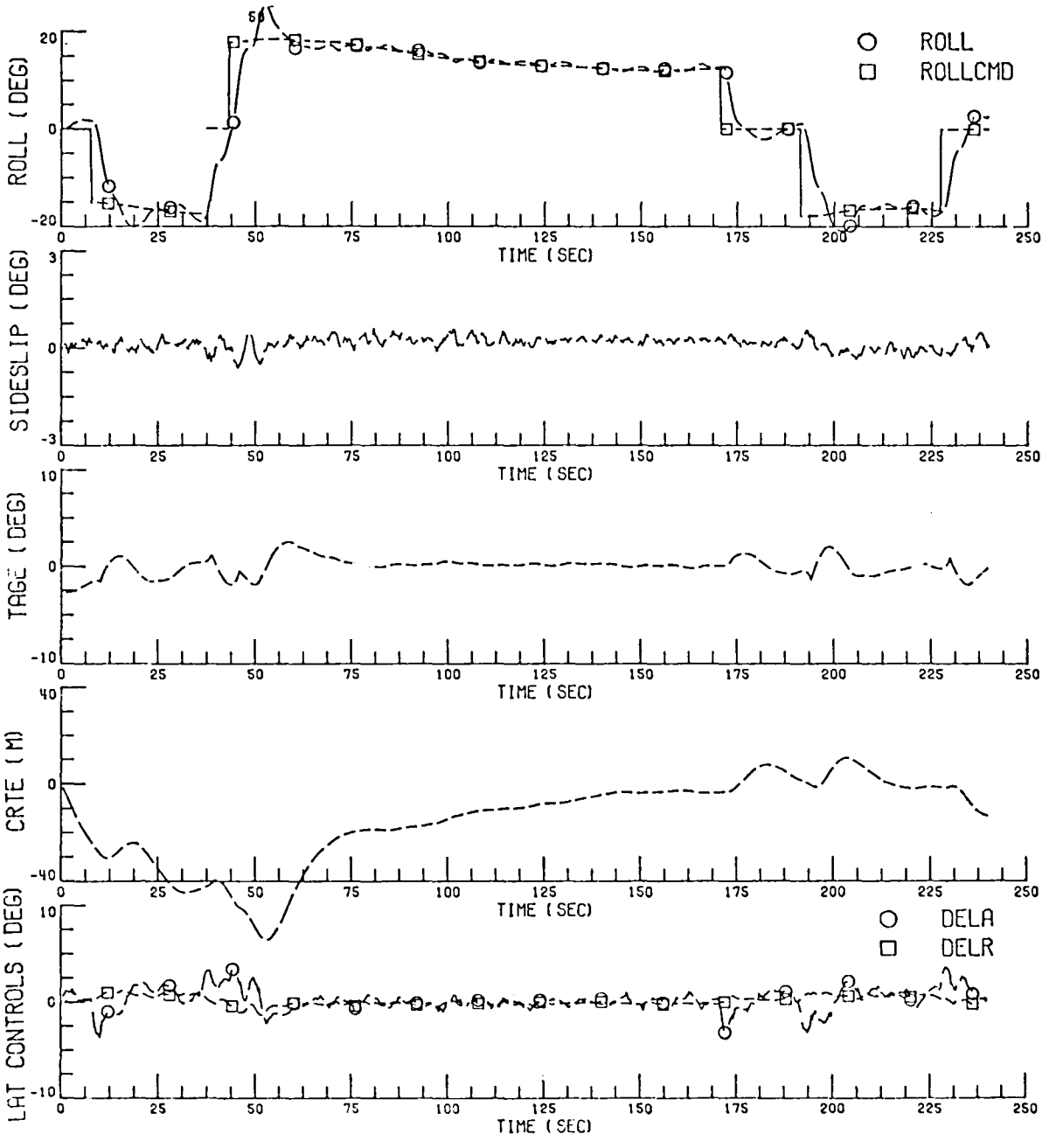

FIGURE 36. LAT2 CURVED TRAJECTORY PERFORMANCE WITH DISTURBANCES, 20 sps

1. Report No.	2. Government Accession No.	3. Recipient's Catalog No.
NASA CR-3829		

4. Title and Subtitle	5. Report Date
INVESTIGATION, DEVELOPMENT, AND APPLICATION OF OPTIMAL OUTPUT FEEDBACK THEORY. Volume II—Development of an Optimal Limited State Feedback Outer-Loop Digital Flight Control System for 3-D Terminal Area Operation	August 1984
	6. Performing Organization Code
7. Author(s)	8. Performing Organization Report No.
John R. Broussard and Nesim Halyo	FR 683111
	10. Work Unit No.
9. Performing Organization Name and Address	
Information & Control Systems, Incorporated 28 Research Drive Hampton, VA 23666	11. Contract or Grant No. NAS1-15759
	13. Type of Report and Period Covered
12. Sponsoring Agency Name and Address	Contractor Report
National Aeronautics and Space Administration Washington, DC 20456	14. Sponsoring Agency Code 534-04-13-54

15. Supplementary Notes

NASA Langley Technical Monitor: Richard M. Hueschen
Final Report

16. Abstract

This report contains the development of a digital outer-loop three dimensional radio navigation (3-D RNAV) flight control system for a small commerical jet transport. The outer-loop control system is designed using optimal stochastic limited state feedback techniques. Options investigated using the optimal limited state feedback approach include integrated versus hierarchical control loop designs, 20 samples per second versus 5 samples per second outer-loop operation and alternative Type 1 integration command errors. Command generator tracking techniques used in the digital control design enable the jet transport to automatically track arbitrary curved flight paths generated by waypoints. The performance of the design is demonstrated using detailed nonlinear aircraft simulations in the terminal area, frequency domain multi-input sigma plots, frequency domain single-input Bode plots and closed-loop poles. The response of the system to a severe wind shear during a landing approach is also presented.

17. Key Words (Suggested by Author(s))

Optimal Control - Theory
Optimal Control - Application
Digital Flight Control System
Autopilot
Output Feedback, Model Following

18. Distribution Statement

Unclassified - Unlimited

Subject Category 08

19. Security Classif. (of this report)	20. Security Classif. (of this page)	21. No. of Pages	22. Price
Unclassified	Unclassified	135	A07

For sale by the National Technical Information Service, Springfield, Virginia 22161

NASA-Langley, 1984

National Aeronautics and Space Administration

Washington, D.C.
20546

Official Business
Penalty for Private Use, $300

THIRD-CLASS BULK RATE

Postage and Fees Paid
National Aeronautics and Space Administration
NASA-451

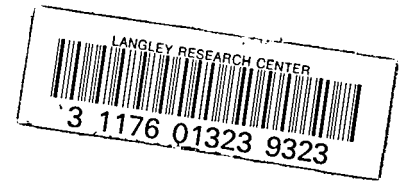

NASA

If Undeliverable (Section 158 Postal Manual) Do Not Return

DO NOT REMOVE SLIP FROM MATERIAL

Delete your name from this slip when returning material to the library.

NAME	MS
DDH	IL
1 MONTH LOAN	

NASA Langley (Rev. May 1988) RIAD N-75